Spring 5-18-2019

Novel Low Shear 3D Bioreactor for the Scaled Production of High Purity Human Mesenchymal Stem Cells

Andrew Burns

Novel Low Shear 3D Bioreactor for the Scaled Production of High Purity Human Mesenchymal Stem Cells

By

Andrew Barney Burns

A Thesis submitted to the Faculty of Keck Graduate Institute of Applied Life Sciences in partial fulfillment of the requirements for the degree of Doctor of Philosophy in Applied Life Sciences

Claremont, California

2019

Approved by:

M. Ian Phillips, Ph.D.

We, the undersigned, certify that we have read the thesis of Andrew Barney Burns and approve it is as adequate in scope and quality for the degree of Doctor of Philosophy.

Thesis Committee:

DocuSigned by:
M. Ian Phillips
09CAD69BC65041C...
5/13/2019

M. Ian Phillips, Ph.D., Chair

DocuSigned by:
Cameron Bardliving
7451127FC51F41E...
5/14/2019

Cameron Bardliving, Ph.D., Member

DocuSigned by:
Vinit Saxena
349CAF23C84F43D...
5/16/2019

Vinit Saxena, Member

DocuSigned by:
E6CBF8D43D374D8...
5/13/2019

Parviz Shamlou, Ph.D., Member

DocuSigned by:
Srikanth Kolluru
151F762EED0745C...
5/13/2019

Srikanth Kolluru, Ph.D., Program Director

Abstract of Thesis

Characterization of a novel, low shear lattice bioreactor for expansion of human mesenchymal stem cells

By Andrew Barney Burns

Keck Graduate Institute of Applied Life Sciences: 2019

Human mesenchymal stem cells are an ideal candidate for stem cell therapies. They have been researched since the 1960's and can differentiate into many desired functional cell types without undergoing teratogenesis. However, higher yields are needed for a marketable, successful stem cell therapy. To accomplish this, cells will have to be cultured to expand them to therapeutically relevant dosages for multiple patients. Bioreactor production is an ideal method to solve this problem.

The aim of this thesis is to test and validate a novel bioreactor for the cultivation of human mesenchymal stem cells. In this work, we investigate a novel suspended matrix for the culture on human mesenchymal stem cells (hMSCs). Initially we investigated various fiber meshes, both random and structured, for stem cell growth and morphology. We also investigated hMSC proliferation on rigid polymers commonly used in 3D printing. We then took the conditions that worked best in 2D culture and tested them in a small-scale model of the Express bioreactor from Sepragen.

We have assessed cell growth on 3D printed Polylactic Acid (PLA) matrices and developed a scale down model bioreactor for development and characterization. Computational Fluid Dynamic (CFD) modeling was used in parallel with the described

in-vitro experimentation to characterize shear profiles. From the CFD we were also able to predict a flow rate which resulted in almost zero shear. What we found was that hMSCs readily form confluent monolayers on the PLA lattice, and retain their surface marker expression and stemness. When combined with a short hypoxic treatment, the cells performed better than control flasks, resulting in a four-fold increase from seed with no impact on biomarker profile and differentiation ability.

Dedication

To my supportive and incredibly patient parents. You sparked my interest in the sciences and helped me through everything. I may finally be done with school.

Para mi Abuelo, sin su ayuda nunca hubiera podido realizar mis sueños de ser un doctor. Tú me enseñaste todo lo que he necesitado para fabricar mi sistema y las herramientas que usé en este proyecto.

Michele, you have always believed in me and supported all my endeavors. You know me better than I know myself, and I could not have done this without your love and guidance.

Acknowledgements

I owe the most thanks to Dr. Ian Phillips. When I first came to KGI it was with the intent of becoming a medical doctor. After my first year we journeyed to Honduras with Global Medical Brigades where we worked together triaging patients in the hallway of an elementary school, and when we returned, he was kind enough to offer me a laboratory coordinator position working with miRNAs while applying for other graduate positions. He was always there to help me and became a true mentor. When he found out I wanted to pursue a doctorate in stem cell bioprocessing he quickly agreed to be my principal investigator. He has been a large factor in my success, and I owe him my deepest gratitude. I could not have conquered this project without his wealth of knowledge.

There are many others I would like to thank at KGI. Kirilynn Svay sought me out and was the professor who helped me put together this project. She saw that I had the ability to conduct a thesis culturing stem cells and helped me see that in myself as well. I would like to thank Dr. Parviz Shamlou for his extreme patience and confidence in my cell culture abilities. In the midst of this project there was much movement in the school, and he saw to it that I would be able to continue my research unimpeded. He was always there to help in both bioprocessing challenges and with life problems. I would also like to thank Dr. Cameron Bardliving, who kept his office door open for me, fielded many oddball questions, and offered life advice.

I would not have been able to finish this project if not for my fellow PhD Students, Corinna Doris, Kevin Vehar, Flaka Radoniqi, Aster Escalante, James Miller, and Elizabeth Henderson. All I had to do was turn around, and every question I had was

answered by any and all of you. Being holed up in our shared office was often loud and sometimes distracting, but I would not have it any other way. Thank you all.

I would also like to take the time to thank Vinit Saxena of Sepragen Inc. The original bioreactor design was spearheaded at Sepragen, and he was kind enough to allow me to test this unique system for stem cell growth, accepting my alterations and listening to my comments. Thank you for trusting your system to me and providing me with an exciting project for my thesis.

I owe my project to KGI along with Dr. Dennis Fenton and Linda Fenton, whose generous donation to KGI funded my stipend and work. If not for their gift to the KGI bioprocessing department I would not have been able to work on this project.

Lastly, I owe much of my knowledge in stem cell biology and laboratory technique to Dr. Drew Glaser and the McCloskey lab at University of California, Merced. Dr. Glaser picked me out from a discussion course in general biology and took on a naive and impressionable nineteen year old. The work I did at UC Merced allowed me to plan out my project with ease from simple cell expansion, to flow cytometry characterization, to stem cell induction. You all cemented my love for stem cell science, and I cannot thank you enough for taking a chance on me.

Contents

Table of Figures

Table of Tables

Table of Equations

Abbreviations

AD-hMSCs and hAD-MSCs	Adipose Derived Human Mesenchymal Stem Cells
ATCC	American Type Culture Collection
b-FGF	Beta – Fibroblast Growth Factor
BM-hMSCs and hBM-MSCs	Bone Marrow Derived Human Mesenchymal Stem Cells
BSA	Bovine Serum Albumin
CDB	Cell Dissociation Buffer
CFD	Computational Fluid Dynamics
DMEM	Dulbecco's Minimum Essential Medium
DO	Dissolved Oxygen
FBS	Fetal Bovine Serum
FDM	Finite Difference Modeling
FEM	Finite Element Modeling
FMO	Fluorescence Minus One
FVM	Finite Volume Modeling
HCT/P	Human Cells and Tissues/Products
hESCs	Human Embryonic Stem Cells
HIFs	Hypoxia Inducible Factors
hiPSCs	Human Induced Pluripotent Stem Cells
HLA	Human Leukocyte Antigen
hMSCs	Human Mesenchymal Stem Cells
IGF-1	Insulin Like Growth Factor – 1
ISCT	International Society for Cell Therapies
KLa	Coefficient of Oxygen Transfer
MI	Myocardial Infarction
miRNA	Micro Ribonucleic Acids
OTR	Oxygen Transfer Rate
PC	Polycarbonate
PCL	Polycaprolactone
PE	Polyethylene
PET	Polyethethylene Terephthalate
PETG	Polyethethylene Terephthalate Glycol
PFA	Paraformaldehyde
P-hMSC and hP-MSCs	Placenta Derived Human Mesenchymal Stem Cells
PLA	Polylactic Acid
pNIPAAM	Poly(N-Isopropylacrylamide)
PS	Polystyrene
T-PU	Thermoplastic Polyurethane
V/V	Volume/Volume
W/V	Weight/Volume

1 INTRODUCTION

1.1 STEM CELL THERAPY

Stem cell are simultaneously novel and well researched. They were first therapeutically used in the 1960's before being formally named, but have recently gained more attention in the field of regenerative medicine.[1] This resurgence in stem cell research is based in its ability to both self-renew and differentiate into functional cell types. Stem cells differ by their time and source of harvest and are classified by their potency; Potency here refers to the number of different cell types the stem cell can become. The potency classifications for stem cells are: totipotent, pluripotent, multipotent, and unipotent. Totipotent cells are able to differentiate into all cell types in the body, as well as placental tissue. Pluripotent cells can become all cells of the body. Multipotent cells can become all cell types of a certain germ layer. Unipotent stem cells are restricted to one cell type and have been simply referred to as progenitor cells.[2] A comparison of stem cell types in regards to therapeutic potential can be found in Table 2-1.

Pluripotent human Embryonic Stem Cells (hESCs) are collected from the inner cell mass of the blastocysts. These cells can differentiate into all three germ layers and their resulting tissues.[3] These cells have had a charged ethical history, as a fertilized oocyte must be sacrificed to harvest these cells. In 2001 the Bush administration placed stringent regulations on hESC research, resulting in defunded embryonic stem cell research using primary harvested lines.[4] Stem cell research was still conducted, but was limited to established lines, such as H7 and H9 hESCs. This complicated hESC research, as laboratories had to split funding and lab space by private investors vs government

funding. It also was detrimental to hESC research, as the available lines were not genetically diverse.[5] Later, the Yamanaka and the Thompson labs both discovered ways to genetically alter cells and induce a pluripotent state in the cells.[6,7] Among the transcription factors the two labs discovered, the two main genes needed are Oct4 and Sox2. Additional alternatives include Nanog, FL4, and C-Myc.[6,7] Cells treated with these factors have been deemed induced pluripotent stem cells (iPSCs). This cell type usually uses a feeder cell culture such as mouse embryonic fibroblast to provide a supportive culture environment for the cells. Additionally, trypsin cannot be used when passaging these cells, as hESCs tend to apoptose when placed into single cell suspension. Because of this, enzymes like accutase are used for cell-substrate detachment to lift cell clusters.

Multipotent stem cells are found in all tissues of the body.[8] They are hypothesized to be surrounded by support cells, forming a favorable niche for the cells to stay quiescent until called to action via cytokines or stress. These stem cells can give rise to cells only of their respective germ layer. Though multipotent stem cells have less potency compared to iPSCs, they are the most studied type of stem cell. This long history stems from their first use as a treatment for Leukemia.

The first stem cell therapy was performed via bone marrow transplant over 50 years ago by Dr. E. Donnall Thomas. This treatment replaced the immune system of a leukemia patient by harvesting bone marrow from a healthy donor and placing it into the ablated bone of the patient.[1] The transplanted bone marrow brought with it both hematopoietic stem cells and bone marrow derived mesenchymal stem cells. Since the donor and recipient were twins, there was no issue of host vs graft disease. As research in tissue transplantation continued, it was discovered that Human Leukocyte Antigen (HLA) was

key in graft vs host disease. Allogenic grafts are now possible by matching donor and recipient based on HLA. This breakthrough opened the door for stem cell treatments. Companies like AlloSource, NuVasive, Osiris, OrthoFix, and others have been approved as combination medical devices and Human Cells and Tissues/Products (HCT/P), and are currently sold in the United States under the guidance of 21 CFR 361.[9] They have been used for bone regeneration, soft tissue repair, and spinal bone regeneration. They have been approved through the 501k pathway, meaning the device must show equivalence to an already approved medical device. For the transplanted cells to remain compliant under 21 CFR 361, the cell product used with these devices must remain minimally manipulated, otherwise it would have to be approved as a BLA or another more complicated avenue. One issue specifically with HCT/P is that they do not have to show equivalence or go through normal clinical trials for approval. This can result in ineffective therapies and can potentially harm patients.

The current demand for stem cells far exceeds their supply. Recent projections estimate a 31.1% compound annual growth rate of the stem cell market from 2016 to 2022.[10] As demand grows, there have been various attempts to culture these cells in the hope of increasing the supply for allogenic stem cell therapies and their testing. Cell culture and cryopreservation are expected to cost over $10 billion by 2020.[11] Conventional culture systems cannot produce these numbers, as culturing stem cells is comparatively harder than other cells.

Stem cells are very sensitive to chemical and mechanical cues. Such forces can cause the cells to differentiate, become quiescent, or apoptose.[12,13] They are also slow growing, which pushes out harvest time and increases the risk of contamination. The media also

must contain recombinant factors, which makes it expensive and usually undefined.[9] Furthermore, they are adherent dependent, and as such will not readily grow in conventional bioreactors for culture of CHO or other suspension-adapted cell lines. Because of this restriction, scale out, rather than scale up, methods of culture are generally adopted.

1.2 AIM AND SCOPE

High purity, high density culture methods for mesenchymal stem cells are necessary for stem cell based therapies to be fully realized. Conventional bioproduction techniques have been used to culture stem cells with cell based therapies in mind, however these techniques are generally cumbersome and prone to contamination which can result in impure cell populations. Here we investigate a custom system for high purity, scalable culture of human mesenchymal stem cells. The main drawbacks of other systems include lack of cell monitoring, shear stress from mixing techniques, and heterogeneity in the system due to a combination of these factors. These prompted the design of the core of the system to facilitate mesenchymal stem cell growth in a homogenous lattice matrix comprised of biocompatible polymers and materials which would not lead to impurities in the cell harvest.

1.3 SIGNIFICANCE OF THE RESEARCH

Stem cell culture is inherently more difficult to scale than conventional cell cultures. hMSCs are very shear sensitive, which leads to low and impure cell harvests. Here we show a system that performs better than conventional spinner flasks and tissue culture flasks. The research was performed as a means of high density, pure stem cell culture.

The footprint is less than that of a standard T75 tissue culture flask, but produces double the yield with better purity.

1.4 Overview of the Study

The background focuses on hMSC bioproduction to provide understanding of existing systems, both in their advances and their shortcomings. The following chapters outline the testing of various polymer types for cell culture and their basic surface chemistries, oxygen tension and its effect on stem cell proliferation and stemness, culture in a dynamic 3D culture system, and computational characterization of the system. The chapters are written in the form of individual manuscripts that together provide a complete overview of the tested system in regards to hMSC bioproduction.

2 Literature Review

2.1 Mesenchymal Stem Cells

Adult Mesenchymal Stem Cells (MSCs) are an anchorage dependent stem cell harvested from adult tissues. Typical sources include the marrow of the iliac crest, the head of the femur, adipose tissue, peripheral blood, Warton jelly, and umbilical cord blood.[14] MSCs were first described by Dr. Friedenstien, who was able to show the existence of a clonal subpopulation of cells in the spleen and blood producing organs of mice.[15] Their harvest amounts vary drastically by their source, with up to 500 times higher yields from fat than from bone.[14,16,17] They are described as fusiform, fibroblast-like cells, and often appear spindle-like under phase contrast.[18] They are characterized via surface marker expression,

gene expression of stemness genes, and the cells that they can differentiate into. Research has shown that hMSCs are positive for the cell surface markers CD166, CD105, CD90 CD73, CD44, CD29, and STRO1 and negative for CD45 CD34, CD19, and CD14.[18–21] Some variation in expression of these markers exist, but this may be explained by variations in the culture methods as well as the age of the cell.[18] Due to variation, the International Society for Cell Therapies (ISCT) has released documentation stating that the minimal criteria to characterize hMSCs for therapies is: greater than 95% expression of CD105, CD73, and CD90, and lack CD45, CD34, CD14 or CD11b, CD79α or CD19, and HLA class II.[22] They must also adhere to plastic, and maintain their osteocyte, adipocyte, and chondrocyte differentiation ability. Though not an ISCT criteria, it has been shown that they express the stemness genes SOX2 and NANOG.[23] They can differentiate into cells of the mesoderm, including adipocytes, osteocytes, chondrocytes, myocytes, cardiomyocytes, and tenocytes (Figure 2-1).[24] There has also been some investigation into the still controversial transdifferentiation of hMSCs, resulting in pancreatic islet cells, corneal epithelium, and nervous tissue.[25–27] This type of change results in the cells entering a dedifferentiated state similar to IPSCs, then differentiating down another germ lineage.

Differentiation is normally controlled through a mix of cytokines, cell mediated cues, and external forces. Cytokines and soluble factors can be added to basal media and change gene expression through cellular pathways.[28–30] External forces such as shear and topologies can also lead to differentiation. Osteocyte differentiation can occur with exposure to as little as 10 dynes/cm^{2,} and higher rates can lead to apoptosis.[31] Culture methods emphasizing strong binding to ECM or substrates show less stemness, while cell

culture comprised of mainly cell-cell junctions promoted stemness.[23] Nanotopographies have also been implicated in stem cell differentiation, leading to osteocyte production.[32,33] Substrate stiffness also plays a large role in hMSC fate; softer substrates tend to produce chondrocytes and adipocytes, while stiffer materials favor osteocyte differentiation.[34–36] The explanation for this is that the culturing substrate matches the final environment of the cell, which leads it to differentiate into the cell best suited for that environment.

hMSCs tend to reach senescence after 24 to 40 population doublings, depending on the age of the donor. The younger the donor, the more doublings were possible before the hMSCs showed signs of senecensce.[18] This is caused by several factors including damages to DNA, changes in mitochondria, abnormal protein accumulation, and the lack of telomerase to maintain proper telomere length.[37–39]

Their ability to differentiate into such a variety of functional cell types, combined with proven benefit in the treatment of inflammatory diseases, along with their ease of culturing compared to other types of stem cells has made them crucial candidates in regenerative medicine.[40,41] This is because hMSCs are immunotolerant and immunomodulatory cells.[42,43] It has been shown that this is partially due to a paracrine signal molecule secreted by hMSCs.[44,45] One example of hMSCs' role in the immune response was shown when hMSC conditioned media inhibited t-cell activation. This immunomodulation has become a unique characteristic used in identifying these cells.[46,47] Part of this ability may come from secretory vesicles known as exosomes, which are discussed later in the text. A brief list of diseases where hMSCs are currently being

investigated includes cardiovascular diseases, diabetes, various immunomodulatory diseases, and bone disorders.

2.1.1 Myocardial Infarction

More commonly known as heart attack, Myocardial Infraction (MI) is caused by ischemia to the heart. This results in damage to cardiomyocytes, decreased heart function, and possibly death. There are approximately 790,000 new MI cases every year in the United States,[48] and costs approximately $108 billion each year.[49] Though hMSCs have the ability to differentiate directly into cardiomyocytes and replace lost function, the exact mechanism of heart repair is still unclear. Resurgence in cardiac function may also come from angiogenesis, which results in the growth of new vessels which reestablish blood flow to infarcted areas of the heart. [50–52] It has also been found that hMSCs have a cytoprotectant effect on cardiomyocytes.[53] In mice, autologous mesenchymal stem cell transplantation into the heart results in a 40% increase in capillary density, as well as increased ventricular contractility.[51] A human clinical study investigating the heart function restoration through hMSC implantation found that left ventricular ejection fraction of the heart increased by 3.84%.[54] Incidence of re-hospitalization for heart failure also dropped in hMSC treated patients.[54]

Research has also shown that the factors released from hMSCs were able protect infarcted regions from cell necrosis and prevent scar tissue formation in rats.[55] This was achieved by transplantation of a cell-laden hydrogel onto the infarcted region. Pore sizes in the gel construct used to anchor cells to the heart were 11nm, small enough to allow signaling molecules, but would stop larger extracellular vesicles or cells themselves from

escaping the hydrogel. $2x10^6$ cells per mL were needed to achieve similar levels of ejection fraction and stroke volume as control groups.

2.1.2 **Diabetes**

Diabetes is a disease in which the body cannot regulate glucose levels in the blood. This can cause complications such as neuropathy and damage to microvasculature.[56,57] Researchers have shown that hMSCs can be used to treat neuropathy and vascular damages resulting from diabetes mellitus.[57] hMSCs have been found to play an important role in in tissue repair to lower blood glucose levels.[58,59] They are also able to treat diabetic neuropathy through a paracrine effect.[56,57,60] Vascular Endothelial Growth Factor is one the many cytokines secreted by hMSCs and is the main chemokine of angiogenesis. When combined with the immunosuppressive properties of hMSCs, this can restore lost microvasculature.[56,57,61] Adult hMSCs also have been implicated in neuroprotection. Implantation of hMSCs into animal models of Parkinson's disease showed a decrease in dopaminergic cell and Perkinje cell loss, showing their neuroprotective nature.[62]

Research has also shown how hMSCs repair both beta islet cells and renal glomeruli in mice models of diabetes. hMSCs lowered blood glucose and increased circulating levels of insulin.[59] The stem cells were introduced through intracardial infusion, but human pancreatic islets and beta cells were found in the pancreas. Human cells were also found in the kidneys, making up parts of the glomerulus.

2.1.3 **Skeletal Diseases**

Osteoarthritis affects 27 million people in the United States and is the most common joint disorder in the country.[63] This disorder causes articular cartilage damage, resulting in bone on bone movement, inflammation of joints, and pain. It is the leading cause of disability in the elderly, and it is estimated that 10-15% of adults over 60 years of age will develop osteoarthritis.[64] Current therapies do not repair the damage causing the pain, and merely treat the symptoms rather than the cause. In a human trial, 10^8 hMSCs were injected into the articular cartilage of patients. The patients showed significant improvement in pain and function with no adverse events.[65] Cartilage defects were also reduced through regeneration of hyaline-like articular cartilage. The hMSC paracrine effect has also shown importance in treatment of osteoarthritis, decreasing inflammatory injury and decreasing chondrocyte migration.[66,67] Because of this, many researchers are currently investigating the secretome of hMSCs for treatment of osteoarthritis.[66,68,69]

Osteoporosis is the progressive loss of bone mass over time. It is generally age related and affects millions of individuals worldwide.[70] Bone loss can be so significant that patients can become bed ridden from sever fractures. Normally osteoblast cells rebuild the bone in balance with osteoclasts resorbing old bone. In osteoporosis, the balance is skewed where breakdown outweighs deposition of new bone. Current therapies mainly prevent further bone loss. Research has shown that hMSCs are a possible means of treating this disease and rebuilding lost bone.[70] This is because of their ability to differentiate into osteoblasts and directly increase bone mass.

One shared problem across these various diseases is that they all theoretically require massive amounts of cells. For MI, it is estimated that up to one billion cells are needed to

substantially reverse damage to the heart.[54,71,72] For diabetes and osteoporosis, it is estimated that hundreds of millions of cells are needed for successful therapies.[65] Harvest alone cannot yield the necessary numbers to treat millions of patients, thus culture is necessary for commercialized allogenic hMSC therapies to become reality.

2.2 hMSC Culture

MSCs are generally regarded as easier to culture than embryonic stem cells and are also of less ethical concern. Unlike ESCs and IPSCs, they do not undergo teratogenesis, which eases regulatory concerns. These cells are described to have a fibrotic morphology, and do not require co-culture with support cells like hESCs have historically needed.[73] Unlike their pluripotent counterparts, they can also be passaged as single cells in which passaging must be done with accutase or collagenase to leave cell clusters.[73,74] This makes subculturing much easier because it is possible to attain distribution of single cells. This also has the added effect of increasing homogeneity in cell culture.

Media used for stem cells is generally costly, and hMSCs are no exception. One reason is because serum and cytokines are needed in the media to maintain stemness. Typically, the two main cytokines for hMSC culture are recombinant human insulin like growth factor one (IGF-1) and recombinant human beta fibroblast growth factor (b-FGF). Fetal Bovine Serum (FBS) is also added to the media. FBS generally ranges from 5% to 10% v/v of media composition, usually in Dulbecco's Minimum Essential Media (DMEM) or alpha MEM.[75] It is supplemented with amino acids and can have antibiotics added to combat microbial contamination. Due to the high cost of media, it is difficult to run such systems in perfusion, especially in academia. Because serum is used, the media is

chemically undefined. For regulatory purposes, there is active research into alternatives for serum. Xeno-free alternatives like human platelet lysate have been used, and though they are generally recognized as safer than serum, there is still a possibility of transmitting human diseases and infectious agents. Human platelet lysate is also expensive, as it must be harvested, stringently tested, and processed before use. Chemically defined media is commercially available as well, which forgoes all serum and its harvested likeness. There is much variation of biomarker characterization, cell proliferation, and subsequent stemness of the cells harvested between all these various types of media,[75,76] all of which are qualities used by the ISCT as means of quality control.

Traditionally hMSCs are cultured on t-flasks. This static 2D culture can produce relatively pure stem cells in a reasonable time. In the lab we found a consistent cell yield of $1.2x10^6$ to $1.4x10^6$ BM-hMSCs from one T75 flask, equating to around 60,000 to 70,000 cells/mL. To scale this method and increase cell yields to meet the quantities needed for successful therapies, researchers have used roller bottles and Multiplate stacks. Roller bottles increase surface area by allowing cells to grow on the walls of the cylinder. The bottles are placed on their sides, filled with just enough media to cover the bottom side, and gently rolled via a rack system. As the bottle turns the cells are systematically washed with media. This style of culture has fallen out of favor for the simpler and larger SA:V ratio of Multiplate flasks. Multiplate stacks like Nunc Cell Factory (Thermo Fisher) and the Corning Cell Stack (Corning) combine many flat culture areas into one flask. They contain between 1 to 40 stacks, with newer system containing up to 120 layers.[77] Both roller bottles and Multiplate systems ease operator burden, but

still have their limitations; it is difficult to monitor and control the cells, and hard to ensure even distribution of the cells across the culture surface. Improper seeding and lack of monitoring can lead to poor yields and heterogeneity in harvest. As such, more controllable bioreactors have been a hot topic of research regarding stem cell culture.

The goal of scale out systems using such bioreactors is to produce high quality stem cells in large enough quantities for therapeutic needs. It is estimated that between 10^6 and 10^9 stem cells per kilogram weight per patient are needed to treat diseases such as diabetes and myocardial infarction.[72,78–81] This large number is due the combination of attrition of stem cells through migration, unwanted differentiation, and apoptosis. The only way to reach the large numbers needed for therapeutic dosages is through cell culture. Furthermore, more than one dose may be necessary to combat this attrition and fully treat the disease. When required the dosage is multiplied across the thousands of patients included in a phase III clinical trial, it becomes clear why the vast majority of allogenic trials currently listed are in Phase I and II. Bioreactors have been investigated for higher density stem cell culture to address this.

2.3 BIOREACTOR CULTURING METHODS

Conventional bioreactors for suspension-adapted cell culture are inherently unfavorable for stem cell culture. They are traditionally impeller driven, resulting in higher than desired shear for the delicate stem cells. They also provide no surface for the cells to adhere and grow. This means that more customized solutions for old reactor styles, or completely new reactors must be made to match the requirements of stem cells. When designing such systems for cell growth, the main points of consideration are: the surface

area available to the cells, the hydrodynamic forces the cells experience in such a system, nutrient gradients in the system that may result from non-impeller driven mixing, and ways of detecting and sampling the cells. With these factors in mind, two main methods have evolved for stem cell culture; suspension cultures using microcarriers, or immobilized/fixed bed reactors. From a research landscape study, it was found that the majority of studies (57%) used bone marrow derived hMSCs (BM-hMSCs).[75] It also found that microcarriers were the favored method of expansion (52.2%). A comparison of fold increase vs hMSC source also showed that adipose derived hMSCs (AD-hMSCs) generally achieved higher average expansion factors compared to other sources. One point worth mentioning is that a group of high performing multiplate static cultures reported in this paper came from the same lab which was seeding at 30-40cells/cm^2 (compared to the recommended 5000cells/cm$^{2)}$.[75] Evidence has shown that lower seed densities increase the rate of population doubling, which increases the expansion factor.[82] Low density seeding also has the benefit of maintaining stemness, as researchers found that cell-cell contact at high confluency decreased CD105 and had a lower percentage of senescent cells.[82] Some other attributes that a reactor should have are: scalability, ease of use, ease of harvest, automation, and cost effectiveness. A comparison table of culture methods can be seen in Table 2-2.

2.3.1 **Microcarrier Based**

The most common route has been to use microcarriers in traditional bioreactors for suspension cell types. These are polymer spheres ranging from 100 to 300 microns in diameter, and provide the stem cells a surface on which to grow while in a suspension system. Using these carriers allow high density cultures because of the large surface area

to volume ratio, with minimal design changes needed on traditional stirred tank bioreactors. Cells are adherent on free-floating structures, so direct sampling of cells is easily performed by a media draw. Microcarriers can vary in composition from non-degradable plastics, to dextran, to enzymatically digestible polymers.[9] Some macroporous carriers allow the stem cells to grow inside of the microcarrier itself, protecting it from strong hydrodynamic forces.[83] These carriers can be used in conjunction with various bioreactor culture systems, the most common being stirred tank reactors and wave bags.

2.3.1.1 Stirred Tank reactors and Spinner Flasks

Traditionally used with CHO and considered the workhorse of bioprocessing, spinner flasks and stirred tank reactors are commonly used for seed train and cell expansion. They consist of a centrally located, magnetically or mechanically driven impeller. The impeller provides even distribution of gas and nutrients to cells. Oxygen transfer can be performed using a submerged sparger below the impeller, or simply though the gas-liquid interface at less than 1 liter.[77] Using such a system provides more control over cell culture conditions than static flasks, as agitation provides a more homogenous environment and inline process parameters can be used to monitor metabolites, pH, temperature, and Dissolved Oxygen (DO).[9,77,84,85] These systems can then be run in fed batch or perfusion to adjust parameters accordingly and maintain an optimal environment for cell growth. Cell expansion varies by harvest source of the mesenchymal stem cells, but falls roughly between $0.2x10^6$ and $2x10^6$ cells/mL.[46,84,86] By using large scale single use STBR researchers were able to achieve 43 and 58 fold increase in adipose derived hMSCs.[24,46] However, the impeller used in this system imparts high shear. hMSCs are very shear

sensitive, and higher than normal values of shear can lead to cell death and differentiation.

2.3.1.2 Wave bags

This system utilizes a flexible bag placed on a rocking table. Bags are loaded with media to the desired volume, and gas is overlaid into the head space to inflate the bag the rest of the way. Gas exchange and media mixing is controlled by rocking the table. Speed and angle are what control the rates of mixing. The resulting back and forth movement results in a wave that moves through the media, mixing the media and suspending MSC laden microcarriers. This system can also have the same inline process monitoring capacity as stirred tank systems. Researchers using this system have reported between $0.9x10^6$ and $1.9x10^6$ cells/mL and an overall 5 to 15 fold increase in adipose and placental derived hMSCs after culture.[87,88] There is some concern that the energy required to keep microcarriers in suspension may be high enough to induce a breaking wave, thus resulting in very high shear.

2.3.1.3 Paddle Driven/Vertical-Wheel bioreactors

These singe use systems are driven by a centrally located paddle wheel. The bottom of the reactor is U-shaped with tight clearance (the wheel is approximately 85% the diameter of the singe use bag insert) between the vertical wheel and the bottom. This provides a strong sweeping force to suspend the cells with low power input.[89] The wheel is mounted horizontally to the systems, such that the direction of motion drives fluid up, while two axial paddles provide sideways liquid handling, generating a folding action.[90] The paddles of the wheel are large enough that very slow rotation provides sufficient

lifting force to mix the microcarriers while inferring relatively low shear, creating a favorable culture environment for microcarrier bound BM-hMSCs.[91]

2.3.2 Non-Microcarrier based systems

Unlike suspended microcarriers, there are other commercially available systems where the culture substrate is stationary. Media is flowed around the substrate or over the cell culture surface. As a whole, these systems offer the same advantages as the microcarrier based systems mentioned previously (real-time measuring of process parameters), but since the culture area is not in free suspension, direct cell sampling and visualization is much harder. However, these systems have the benefit of incredibly high SA:V ratios and decreased purification at cell harvest because of the geometry and immobility of the culture substrate. As with microcarriers, enzymes are typically used to detach the cells from their substrate and from other cells.

2.3.2.1 Packed bed

Another avenue of stem cell bioproduction includes immobilized/fixed bed reactor-based systems. The culture material can either be packed or held in place (fixed bed) while media is perfused through the system, or the material can be floating (fluidized bed) in a chamber while the media is perfused through it. These systems generally use randomized fibers to provide a large surface area to volume ratio for stem cell culture. Cells grow adherently on the surface of fibers while media is perfused through the porous fiber matrix. Researchers have reported fold expansions of 9.2 to 38.7 in such systems using bone marrow and umbilical cord hMSCs.[24,92] The iCELLis by Pall is a commercially sold fixed bed system which uses PET as its culture substrate.

2.3.2.2 Hollow fiber

Normally used in downstream filtration, cells can grow in either the lumen or around the outside of such fibers, and media can be passed through the fibers. An advantage of this system is can mimic laminar flow through vessel very well. However, as mixing is not handled in a turbulent manner, media gradients can form in such fiber-based systems. And since the fibers are locked in place, direct sampling of cells is much more difficult than with microcarrier based systems. Papers report successful hMSC expansion in GMP compliant quantum cell hollow fiber system.[93–95] and expansion factors of 6.7 to 31.4 were reached using BM-hMSCs.[93,94,96,97]

2.3.2.3 Parallel plate

Lastly, a derivative of Multiplate systems is the parallel plate bioreactor. This system is a stack of plastic plates much like static multistack/multiplate flasks already mentioned. The difference here is that media is flowed from the center radially outward on multiple plates stacked in one system. Much like hollow fiber-based reactors, nutrient gradients can form, and direct sampling of the cells is near impossible in such a system. However, both fiber based and microcarrier based systems boast more surface area to volume than these systems. One study reported an expansion factor of 3.9 using periosteum derived hMSCs.[98]

2.4 POLYMERS USED IN CULTURE

Polymer composition and stiffness are integral in stem cell culture. Stiffer materials have been shown to increase osteogenesis in hMSCs.[36] Cells cultured on polymers with similar elastic modulus to cancellous bone have been shown to readily differentiate into

osteocytes and start calcium deposition. Conversely, hMSCs cultured on more elastic substrates will differentiate into chondrocytes.[34] The hydrophilicity also has a direct impact on cell stemness and proliferation. Hydrophilic surfaces decrease cell binding, which in turn increases cell stemness.[23] The reverse is also true, where the greater the cell adhesion to the substrate due to hydrophilic surfaces decreases differentiation potential.

Polyethylene Terephthalate (PET) and Polyethylene Terephthalate Glycol (PETG) are both thermoplastic polymer resins from the polyester family. PET and its blends have been used as a cell culture substrate. It can be electrospun in nanofibers or 3D printed into shapes.[99] PET fibers are currently used as the cell scaffold in the iCELLis reactor. Researchers discovered that a PET 3D fiber matrix used in the iCELLis reactor both sustained hMSC culture for 21 days, and increased both CD105 and CD29 markers.[100]

Polystyrene (PS) is the plastic of choice for cell culture. Tissue culture flasks are made of PS and treated with plasma or exposed to radiation to expose hydroxyl groups on the surface.[101] These functional groups promote cell attachment and proliferation. This process exposes hydroxyl groups, which can be used to both coat the dishes with proteins, and directly promote cell adhesion.

Polycaprolactone (PCL) is a synthetic polymer that has gained interested in cell culture due to its biocompatibility and biochemical properties.[102] It has been electrospun into nanofibers for the culture of hMSCs and their differentiation into osteocytes.[103]

Poly Lactic Acid (PLA) is easily 3D printed and generally recognized as safe by the FDA. It has a Young's modulus similar to bone, matching the niche of bone derived hMSCs. Its hydrolysis product is lactic acid, a compound normally found produced by

metabolism. Previous research has shown that plasma treatment of nonwoven PLA scaffolds promotes stem cell adhesion and growth.[104,105]

Hydrogels are an alternative to rigid polymers and plastics. They have been successfully used for both stem cell culture as well as a means of directing stem cell fate.[106] Some natural polymers used include alginate, Hyaluronic acid, Chitosan, Collagen, and gelatin. Artificial hydrogels have also been used for this purpose and result in a Xeno-free culture surface. These include polyvinyl alcohol, polyethylene glycol, and polyacrylamide. Special polyacrylamide gels are thermoresponsive, allowing different characteristics by varying temperature. Poly(N-isopropyl acrylamide) (pNIPAAM) has been used to culture stem cells and allows for non-enzymatic cell lifting.[107–109]

These polymers have been blended, electrospun, and coated to modulate biocompatibility, increase binding and proliferation, and allow for resorption into the body. The latter is done with the intent of stopping stem cells from migrating away from the surgical site, thus increasing the effectiveness of the stem cell therapy.

2.4.1 **Coatings**

Most polymers used for cell culture are blended with proteins or coated with proteins after manufacturing to promote cell adhesion and growth. The most common coatings are animal derived, and the choice is largely dictated by the cell that is being cultured. However, the most ubiquitous is gelatin, a denatured form of collagen.

Usually provided as a powder, porcine gelatin is dissolved into deionized water to make a 0.1% solution. This can then be plated onto cell culture surfaces to deposit denatured

collagen onto the surface.[110] This provides a more favorable surface for cells to adhere to by providing RGD residues for integrin mediated binding.[111]

Collagen anchorage is dependent on cell recognition of GxOGER residues.[110] Collagen I, II, and II are rich in this peptide sequence.[112] Researchers have found that there is more cross-linking between collagen fibers in 3D culture, decreasing integrin mediated binding of cells.[110] They deduced that cell adhesion was mainly due to entrapment of cells within the cross-linked ECM.

Laminin is normally found in the basement membrane separating epithelium from the underlying tissue.[113] In studies conducted with cancer cell lines it was found that laminin promoted cell motility.[114] This may be useful as a cell coating where passaging is performed by addition of new surface area for the cells to migrate to and culture out, eliminating the need for enzymatic digestion based passaging.

Cell adhesion to fibronectin is integrin mediated via RGDS recognition sites.[115] Fibronectin has been shown to promote osteocyte differentiation in hMSCs.[116] It is normally found circulating in blood plasma and plays a large role in wound healing.[117]

Vitronectin is a glycoprotein found predominately in the serum and in bone.[118] It binds integrin to promote cell adhesion and migration.[119] A recombinant form of fibronectin is commercially available, easing regulatory concerns.

2.5 ADDITIONAL PARAMETERS IN STEM CELL PROLIFERATION AND PURITY

2.5.1 Gas control

Research has shown that another method of controlling hMSC proliferation and stemness is through control of gasses. Physiological oxygen percent in the bone marrow is between 1% and 5%.[120,121] By matching oxygen tension normally found in their niche, researchers have seen significant increases over conventional culture techniques.[122,123] Biomarker profile does not suffer, and cells can still readily differentiate into normal cell types.[124,125] Companies like Xcell Biosciences have integrated hypoxic culturing options into their Avatar incubators, as well as hyperbaric conditions, and have shown that this combination increases marker expression and proliferation with stem cells.[126] This effect is through hypoxia inducible factors (HIFs) and their downstream effects.[123,127] HIF has also been shown to increase stem cell survival and proliferation.[128] Genetically modified stromal cells showed increased engraftment in ischemic heart tissue.[129]

2.6 OTHER CONSIDERATIONS

2.6.1 Downstream processes

One commonly overlooked hurdle in stem cell therapy is the downstream purification of these cells.[75] The level of purification needed is heavily reliant on the quality of cells produced, as well as the materials used in the culture of these cells. As such, some focus has been placed on microcarrier composition, resulting in digestible polymers and simple filtration devices to remove microcarriers.[9,130–132] This removes the otherwise required

filtration step to ensure complete removal of microcarriers from cell harvest. The same applies to porous medium, where thermoresponsive coatings aim to eliminate enzymatic cell lifting steps altogether.[109,133–135] Biocompatible polymers have also shown some promise in reactor culture, cutting the concern of leachables considerably, while also possibly eliminating cell removal altogether.[108] Implantation of a cell laden scaffold make of a biocompatible or biodegradable polymer would also help stop stem cell migration to other parts of the body, theoretically increasing efficacy of the therapy and would also eliminate the need for cell removal from the culture substrate.[103,104,131,136] Such processes would drastically decrease downstream requirements, though buffer exchange may still be necessary.

2.6.2 **Cryopreservation**

An allogenic process for hMSC production would need to be cryopreserved for large scale distribution. The cells would be shipped to centers where administration would occur, as it is not feasible to ship and store non-cryopreserved cells. Researchers have shown that high viability cell recovery under serum free culture and freezing conditions is possible.[137] It is worth noting that this process still uses conventional centrifugation steps to both suspend cells in cryopreservation media before freezing, and to remove cryopreservatives. These techniques do not scale well, and concentration and buffer exchange steps may be better scaled using Tangential Flow filtration.

This downstream step has been tested for hMSC concentration and media exchange with good results. Researchers found that though the stem cells are easily damaged by shear in such a system, it can still be used to clarify BM-hMSCs from microcarriers and concentrate them for further processing.[138,139]

2.6.3 **Secretome**

Exosomes are extracellular vesicles secreted by hMSCs. They are between 30nm and 150nm in diameter and contain cytokines, various types of RNA, and DNA.[140–142] Exosomes originate from early endosomes that are modified by the fusion of other intraluminal vesicles.[143] They are released after fusion with the plasma membrane. Exosomes have been shown to help heal wounds and decrease inflammation.[144] MicroRNAs (miRNAs) are one part of these vesicles, and it is thought that they are a main contributor of free miRNA in circulation.[145,146] miRNAs have been shown to play a role in disease and have been investigated as therapies for inflammatory diseases, ocular diseases, bone and cartilage disorders, and even some forms of cancer. [66,69,142,144,145]

Because exosome-based therapies do not use the whole cell itself, the road to market approval may be easier and faster. The exosomes can be characterized and do not pose the same risks as stem cells such as off target differentiation, rare occurrence of malignancies, and infection.[147,148] A perfusion reactor would be a viable option to produce exosomes, as TFF would stop any cell contamination into the product while constant media exchange would help guard against product degradation.

2.6.4 **Lab on a chip**

Drug discovery and testing are currently the costliest steps in producing drugs. Therapeutic candidates are screened for reactivity in vitro, and when positive targets are found they are progressed to animal studies to test safety and efficacy. However, animal testing and its overhead is very costly, and not always predictive of safety in humans.[149] One theoretical method to test drug safety on human tissue in a repeatable manner is to create a tissue or organ sample on a chip.[150,151] The goal is not to create the entire organ

or structure, but merely a functional subunit of the tissue.[150] This technology stems from the ability of a stem cell to give rise to functional cell types which make up specific tissues. A stem cell can be cultured out and differentiated, resulting in a functional tissue. The resulting tissue can be tested for drug interaction more holistically than could otherwise be done with a specific cell type. A therapeutic agent can be tested for toxicity and effectiveness in closer relation to what would happen in the body. Moreover, stem cells from diseased patients can be used for disease modeling.[152] This has mainly been advocated with the use of IPSCs, but may also prove useful in MSCs for testing drug targets for diseases of tissues derived from the mesoderm.

2.7 CONCLUSION

hMSCs have much potential as a marketable autologous and allogenic stem cell therapy. Over the past few decades scientists have made large leaps in understanding these extraordinary cells. One general agreement is that large scale culture is needed for a successful allogenic therapy to be realized. This is because of the theoretically large cell numbers needed for a therapeutic dose, due to in part to the sensitive nature of stem cells. There is no consensus on approach, as each system has its own advantages and disadvantages. Microcarrier based culture utilizes more characterized systems, making translation into bioreactors simpler. However, the impeller used in stirred tank systems can result in high shear. Fixed bed reactors and parallel plate reactors remove the need for an impeller but make it difficult to sample the system and characterize cell morphology. One commonality in these systems is the need for polymer selection.

To increase binding and stemness of the cells cultured in such systems material scientists have investigated polymers and polymer blends. hMSCs respond to mechanical cues,

allowing scientist to drive purity and differentiation without the need of cytokines. Polymer science has also been used to create a more physiologically similar environment to the normal cell niche. Microcarriers and fiber based systems have both benefitted from this, as seen by the use of biocompatible materials, special topologies, and coatings of the materials.

Hypoxia has been shown in increase both stemness and cell proliferation in hMSC cultures. Decreasing oxygen percentage mimics the natural niche in bone, much like the mentality of altering polymer stiffness. This has worked as an effective and simple means of increase stem cell yields while maintaining cell purity.

Cells grown in these methods have other uses than being implanted as a therapy. Secreted proteins and vesicles can be harvested from such systems and used themselves as a possible therapies. Healthy and diseased cells can be cultured out in a bioprocess and differentiated into tissues. The resulting lab grown tissue can be used as a test for drug interaction and efficacy. Both of these processes may have a more defined route to approval and usage then whole cell therapies.

1. Fredhutch.org. History of Transplantation. https://www.fredhutch.org/en/treatment/long-term-follow-up/FAQs/transplantation.html. Accessed March 12, 2019.

2. Busengdal H, Rentzsch F. Unipotent progenitors contribute to the generation of sensory cell types in the nervous system of the cnidarian Nematostella vectensis. *Dev Biol*. 2017;431(1):59-68. doi:10.1016/j.ydbio.2017.08.021.

3. Thomson JA, Itskovitz-Eldor J, Shapiro SS, et al. Embryonic stem cell lines derived from human blastocysts. *Science*. 1998;282(5391):1145-1147. doi:10.1126/science.282.5391.1145.

4. Murugan V. Embryonic stem cell research: a decade of debate from Bush to Obama. *Yale J Biol Med*. 2009;82(3):101-103. http://www.ncbi.nlm.nih.gov/pubmed/19774120. Accessed March 12, 2019.

5. Daley GQ. Missed Opportunities in Embryonic Stem-Cell Research. *N Engl J Med*. 2004;351(7):627-628. doi:10.1056/NEJMp048200.

6. Takahashi K, Yamanaka S. Induction of Pluripotent Stem Cells from Mouse Embryonic and Adult Fibroblast Cultures by Defined Factors. doi:10.1016/j.cell.2006.07.024.

7. Yu J, Vodyanik MA, Smuga-Otto K, et al. *Induced Pluripotent Stem Cell Lines Derived from Human Somatic Cells*. http://science.sciencemag.org/. Accessed March 12, 2019.

8. National Institute of Health. NIH Stem Cell Information. Stem Cell Information . stemcells.nih.gov/info/basics/4.htm. Published 2016. Accessed March 12, 2019.

9. Jossen V, van den Bos C, Eibl R, Eibl D. Manufacturing human mesenchymal stem cells at clinical scale: process and regulatory challenges. *Appl Microbiol Biotechnol*. 2018;102(9):3981-3994. doi:10.1007/s00253-018-8912-x.

10. Stem Cell Therapy Market Worth USD 60.94 Billion by 2022 - Scalar Market Research. http://www.aboutpharma.com/blog/2016/11/01/stem-cell-therapy-market-worth-usd-60-94-billion-by-2022-scalar-market-research/. Accessed March 26, 2017.

11. Harvesting stem cells - Canadian Cancer Society. http://www.cancer.ca/en/cancer-information/diagnosis-and-treatment/stem-cell-transplant/harvesting-stem-cells/?region=bc. Accessed March 26, 2017.

12. Tower J. Stress and stem cells. 2012. doi:10.1002/wdev.56.

13. Vining KH, Mooney DJ. Mechanical forces direct stem cell behaviour in development and regeneration. doi:10.1038/nrm.2017.108.

14. Hass R, Kasper C, Böhm S, Jacobs R. Different populations and sources of human mesenchymal stem cells (MSC): A comparison of adult and neonatal tissue-derived MSC. *Cell Commun Signal*. 2011;9(1):12. doi:10.1186/1478-811X-9-12.

15. Friedenstein AJ, Gorskaja JF, Kulagina NN. Fibroblast precursors in normal and irradiated mouse hematopoietic organs. *Exp Hematol*. 1976;4(5):267-274. http://www.ncbi.nlm.nih.gov/pubmed/976387. Accessed March 15, 2019.

16. Fraser JK, Wulur I, Alfonso Z, Hedrick MH. Fat tissue: an underappreciated source of stem cells for biotechnology. *Trends Biotechnol*. 2006;24(4):150-154. doi:10.1016/j.tibtech.2006.01.010.

17. Kitagawa Y, Korobi M, Toriyama K, Kamei Y, Torii S. History of Discovery of Human Adipose-Derived Stem Cells and Their Clinical Application. January 2006. https://www.scienceopen.com/document?vid=da6cfed7-2179-4f7f-b98f-4b6b4f773dd2. Accessed March 13, 2019.

18. Abdallah BM, Kassem M. Human mesenchymal stem cells: from basic biology to clinical applications. *Gene Ther*. 2008;15(2):109-116. doi:10.1038/sj.gt.3303067.

19. Rojewski MT, Weber BM, Schrezenmeier H. Phenotypic Characterization of Mesenchymal Stem Cells from Various Tissues. *Transfus Med Hemother*. 2008;35(3):168-184. doi:10.1159/000129013.

20. Lv F-J, Tuan RS, Cheung KMC, Leung VYL. Concise Review: The Surface Markers and Identity of Human Mesenchymal Stem Cells. *Stem Cells*. 2014;32(6):1408-1419. doi:10.1002/stem.1681.

21. Lin C-S, Xin Z-C, Dai J, Lue TF. *Commonly Used Mesenchymal Stem Cell Markers and Tracking Labels: Limitations and Challenges*. https://www.ncbi.nlm.nih.gov/pmc/articles/PMC3839663/pdf/nihms-530000.pdf. Accessed March 13, 2019.

22. Dominici M, Le Blanc K, Mueller I, et al. Minimal criteria for defining multipotent mesenchymal stromal cells. The International Society for Cellular Therapy position statement. doi:10.1080/14653240600855905.

23. Balikov DA, Crowder SW, Boire TC, et al. Tunable Surface Repellency Maintains Stemness and Redox Capacity of Human Mesenchymal Stem Cells. *ACS Appl Mater Interfaces*. 2017;9(27):22994-23006. doi:10.1021/acsami.7b06103.

24. Schirmaier C, Jossen V, Kaiser SC, et al. Scale-up of adipose tissue-derived mesenchymal stem cell production in stirred single-use bioreactors under low-serum conditions. *Eng Life Sci*. 2014;14(3):292-303. doi:10.1002/elsc.201300134.

25. Pokrywczynska M, Lewandowska MA, Krzyzanowska S, et al. Transdifferentiation of Bone Marrow Mesenchymal Stem Cells into the Islet-Like Cells: the Role of Extracellular Matrix Proteins. *Arch Immunol Ther Exp (Warsz)*. 2015;63(5):377-384. doi:10.1007/s00005-015-0340-3.

26. Ullah M, Stich S, Notter M, Eucker J, Sittinger M, Ringe J. Transdifferentiation of mesenchymal stem cells-derived adipogenic-differentiated cells into osteogenic- or chondrogenic-differentiated cells proceeds via dedifferentiation and have a correlation with cell cycle arresting and driving genes. *Differentiation*. 2013;85(3):78-90. doi:10.1016/j.diff.2013.02.001.

27. Jiang T-S, Cai L, Ji W-Y, et al. Reconstruction of the corneal epithelium with induced marrow mesenchymal stem cells in rats. *Mol Vis*. 2010;16:1304-1316. http://www.ncbi.nlm.nih.gov/pubmed/20664793. Accessed March 13, 2019.

28. Beederman M, Lamplot JD, Nan G, et al. BMP signaling in mesenchymal stem cell differentiation and bone formation. *J Biomed Sci Eng*. 2013;6(8A):32-52. doi:10.4236/jbise.2013.68A1004.

29. Kurpinski K, Lam H, Chu J, et al. Transforming Growth Factor-β and Notch Signaling Mediate Stem Cell Differentiation into Smooth Muscle Cells. *Stem Cells*. 2010;28(4):734-742. doi:10.1002/stem.319.

30. Almalki SG, Agrawal DK. Key transcription factors in the differentiation of mesenchymal stem cells. *Differentiation*. 2016;92(1-2):41-51. doi:10.1016/j.diff.2016.02.005.

31. Yourek G, Mccormick SM, Mao JJ, Reilly GC. Shear stress induces osteogenic differentiation of human mesenchymal stem cells. *Regen Med*. 2010;5(5):713-724. doi:10.2217/rme.10.60.

32. Kulangara K, Yang Y, Yang J, Leong KW. Nanotopography as Modulator of Human Mesenchymal Stem Cell Function. 2012. doi:10.1016/j.biomaterials.2012.03.053.

33. Qian W, Gong L, Cui X, et al. Nanotopographic Regulation of Human Mesenchymal Stem Cell Osteogenesis. *ACS Appl Mater Interfaces*. 2017;9(48):41794-41806. doi:10.1021/acsami.7b16314.

34. Singh N, Rahatekar SS, Koziol KKK, et al. Directing Chondrogenesis of Stem Cells with Specific Blends of Cellulose and Silk. *Biomacromolecules*. 2013;14(5):1287-1298. doi:10.1021/bm301762p.

35. Park JS, Chu JS, Tsou AD, et al. The Effect of Matrix Stiffness on the Differentiation of Mesenchymal Stem Cells in Response to TGF-β. *Biomaterials*. 2011;32(16):3921-3930. doi:10.1016/j.biomaterials.2011.02.019.

36. Sun M, Chi G, Xu J, et al. Extracellular matrix stiffness controls osteogenic differentiation of mesenchymal stem cells mediated by integrin α5. doi:10.1186/s13287-018-0798-0.

37. Wagner W, Bork S, Horn P, et al. Aging and replicative senescence have related effects on human stem and progenitor cells. *PLoS One*. 2009;4(6):e5846. doi:10.1371/journal.pone.0005846.

38. Samsonraj RM, Raghunath M, Hui JH, Ling L, Nurcombe V, Cool SM. Telomere length analysis of human mesenchymal stem cells by quantitative PCR. *Gene*. 2013;519(2):348-355. doi:10.1016/J.GENE.2013.01.039.

39. Yang Y-HK. Aging of mesenchymal stem cells: Implication in regenerative medicine. *Regen Ther*. 2018;9:120-122. doi:10.1016/j.reth.2018.09.002.

40. Newman RE, Yoo D, LeRoux MA, Danilkovitch-Miagkova A. Treatment of

inflammatory diseases with mesenchymal stem cells. *Inflamm Allergy Drug Targets*. 2009;8(2):110-123. http://www.ncbi.nlm.nih.gov/pubmed/19530993. Accessed March 13, 2019.

41. Singer NG, Caplan AI. Mesenchymal Stem Cells: Mechanisms of Inflammation. *Annu Rev Pathol Mech Dis*. 2011;6:457-478. doi:10.1146/annurev-pathol-011110-130230.

42. de Witte SFH, Luk F, Sierra Parraga JM, et al. Immunomodulation By Therapeutic Mesenchymal Stromal Cells (MSC) Is Triggered Through Phagocytosis of MSC By Monocytic Cells. *Stem Cells*. 2018;36(4):602-615. doi:10.1002/stem.2779.

43. De Miguel MP, Fuentes-Julián S, Blázquez-Martínez A, et al. Immunosuppressive properties of mesenchymal stem cells: advances and applications. *Curr Mol Med*. 2012;12(5):574-591. http://www.ncbi.nlm.nih.gov/pubmed/22515979. Accessed March 13, 2019.

44. Ranganath SH, Levy O, Inamdar MS, Karp JM. Harnessing the mesenchymal stem cell secretome for the treatment of cardiovascular disease. *Cell Stem Cell*. 2012;10(3):244-258. doi:10.1016/j.stem.2012.02.005.

45. Linero I, Chaparro O. Paracrine Effect of Mesenchymal Stem Cells Derived from Human Adipose Tissue in Bone Regeneration. Camussi G, ed. *PLoS One*. 2014;9(9):e107001. doi:10.1371/journal.pone.0107001.

46. Lawson T, Kehoe DE, Schnitzler AC, et al. Process development for expansion of human mesenchymal stromal cells in a 50 L single-use stirred tank bioreactor. *Biochem Eng J*. 2017;120:49-62. doi:10.1016/J.BEJ.2016.11.020.

47. Uccelli A, Pistoia V, Moretta L. Mesenchymal stem cells: a new strategy for immunosuppression? *Trends Immunol*. 2007;28(5):219-226. doi:10.1016/J.IT.2007.03.001.

48. Benjamin EJ, Blaha MJ, Chiuve SE, et al. Heart Disease and Stroke Statistics—2017 Update: A Report From the American Heart Association. *Circulation*. 2017;135(10). doi:10.1161/CIR.0000000000000485.

49. Johnson T. Reducing the Prevalence and Costs of Heart Disease. NCLS. http://www.ncsl.org/research/health/reducing-the-prevalence-and-costs-of-heart-disease.aspx. Published 2015. Accessed March 19, 2019.

50. Ohnishi S, Ohgushi H, Kitamura S, Nagaya N. Mesenchymal Stem Cells for the Treatment of Heart Failure. *Int J Hematol*. 2007;86(1):17-21. doi:10.1532/IJH97.07041.

51. Tang YL, Zhao Q, Qin X, et al. Paracrine Action Enhances the Effects of Autologous Mesenchymal Stem Cell Transplantation on Vascular Regeneration in Rat Model of Myocardial Infarction. *Ann Thorac Surg*. 2005;80(1):229-237. doi:10.1016/j.athoracsur.2005.02.072.

52. Tang YL, Zhao Q, Zhang YC, et al. Autologous mesenchymal stem cell transplantation induce VEGF and neovascularization in ischemic myocardium.

Regul Pept. 2004;117(1):3-10. doi:10.1016/J.REGPEP.2003.09.005.

53. Gnecchi M, He H, Liang OD, et al. Paracrine action accounts for marked protection of ischemic heart by Akt-modified mesenchymal stem cells. *Nat Med*. 2005;11(4):367-368. doi:10.1038/nm0405-367.

54. Yim HW, Jeong H, Park H-J, et al. Mesenchymal Stem Cell Therapy for Ischemic Heart Disease: Systematic Review and Meta-analysis. *Int J Stem Cells*. 2018;11(1):1-12. doi:10.15283/ijsc17061.

55. Melhem MR, Park J, Knapp L, et al. 3D Printed Stem-Cell-Laden, Microchanneled Hydrogel Patch for the Enhanced Release of Cell-Secreting Factors and Treatment of Myocardial Infarctions. *ACS Biomater Sci Eng*. 2017;3(9):1980-1987. doi:10.1021/acsbiomaterials.6b00176.

56. Zhou JY, Zhang Z, Qian GS. Mesenchymal stem cells to treat diabetic neuropathy: a long and strenuous way from bench to the clinic. *Cell death Discov*. 2016;2:16055. doi:10.1038/cddiscovery.2016.55.

57. Davey GC, Patil SB, O'Loughlin A, O'Brien T. Mesenchymal stem cell-based treatment for microvascular and secondary complications of diabetes mellitus. *Front Endocrinol (Lausanne)*. 2014;5:86. doi:10.3389/fendo.2014.00086.

58. Domouky AM, Hegab AS, Al-Shahat A, Raafat N. Mesenchymal stem cells and differentiated insulin producing cells are new horizons for pancreatic regeneration in type I diabetes mellitus. *Int J Biochem Cell Biol*. 2017;87:77-85. doi:10.1016/j.biocel.2017.03.018.

59. Lee RH, Seo MJ, Reger RL, et al. *Multipotent Stromal Cells from Human Marrow Home to and Promote Repair of Pancreatic Islets and Renal Glomeruli in Diabetic NODscid Mice*.; 2006. www.pnas.orgcgidoi10.1073pnas.0608249103. Accessed March 15, 2019.

60. Han JW, Sin MY, Yoon Y-S. Cell therapy for diabetic neuropathy using adult stem or progenitor cells. *Diabetes Metab J*. 2013;37(2):91-105. doi:10.4093/dmj.2013.37.2.91.

61. Morris AD, Dalal S, Li H, Brewster LP. Human diabetic mesenchymal stem cells from peripheral arterial disease patients promote angiogenesis through unique secretome signatures. *Surgery*. 2018;163(4):870-876. doi:10.1016/j.surg.2017.11.018.

62. Kitada M, Dezawa M. Parkinson's disease and mesenchymal stem cells: potential for cell-based therapy. *Parkinsons Dis*. 2012;2012:873706. doi:10.1155/2012/873706.

63. Osteoarthritis: Symptoms, Causes, Diagnosis, Treatment. https://www.webmd.com/osteoarthritis/guide/osteoarthritis-basics#1. Accessed March 15, 2019.

64. Kong L, Zheng L-Z, Qin L, Ho KKW. Role of mesenchymal stem cells in osteoarthritis treatment. *J Orthop Transl*. 2017;9:89-103.

doi:10.1016/j.jot.2017.03.006.

65. Emadedin M, Aghdami N, Taghiyar L, et al. Intra-articular injection of autologous mesenchymal stem cells in six patients with knee osteoarthritis. *Arch Iran Med*. 2012;15(7):422-428. doi:012157/AIM.0010.

66. Liu Y, Zou R, Wang Z, Wen C, Zhang F, Lin F. Exosomal KLF3-AS1 from hMSCs promoted cartilage repair and chondrocyte proliferation in osteoarthritis. 2018. doi:10.1042/BCJ20180675.

67. Pan L, Liu D, Zhao L, Wang L, Xin M, Li X. Long noncoding RNA MALAT1 alleviates lipopolysaccharide-induced inflammatory injury by upregulating microRNA-19b in murine chondrogenic ATDC5 cells. *J Cell Biochem*. 2018;119(12):10165-10175. doi:10.1002/jcb.27357.

68. Mao G, Kang Y, Zhang Z, Zhang Z, Liao W. Exosomes derived from miR-92a-3p-overexpressing human mesenchymal stem cells enhance chondrogenesis and prevent the development of osteoarthritis. *Osteoarthr Cartil*. 2018;26:S103. doi:10.1016/j.joca.2018.02.222.

69. Elisabetta M, Palamà F, Carluccio S, et al. *Exosomes Derived from Mesenchymal Stem Cells as a Possible Therapy for Osteoarthritis*. https://search.proquest.com/openview/43e4dee74534ebef0324369873d94c0f/1?cbl=2030046&pq-origsite=gscholar. Accessed March 14, 2019.

70. Phetfong J, Sanvoranart T, Nartprayut K, et al. Osteoporosis: the current status of mesenchymal stem cell-based therapy. *Cell Mol Biol Lett*. 2016;21:12. doi:10.1186/s11658-016-0013-1.

71. Brewer C, Chu E, Chin M, Lu R. Transplantation dose alters the differentiation program of hematopoietic stem cells HHS Public Access. *Cell Rep*. 2016;15(8):1848-1857. doi:10.1016/j.celrep.2016.04.061.

72. Schnitzler AC, Verma A, Kehoe DE, et al. Bioprocessing of human mesenchymal stem/stromal cells for therapeutic use: Current technologies and challenges. *Biochem Eng J*. 2016;108:3-13. doi:10.1016/j.bej.2015.08.014.

73. Glaser DE, Turner WS, Madfis N, et al. Multifactorial Optimizations for Directing Endothelial Fate from Stem Cells. Rajasingh J, ed. *PLoS One*. 2016;11(12):e0166663. doi:10.1371/journal.pone.0166663.

74. Glaser DE, Burns AB, Hatano R, Medrzycki M, Fan Y, McCloskey KE. Specialized mouse embryonic stem cells for studying vascular development. *Stem Cells Cloning*. 2014;7:79-88. doi:10.2147/SCCAA.S69554.

75. Lambrechts T, Sonnaert M, Schrooten J, Luyten FP, Aerts J-M, Papantoniou I. Large-Scale Mesenchymal Stem/Stromal Cell Expansion: A Visualization Tool for Bioprocess Comparison. doi:10.1089/ten.teb.2016.0111.

76. Hagmann S, Moradi B, Frank S, et al. *Different Culture Media Affect Growth Characteristics, Surface Marker Distribution and Chondrogenic Differentiation of Human Bone Marrow-Derived Mesenchymal Stromal Cells*. Vol 14.; 2013.

doi:10.1186/1471-2474-14-223.

77. Panchalingam KM, Jung S, Rosenberg L, Behie LA. Bioprocessing strategies for the large-scale production of human mesenchymal stem cells: a review. 2015. doi:10.1186/s13287-015-0228-5.

78. Jossen V, Schirmer C, Mostafa Sindi D, et al. Theoretical and Practical Issues That Are Relevant When Scaling Up hMSC Microcarrier Production Processes. *Stem Cells Int*. 2016;2016:1-15. doi:10.1155/2016/4760414.

79. Kempf H, Andree B, Zweigerdt R. Large-scale production of human pluripotent stem cell derived cardiomyocytes. *Adv Drug Deliv Rev*. 2016;96:18-30. doi:10.1016/j.addr.2015.11.016.

80. Kebriaei P, Isola L, Bahceci E, et al. Adult Human Mesenchymal Stem Cells Added to Corticosteroid Therapy for the Treatment of Acute Graft-versus-Host Disease. doi:10.1016/j.bbmt.2008.03.012.

81. Yuan Y, Kallos MS, Hunter C, Sen A. Improved expansion of human bone marrow-derived mesenchymal stem cells in microcarrier-based suspension culture. *J Tissue Eng Regen Med*. 2014;8(3):210-225. doi:10.1002/term.1515.

82. Balint R, Richardson SM, Cartmell SH. Low-density subculture: a technical note on the importance of avoiding cell-to-cell contact during mesenchymal stromal cell expansion. *J Tissue Eng Regen Med*. 2015;9(10):1200-1203. doi:10.1002/term.2051.

83. Gepp MM, Fischer B, Schulz A, et al. Bioactive surfaces from seaweed-derived alginates for the cultivation of human stem cells. *J Appl Phycol*. 2017;29(5):2451-2461. doi:10.1007/s10811-017-1130-6.

84. Jossen V, Pörtner R, Kaiser SC, Kraume M, Eibl D, Eibl R. Mass Production of Mesenchymal Stem Cells — Impact of Bioreactor Design and Flow Conditions on Proliferation and Differentiation. In: *Cells and Biomaterials in Regenerative Medicine*. InTech; 2014. doi:10.5772/59385.

85. Liu N, Zang R, Yang S-T, Li Y. Stem cell engineering in bioreactors for large-scale bioprocessing. *Eng Life Sci*. 2014;14(1):4-15. doi:10.1002/elsc.201300013.

86. Nienow AW, Hewitt CJ, Heathman TRJ, et al. Agitation conditions for the culture and detachment of hMSCs from microcarriers in multiple bioreactor platforms. *Biochem Eng J*. 2016;108:24-29. doi:10.1016/J.BEJ.2015.08.003.

87. Timmins NE, Kiel M, Günther M, et al. Closed system isolation and scalable expansion of human placental mesenchymal stem cells. *Biotechnol Bioeng*. 2012;109(7):1817-1826. doi:10.1002/bit.24425.

88. Giroux D, Wesselschmidt R, Hashimura Y, et al. *Development of Scalable Manufacturing Processes for Bone-Marrow Derived Mesenchymal Stem Cells in a Low Shear, Single Use Bioreactor System*.; 2014. https://www.pbsbiotech.com/uploads/1/7/9/9/17996975/chi_poster-final_v.140817.pdf. Accessed May 5, 2018.

89. Jung S, Panchalingam KM, Lee B, et al. Quality Manufacturing of Mesenchymal Stem/Stromal Cells Using Scalable and Controllable Bioreactor Platforms. In: *Bioreactors for Stem Cell Expansion and Differentiation*. CRC Press; 2018:201-242. doi:10.1201/9780429453144-8.

90. Croughan MS, Giroux D, Fang D, Lee B. Novel Single-Use Bioreactors for Scale-Up of Anchorage-Dependent Cell Manufacturing for Cell Therapies. *Stem Cell Manuf*. January 2016:105-139. doi:10.1016/B978-0-444-63265-4.00005-4.

91. Sousa MFQ, Silva MM, Giroux D, et al. Production of oncolytic adenovirus and human mesenchymal stem cells in a single-use, Vertical-Wheel bioreactor system: Impact of bioreactor design on performance of microcarrier-based cell culture processes. *Biotechnol Prog*. 2015;31(6):1600-1612. doi:10.1002/btpr.2158.

92. Tsai A-C, Liu Y, Ma T. Expansion of human mesenchymal stem cells in fibrous bed bioreactor. *Biochem Eng J*. 2016;108:51-57. doi:10.1016/j.bej.2015.09.002.

93. Rojewski MT, Fekete N, Baila S, et al. GMP-Compliant Isolation and Expansion of Bone Marrow-Derived MSCs in the Closed, Automated Device Quantum Cell Expansion System. *Cell Transplant*. 1981;22. doi:10.3727/096368912X657990.

94. Lechanteur C, Baila S, Janssens ME, et al. Stem Cell Large-Scale Clinical Expansion of Mesenchymal Stem Cells in the GMP-Compliant, Closed Automated Quantum ® Cell Expansion System: Comparison with Expansion in Traditional T-Flasks Large-Scale Clinical Expansion of Mesenchymal Stem Cells in the GM. *J Stem Cell Res Ther Lechanteur*. 2014;4(8):222. doi:10.4172/2157-7633.1000222.

95. Jones ME, Nankervis BJ, Fuerst KE, Dodd JA. Cell Growth with Mechanical Stimuli. May 2018. http://www.freepatentsonline.com/y2018/0142199.html. Accessed February 20, 2019.

96. Hanley PJ, Mei Z, Durett AG, et al. Efficient Manufacturing of Therapeutic Mesenchymal Stromal Cells Using the Quantum Cell Expansion System. doi:10.1016/j.jcyt.2014.01.417.

97. Jones M, Varella-Garcia M, Skokan M, et al. Genetic stability of bone marrow-derived human mesenchymal stromal cells in the Quantum System. *Cytotherapy*. 2013;15(11):1323-1339. doi:10.1016/j.jcyt.2013.05.024.

98. Lambrechts T, Papantoniou I, Viazzi S, et al. Evaluation of a monitored multiplate bioreactor for large-scale expansion of human periosteum derived stem cells for bone tissue engineering applications. *Biochem Eng J*. 2016;108:58-68. doi:10.1016/J.BEJ.2015.07.015.

99. Biazar E, Ahmadian M, Heidari K S, et al. Electro-spun Polyethylene Terephthalate (PET) Mat as a Keratoprosthesis Skirt and Its Cellular Study. *Fibers Polym*. 2017;18(8):1545-1553. doi:10.1007/s12221-017-7345-y.

100. Cao Y, Li D, Shang C, Yang S-T, Wang J, Wang X. Three-dimensional culture of human mesenchymal stem cells in a polyethylene terephthalate matrix. *Biomed Mater*. 2010;5(6):065013. doi:10.1088/1748-6041/5/6/065013.

101. Curtis ASG, Forrester J V, Mclnnes C, Lawrie F, McInnes C, Lawrie F. Adhesion of cells to polystyrene surfaces. *J Cell Biol*. 1983;97(5 Pt 1):1500-1506. http://www.ncbi.nlm.nih.gov/pubmed/6355120. Accessed March 14, 2019.

102. Xue R, Qian Y, Li L, Yao G, Yang L, Sun Y. Polycaprolactone nanofiber scaffold enhances the osteogenic differentiation potency of various human tissue-derived mesenchymal stem cells. *Stem Cell Res Ther*. 2017;8(1):148. doi:10.1186/s13287-017-0588-0.

103. Miyagi Y, Zeng F, Huang X-P, et al. Surgical ventricular restoration with a cell- and cytokine-seeded biodegradable scaffold. 2010. doi:10.1016/j.biomaterials.2010.06.048.

104. Zong X, Bien H, Chung C, et al. Electrospun fine-textured scaffolds for heart tissue constructs. *Biomaterials*. 2005;26(26):5330-5338. doi:10.1016/j.biomaterials.2005.01.052.

105. Hanson AD, Wall ME, Pourdeyhimi B, Loboa EG. Effects of oxygen plasma treatment on adipose-derived human mesenchymal stem cell adherence to poly(L-lactic acid) scaffolds. *J Biomater Sci Polym Ed*. 2007;18(11):1387-1400. doi:10.1163/156856207782246812.

106. Tsou Y-H, Khoneisser J, Huang P-C, Xu X. Hydrogel as a bioactive material to regulate stem cell fate. *Bioact Mater*. 2016;1(1):39-55. doi:10.1016/J.BIOACTMAT.2016.05.001.

107. Turner WS, Sandhu N, McCloskey KE. Tissue engineering: construction of a multicellular 3D scaffold for the delivery of layered cell sheets. *J Vis Exp*. 2014;(92):e51044. doi:10.3791/51044.

108. Tang J, Cui X, Caranasos TG, et al. Heart Repair Using Nanogel-Encapsulated Human Cardiac Stem Cells in Mice and Pigs with Myocardial Infarction. *ACS Nano*. 2017;11(10):9738-9749. doi:10.1021/acsnano.7b01008.

109. Yang HS, Jeon O, Bhang SH, Lee S-H, Kim B-S. Suspension Culture of Mammalian Cells Using Thermosensitive Microcarrier That Allows Cell Detachment Without Proteolytic Enzyme Treatment. *Cell Transplant*. 2010;19(9):1123-1132. doi:10.3727/096368910X516664.

110. Davidenko N, Schuster CF, Bax D V, et al. Evaluation of cell binding to collagen and gelatin: a study of the effect of 2D and 3D architecture and surface chemistry. *J Mater Sci Mater Med*. 2016;27(10):148. doi:10.1007/s10856-016-5763-9.

111. Davis GE. Affinity of integrins for damaged extracellular matrix: αvβ3 binds to denatured collagen type I through RGD sites. *Biochem Biophys Res Commun*. 1992;182(3):1025-1031. doi:10.1016/0006-291X(92)91834-D.

112. Hamaia S, Farndale RW. Integrin Recognition Motifs in the Human Collagens. In: *Advances in Experimental Medicine and Biology*. Vol 819. Springer, Dordrecht; 2014:127-142. doi:10.1007/978-94-017-9153-3_9.

113. Godfrey M. Laminin - an overview | ScienceDirect Topics. Asthma and COPD

(Second Edition). https://www.sciencedirect.com/topics/neuroscience/laminin. Published 2009. Accessed March 20, 2019.

114. Liberio MS, Sadowski MC, Soekmadji C, Davis RA, Nelson CC. Differential effects of tissue culture coating substrates on prostate cancer cell adherence, morphology and behavior. *PLoS One*. 2014;9(11):e112122. doi:10.1371/journal.pone.0112122.

115. Moritz T, Dutt P, Xiao X, et al. *Fibronectin Improves Transduction of Reconstituting Hematopoietic Stem Cells by Retroviral Vectors: Evidence of Direct Viral Binding to Chymotryptic Carboxy-Terminal Fragments*. www.bloodjournal.org. Accessed March 20, 2019.

116. Linsley C, Wu B, Tawil B. The Effect of Fibrinogen, Collagen Type I, and Fibronectin on Mesenchymal Stem Cell Growth and Differentiation into Osteoblasts. *Tissue Eng Part A*. 2013;19(11-12):1416-1423. doi:10.1089/ten.tea.2012.0523.

117. To WS, Midwood KS. Plasma and cellular fibronectin: distinct and independent functions during tissue repair. *Fibrogenesis Tissue Repair*. 2011;4:21. doi:10.1186/1755-1536-4-21.

118. su Y-C, Riesbeck K. Vitronectin - an overview | ScienceDirect Topics. The Complement FactsBook. https://www.sciencedirect.com/topics/neuroscience/vitronectin. Published 2018. Accessed March 20, 2019.

119. Hayman EG, Pierschbacher MD, Suzuki S, Ruoslahti E. Vitronectin--a major cell attachment-promoting protein in fetal bovine serum. *Exp Cell Res*. 1985;160(2):245-258. http://www.ncbi.nlm.nih.gov/pubmed/2412864. Accessed March 20, 2019.

120. Méndez-Ferrer S, Michurina T V, Ferraro F, et al. Mesenchymal and haematopoietic stem cells form a unique bone marrow niche. *Nature*. 2010;466(7308):829-834. doi:10.1038/nature09262.

121. Parmar K, Mauch P, Vergilio J-A, Sackstein R, Down JD. Distribution of hematopoietic stem cells in the bone marrow according to regional hypoxia. *Proc Natl Acad Sci U S A*. 2007;104(13):5431-5436. doi:10.1073/pnas.0701152104.

122. Ito A, Aoyama T, Yoshizawa M, et al. *The Effects of Short-Term Hypoxia on Human Mesenchymal Stem Cell Proliferation, Viability and P16 INK4A MRNA Expression: Investigation Using a Simple Hypoxic Culture System with a Deoxidizing Agent*. Vol 11. Journal of Stem Cell & Regenerative Medicine; 2015. http://www.ncbi.nlm.nih.gov/pubmed/26195892. Accessed March 16, 2019.

123. Ejtehadifar M, Shamsasenjan K, Movassaghpour A, et al. The Effect of Hypoxia on Mesenchymal Stem Cell Biology. *Adv Pharm Bull*. 2015;5(2):141-149. doi:10.15171/apb.2015.021.

124. Shearier E, Xing Q, Qian Z, Zhao F. Physiologically Low Oxygen Enhances

Biomolecule Production and Stemness of Mesenchymal Stem Cell Spheroids. doi:10.1089/ten.tec.2015.0465.

125. Ahmed Mohyeldin, Tomas Garzon-Muvdi AQ-H. Oxygen in Stem Cell Biology: A Critical Component of the Stem Cell Niche. *Cell Stem Cell*. 2010;7. doi:10.1016/j.stem.2010.07.007.

126. Xcell Biosciences. *Next Generation Primary Cell Culture and AVATAR Analysis Platform*. http://www.gendiscovery.com.tw/pdf/XcellAvatar.pdf. Accessed March 16, 2019.

127. Majmundar AJ, Wong WJ, Simon MC. Hypoxia-Inducible Factors and the Response to Hypoxic Stress. *Mol Cell*. 2010;40(2):294-309. doi:10.1016/j.molcel.2010.09.022.

128. Tamama K, Kawasaki H, Kerpedjieva SS, Guan J, Ganju RK, Sen CK. Differential roles of hypoxia inducible factor subunits in multipotential stromal cells under hypoxic condition. *J Cell Biochem*. 2011;112(3):804-817. doi:10.1002/jcb.22961.

129. Tang YL, Tang Y, Zhang YC, Qian K, Shen L, Phillips MI. Improved Graft Mesenchymal Stem Cell Survival in Ischemic Heart With a Hypoxia-Regulated Heme Oxygenase-1 Vector. *J Am Coll Cardiol*. 2005;46(7):1339-1350. doi:10.1016/J.JACC.2005.05.079.

130. Yu C, Kornmuller A, Brown C, Hoare T, Flynn LE. Decellularized adipose tissue microcarriers as a dynamic culture platform for human adipose-derived stem/stromal cell expansion. *Biomaterials*. 2017;120:66-80. doi:10.1016/J.BIOMATERIALS.2016.12.017.

131. Bertolo A, Taddei AR, Baur M, Kantonsspital L, Pötzel T, Stoyanov J. Injectable Microcarriers as Human Mesenchymal Stem Cell Support and their Application for Cartilage and Degenerated Intervertebral Disc Repair Mesenchymal Stem Cells View project copper regulation View project. *Eur Cells Mater*. 2015;29:70-81. www.ecmjournal.org. Accessed March 16, 2019.

132. Caracci SJ, Henry D, Walerack C, Zhou Y. Digestible substrates for cell culture. June 2016. https://patents.google.com/patent/US20180179489A1/en. Accessed March 16, 2019.

133. Kim H, Kim K, Lee SJ. Nature-inspired thermo-responsive multifunctional membrane adaptively hybridized with PNIPAm and PPy. *NPG Asia Mater*. 2017;9(10):e445. doi:10.1038/am.2017.168.

134. Sutherland AB. *Fabrication of Responsive Polymer Brushes for Patterned Cell Growth and Detachment Repository Citation "Fabrication of Responsive Polymer Brushes for Patterned Cell Growth and Detachment" (2013). Browse All Theses and Dissertations*. https://corescholar.libraries.wright.edu/etd_all.748.https://corescholar.libraries.wright.edu/etd_all/748. Accessed March 16, 2019.

135. Nash ME, Healy D, Carroll WM, Elvira C, Rochev YA. Cell and cell sheet

recovery from pNIPAm coatings; motivation and history to present day approaches. *J Mater Chem*. 2012;22(37):19376. doi:10.1039/c2jm31748f.

136. Jin J, Jeong SI, Shin YM, et al. Transplantation of mesenchymal stem cells within a poly(lactide- *co* -ε-caprolactone) scaffold improves cardiac function in a rat myocardial infarction model. *Eur J Heart Fail*. 2009;11(2):147-153. doi:10.1093/eurjhf/hfn017.

137. Heathman TRJ, Glyn VAM, Picken A, et al. Expansion, harvest and cryopreservation of human mesenchymal stem cells in a serum-free microcarrier process. *Biotechnol Bioeng*. 2015;112(8):1696-1707. doi:10.1002/bit.25582.

138. Cunha B, Peixoto C, Silva MM, Carrondo MJT, Serra M, Alves PM. Filtration methodologies for the clarification and concentration of human mesenchymal stem cells. *J Memb Sci*. 2015;478:117-129. doi:10.1016/J.MEMSCI.2014.12.041.

139. Popova D, Dhadda P, Bell M, et al. Developing integrated single-use upstream and downstream platform processing options for allogeneic cell therapy applications: Linking the stirred tank bioreactor to the TFF. *Cytotherapy*. 2017;19(5):S124. doi:10.1016/j.jcyt.2017.02.203.

140. Wang X, Omar O, Vazirisani F, Thomsen P, Ekström K. Mesenchymal stem cell-derived exosomes have altered microRNA profiles and induce osteogenic differentiation depending on the stage of differentiation. *PLoS One*. 2018;13(2):e0193059. doi:10.1371/journal.pone.0193059.

141. Vishnubhatla I, Corteling R, Stevanato L, Hicks C, Sinden J. The Development of Stem Cell-derived Exosomes as a Cell-free Regenerative Medicine. 2014. doi:10.5772/58597.

142. Hu L, Wang J, Zhou X, et al. Exosomes derived from human adipose mensenchymal stem cells accelerates cutaneous wound healing via optimizing the characteristics of fibroblasts. *Nat Publ Gr*. 2016. doi:10.1038/srep32993.

143. Phinney DG, Pittenger MF. Concise Review: MSC-Derived Exosomes for Cell-Free Therapy. *Stem Cells*. 2017;35(4):851-858. doi:10.1002/stem.2575.

144. Kim SH, Bianco NR, Shufesky WJ, Morelli AE, Robbins PD. Effective treatment of inflammatory disease models with exosomes derived from dendritic cells genetically modified to express IL-4. *J Immunol*. 2007;179(4):2242-2249. http://www.ncbi.nlm.nih.gov/pubmed/17675485. Accessed March 2, 2019.

145. Vallabhaneni KC, Penfornis P, Dhule S, et al. Extracellular vesicles from bone marrow mesenchymal stem/stromal cells transport tumor regulatory microRNA, proteins, and metabolites. *Oncotarget*. 2015;6(7):4953-4967. doi:10.18632/oncotarget.3211.

146. Alexander M, Hu R, Runtsch MC, et al. Exosome-delivered microRNAs modulate the inflammatory response to endotoxin. *Nat Commun*. 2015;6:7321. doi:10.1038/ncomms8321.

147. Barkholt L, Flory E, Jekerle V, et al. Risk of tumorigenicity in mesenchymal

stromal cell–based therapies—Bridging scientific observations and regulatory viewpoints. *Cytotherapy*. 2013;15(7):753-759. doi:10.1016/J.JCYT.2013.03.005.

148. Prockop DJ, Brenner M, Fibbe WE, et al. Defining the risks of mesenchymal stromal cell therapy. *Cytotherapy*. 2010;12(5):576-578. doi:10.3109/14653249.2010.507330.

149. Lin JH. Species similarities and differences in pharmacokinetics. *Drug Metab Dispos*. 1995;23(10).

150. Ronaldson-Bouchard K, Vunjak-Novakovic G. Organs-on-a-Chip: A Fast Track for Engineered Human Tissues in Drug Development. *Cell Stem Cell*. 2018;22(3):310-324. doi:10.1016/J.STEM.2018.02.011.

151. Kimura H, Sakai Y, Fujii T. Organ/body-on-a-chip based on microfluidic technology for drug discovery. *Drug Metab Pharmacokinet*. 2018;33(1):43-48. doi:10.1016/J.DMPK.2017.11.003.

152. Park I-H, Arora N, Huo H, et al. Disease-Specific Induced Pluripotent Stem Cells. *Cell*. 2008;134(5):877-886. doi:10.1016/J.CELL.2008.07.041.

153. Rodrigues C, Fernandes T, Diogo M, da Silva C, Cabral J. Bioreactors for Stem Cell Expansion and Differentiation. In: *Stem Cell Engineering*. CRC Press; 2012:1-28. doi:10.1201/b12942-11.

154. Hookway TA, Butts JC, Lee E, Tang H, Mcdevitt TC. Aggregate formation and suspension culture of human pluripotent stem cells and differentiated progeny. 2016. doi:10.1016/j.ymeth.2015.11.027.

155. Chen VC, Couture SM, Ye J, et al. Scalable GMP compliant suspension culture system for human ES cells. *Stem Cell Res*. 2012;8(3):388-402. doi:10.1016/j.scr.2012.02.001.

156. Healthcare G. Cytodex ™ surface microcarriers. https://www.gelifesciences.co.jp/catalog/pdf/18106061_cytodex.pdf. Accessed May 5, 2018.

157. Czermak P, Freimark D, Pino-Grace P, et al. Use of Encapsulated Stem Cells to Overcome the Bottleneck of Cell Availability for Cell Therapy Approaches. *Transfus Med Hemother*. 2010;37:66-73. doi:10.1159/000285777.

158. Singh V. Disposable bioreactor for cell culture using wave-induced agitation. *Cytotechnology*. 1999;30(1/3):149-158. doi:10.1023/A:1008025016272.

159. Piret JM, Cooney CL. Model of oxygen transport limitations in hollow fiber bioreactors. *Biotechnol Bioeng*. 1991;37(1):80-92. doi:10.1002/bit.260370112.

160. Mizukami A, de Abreu Neto MS, Moreira F, et al. A Fully-Closed and Automated Hollow Fiber Bioreactor for Clinical-Grade Manufacturing of Human Mesenchymal Stem/Stromal Cells. *Stem Cell Rev Reports*. 2018;14(1):141-143. doi:10.1007/s12015-017-9787-4.

161. Osiecki MJ, Michl TD, Kul Babur B, et al. Packed Bed Bioreactor for the Isolation and Expansion of Placental-Derived Mesenchymal Stromal Cells. *PLoS One*. 2015;10(12):e0144941. doi:10.1371/journal.pone.0144941.

162. Placzek MR, Chung I-M, Macedo HM, et al. Stem cell bioprocessing: fundamentals and principles. *J R Soc Interface*. 2009;6:209–232. doi:10.1098/rsif.2008.0442.

163. Dougherty E. Living, breathing human lung-on-a-chip: A potential drug-testing alternative. https://wyss.harvard.edu/living-breathing-human-lung-on-a-chip-a-potential-drug-testing-alternative/. Accessed April 4, 2019.

Table 2-1: Pros and Cons of stem cell types in regard to bioproduction and therapeutic potential.

Stem Cell Type	*Advantages*	*Disadvantages*
Embryonic	- High Differentiation Potential - High Passage Potential	- Hard to Source (ethical issues) - Immune Response - Teratogenic Phase
Induced Pluripotent	- High Differentiation Potential - High Passage Potential - Easily Sourced	- Patient Specific - Teratogenic Phase - Still Carry Genetic Defects
Adult (Mesenchymal) Stem Cell	- HLA Typed and Banked - Immunoprivilaged - Easy Culture - Historical Use and Widely Researched	- Low Passage Potential - Multipotent

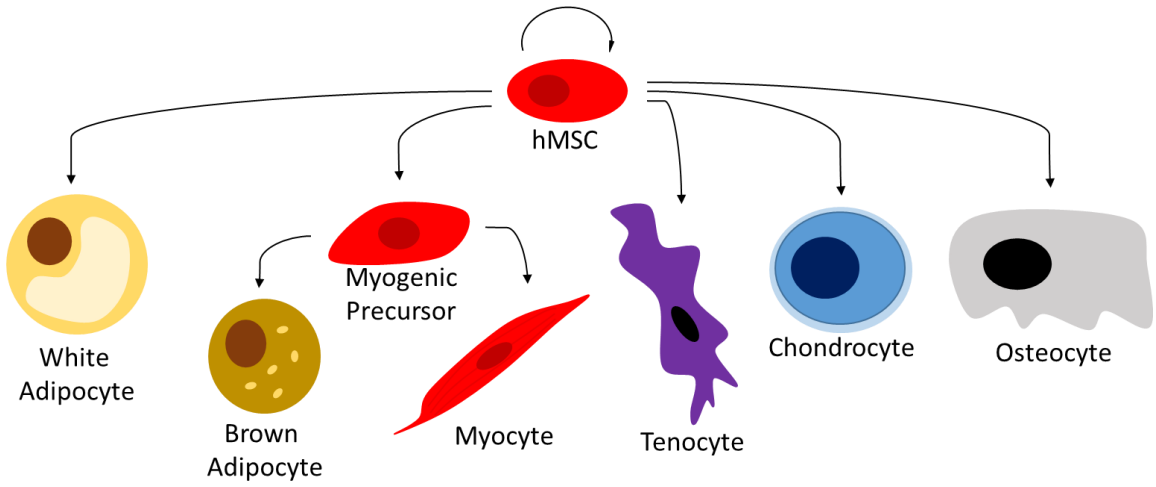

Figure 2-1: Brief diagram of differentiation potential of hMSCs. Using factors and seeding techniques hMSCs can become many desired functional cell types.

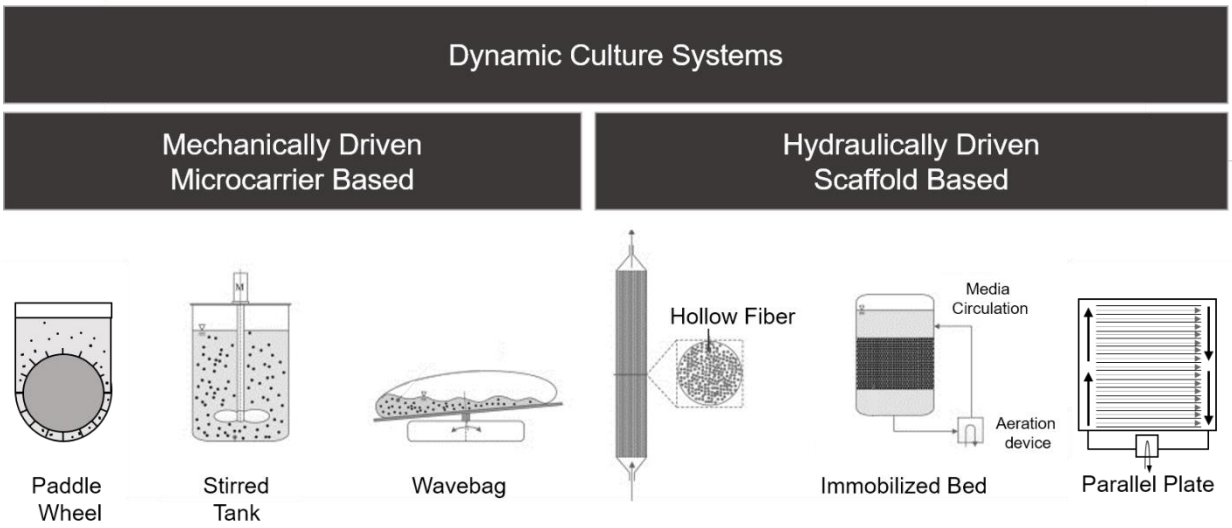

Figure 2-2: Various bioreactor systems for the culture of hMSCs. On the left are common microcarrier based systems, and on the left are commonly used scaffold based bioreactors. Adapted from Jossen et al.[9]

Table 2-2: Bioreactor systems advantages and disadvantages for the bioproduction of hMSCs.

Method	*Bioreactor type*	*Advantages*	*Disadvantages*	*Source*
Adherent/ Suspension	Aggregate-based stirred tank bioreactor	Homogeneous culture environment; easy to scale up.	High shear stress. Little nutrient diffusion into center of aggregate causing apoptosis.	[153–155]
Adherent/ Suspension	Microcarrier-based bioreactor: Stirred tank, RCCS	Support high density cell culture; regulate cell growth and differentiation; serve as cell delivery systems; easy to scale up.	Difficult to harvest cells. Still some possible shear issues. Limited growth area on microcarriers.	[78,88,109,156]
Adherent/ Suspension	Microencapsulation-based bioreactor stirred tank, RCCS	Protection from shear stress; provide 3D microenvironment.	Need to release the cells from the hydrogels. Can affect stemness of cells.	[157]
Adherent/ Suspension	Microcarrier-based Wave bioreactor	Suitable for hematopoietic stem cell culture; gentle mixing, low shear stress, easy to scale up.	Costly. Possible sampling issues. Required energy for suspension causing high shear.	[78,158]
Adherent	Hollow fiber membrane bioreactor	Low shear stress, better mimics cellular microenvironment.	Difficult to scale up and the culture environment is inhomogeneous due to the nutrient and oxygen gradient. Difficult to monitor and sample cells.	[159]
Adherent	Immobilized cells in 3D scaffolds: Fixed bed, fluidized bed, fibrous bed	Provide 3D microenvironment; allow cell spatial organization; regulate proliferation, differentiation and tissue formation.	Difficult to harvest cells. Hard to visualize cells.	[78,160,161]
Adherent	Rotary cell culture system (RCCS)	Low shear stress; good mass transfer; controlled oxygenation.	Limited in size; hard to scale up; may not be able to produce the quantities of cells needed for some applications.	[162]

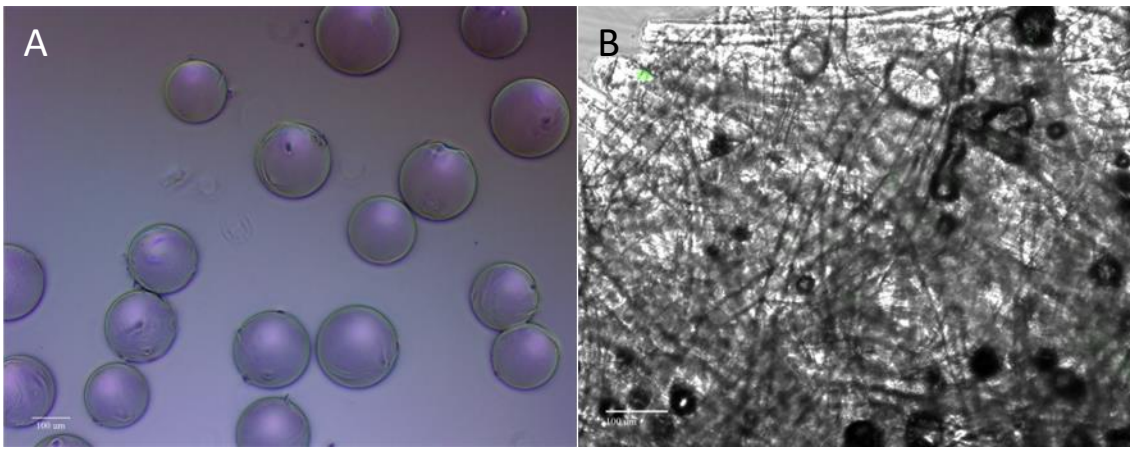

Figure 2-3: Different culture methods for reactor culture. A) Cytodex 1 microcarriers with cells adherent to surface. B) Randomized cellulosic fiber matrix with cells on it. Cells stained with phalloidin green for imaging purposes. Scale bars are 100 microns

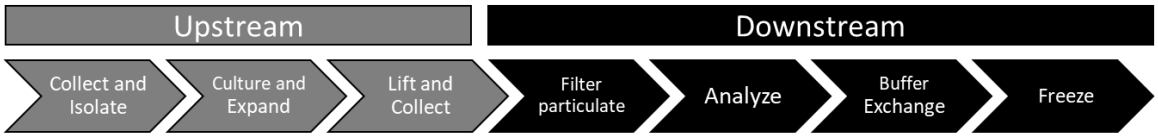

Figure 2-4: Flow chart of process for whole cell therapy. Upstream processes involve the culture of the cells, and downstream is comprised of steps to increase purity of the resulting therapeutic.

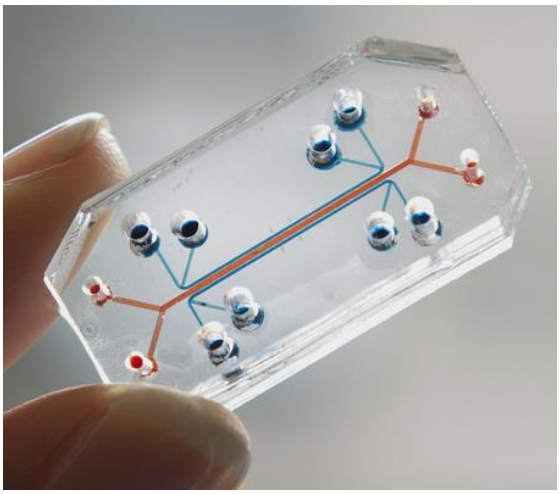

Figure 2-5: Lung on a chip. Developed for testing effects safety and efficacy of drugs on lung cells in vitro accurately. Developed by Wyss Institute for Biologically inspired Engineering and Harvard University.[163]*This technology can be used in conjunction with bioproduced human stem cells, providing effective tissue modeling of both normal and potentially diseases tissues and the effects drugs can have on them.*

3 POLYMERS AND TREATMENTS

3.1 ABSTRACT

In order to reach clinically relevant numbers of hMSCs for stem cell based therapies, culture techniques must be used. To achieve this, fiber matrices and 3D printed polymers have been tested. In this work we test stem cell adhesion and growth to PE, silk, and cellulosic fibers, as well as PETG, T-PU, and PLA 3D printable polymers for used in a novel 3D bioreactor. Cellulosic fibers supported cell growth, but cells tended to form undesirable clusters. Gelatinized PLA showed the best cell adhesion and proliferation, forming monolayers akin to culture on 2D tissue culture dishes. hMSCs were easily removed and maintained their biomarker phenotype after seven days of culture.

3.2 BACKGROUND AND INTRODUCTION

Mesenchymal stem cells (MSCs) are promising candidates for therapies in the field of regenerative medicine. They have the ability to differentiate into mesoderm derived cell types including osteocytes, chondrocytes, adipocytes, and myocytes.[1] They are described as fibrotic and are anchorage dependent cells.[2] Factors such as topology and surface chemistry have been proven to affect the potency of hMSCs.[3] As such, proper culture is heavily reliant on the choice of substrate the cell is grown on.

Softer polymers and blends have been shown to induce hMSCs to a chondrocyte or adipocyte fate.[4] Harder substrates have shown to promote cell elongation and osteocyte differentiation.[5–7] This is thought to be because cartilage has a relatively pliant ECM,

whereas cancellous bone is comparatively stiffer. This is due in part to their ability to test the substrate on which they reside, contracting to determine the stiffness of the ECM.[8] The cells are therefore fated to become the cells which reside in that level of rigidity.

Researchers in polymer sciences have found that much of cell-substrate binding is through integrin mediated adhesion.[9,10] The Integrin receptors on the surface of the hMSC recognize certain residues in the extracellular matrix proteins, leading to cell adhesion.[11] The recognition and binding to basal membrane proteins such as collagen, laminin, and fibronectin are also through integrin binding. The selectivity of the integrin receptor comes from two subunits which form a dimer, and can vary widely based on the subunits combined. For example, B1 and A2 dimers selectively recognize DGEA residues of various collagens and laminin, while B3 AV has been shown to bind RGD sequences of vitronectin, fibrogen, Von Willebrand factor, thrombospondin, fibronectin, osteopontin, and collagen.[11]

hMSCs also rely on cadherin to maintain stemness.[12] N-cadherin is involved in cell migration and wound healing, and is an important protein in connective tissues.[13,14] Cadherin is mainly found in cell junctions, binding cells together in tissues.[15] it is through the combination of cadherin and integrin that cells adhere, grow, and proliferate, making surface chemistry very important in the culture of sensitive cells such as hMSCs.[15]

Another method of cell adhesion is through exposed hydroxyl groups.[16] This is important for cell adhesion to plastics, a defining characteristic of MSCs.[17] Interestingly, carboxyl groups inhibit cell adhesion.[18] Using hydroxyl groups is a good way of reducing the cell culture reliance on xeno-sourced products, easing regulatory concerns for cell based products. Secondary to exposing hydroxyl groups, synthetic polymers like poly-D-lysine

can be bound to plasma treated surfaces to further enhance cell adhesion.[19] This is a means of treating plastics and polymers, therefore, plasma treatment and subsequent coating has its usefulness in polymer-based 3D scaffolds.[20,21]

Scaffolds are used when growing cells in 3D cultures. This can be used to both increase usable surface area and to culture cells into a desired shape. The two main 3D culture methods are either hydrogel based or hard material support based. Hydrogels are polymers which swell with water.[22] There are both natural ECM based hydrogels and fully synthetic hydrogels. Both scaffolds and hydrogels are common methods of culturing cells in 3D. Culturing cells in 3D has shown to increase cell-cell connections, mimicking natural environments.[23] This increase in cell communication has also been linked to maintaining the stemness of mesenchymal stem cells.[12] One way to orient and increase surface area in such hydrogels and rigid polymer scaffolds is through 3D printing.

3D printing has proven to be a valuable tool in cell culture, specifically in regenerative medicine and stem cell culture.[24] Scientist have been able to regrow bone in sheep using FDM 3D printing of Polybutylene Terephthalate for MSC growth and differentiation.[25] Other common 3D printing thermoplastics used in cell culture are Poly Lactic Acid (PLA), Polycaprolactone (PCL), and Polyethylene Terephthalate Glycol (PETG).[26–29] 3D printing of hydrogels has also proven useful for hindering hMSC mobility and attrition, which has been hypothesized to decrease effectiveness of hMSC therapies.[30] Another feature of 3D printing is that the shape of the overall scaffold can be tailored to the intended therapy.

In this work we investigate the effectiveness of various polymers on hMSC growth. Because of the significant increase in surface area, as well as rigidity desired in potential

hMSC scaffolds, we focused on both fibers and hard polymers. Cellulosic, silk, polyethylene, and various polymers used in 3D printing were tested to see if they would support hMSC culture. Simple surface treatment of PLA was also tested as a means of increasing cell adhesion. The intention was to see which polymer best sustained hMSC culture to use in a scale-down model of the Express bioreactor from Sepragen Corporation (Hayward, CA).

3.3 MATERIALS AND METHODS

3.3.1 Cell culture

3.3.1.1 BEND3 Culture

Murine BEND3 brain endothelial cells were used for cell culture feasibility studies. They were cultured as per ATCC recommendations. Cells were seeded at 5,000 cells/cm^2 for culture propagation. Media was a high glucose DMED base containing sodium pyruvate (GIBCO 11995065), supplemented with 10% FBS (ATCC 30-2021) and 1% penicillin-streptomycin (ATCC 30-2300). Cells were passaged using 0.25% Trypsin and 0.53 mM EDTA solution (ATCC 30-2101). Cells were fed on day 3 and passaged on day 6 or when confluency reached 90%. Experiments were conducted between passage 5 and 30.

3.3.1.2 hMSC Culture

hMSCs were cultured according to guidelines provided from ATCC. Briefly, cells were cultured in hMSC media (ATCC PCS-500-030) supplemented with the bone marrow derived hMSC bullet kit (ATCC PCS-500-041) at 37°C and 5% CO2. A ¾ media exchange was performed on day 3, and cells were passaged at 80-90% confluency,

usually on day 6. Cells were lifted using 3.5mL of 0.25% Trypsin and 0.53 mM EDTA solution (ATCC 30-2101) for regular passaging of T-75 flasks, and cells were re-plated at 5,000 cells cm^{-2}. Working cell bank was created from pass 4 hMSCs and stored in liquid nitrogen. Experiments using hMSCs were conducted on cells between passage 5 and 9.

3.3.2 **Cellulosic scaffold**

Cellulosic samples were provided by Sepragen Corporation (Hayward, CA). This scaffold material is treated to promote cell adhesion and is currently used in their Express bioreactor line. For test cultures $1cm^2$ swatches were cut to fit into 12 well plates. Seeding experiments varied, but included static adhesion, rocking, and gelatin vs untreated samples. For static seeding a rough estimate of surface area was taken using porosity found using FIJI. The appropriate cell number was suspended in the volume necessary to wet the swatch and set overnight in the incubator. The well was then brought to appropriate volume. Cells were then cultured out for seven days.

For rocking the cells were place in total well volume and the swatch was place with the cell laden media. The culture plate was then place on an oscillating rocker (Adams Nutator Model 1105) overnight in 37°C and 5% CO_2 incubator.

Cellulosic scaffolds were gelatinized by placing swatches in filtered and autoclave-sterilized 0.1% (W/V) porcine gelatin (Fisher 9000-70-8) solution in MQ water. The submerged swatches were placed at 37°C for 30 minutes. Swatches were then washed with PBS and cell inoculum was added to the wells or directly to the scaffold depending on adhesion and culture study.

For bioreactor studies a swatch of cellulosic was cut, sterilized and gelatinized according to previous methods. A 50mL conical tube cap was fitted with four ports. One extended to the middle of the tube, one to the bottom, and two had no extensions. The two without any internal attachments were for gas exchange. 10^6 hMSCs were suspended into 15mL of media and added to the reactor. Seeding circulation started at 5mL min^{-1} for one hour, then was set to 2.5mL/min for one hour, then brought down to 1.5mL min^{-1}. Media circulation was tested between 1.0-2.0mL min^{-1} for the remainder of the seven days.

3.3.3 **Silk and polyester**

100% Silk fabric purchased from fabric store was cleaned with hot water and soap. Swatches were cut and autoclave sterilized for 15 minutes at 112°C. Four swatches of silk fibers were rewetted in PBS and placed into well plates. Two control wells, two ungelatinized swatches, and two gelled swatches were seeded at a density of 5,000 cells cm^{-2} based on well area. At day seven cells were fixed and stained for visualization using fluorescent microscopy.

Polyester was sterilized and prepared in the same way as silk fibroin swatches. After a 15 minute autoclave cycle the fabric shape and texture was altered, but still stable enough for culture. Cells were plated at 5,000 cells cm^{-2} and cultured for seven days. After which cells were stained and imaged by fluorescent microscopy.

3.3.4 **PLA and plasma etching**

PLA scaffolds were 3D printed using a PrintrBot Simple Metal (Printrbot) and Cura 3.2.1 slicing software. Translucent high temperature PLA (Protoplant) was used. PLA was printed at 212°C. PLA was autoclaved at 121°C for 15 minutes to both sterilize and heat

treat the PLA. For plasma treatment, samples were first placed in plasma cleaner (Harrick Plasma, model PDC-32G) set on high for three minutes. Plasma was created under vacuum without addition of argon or oxygen. Samples were then wetted with MQ water and autoclave sterilized for 15 minutes before culture.

3.3.5 **PETG and T-PU**

Polyethylene Terephthalate Glycol (PETG) (3D Solutech) was printed at 207°C. It was autoclave sterilized for 15 minutes at 121°C. Like the PLA, it was printed in both flat sheet and lattice form to test cell growth and adhesion. A comparison of gelatinized and control PET scaffolds was also performed. Thermoplastic Polyurethane (SainSmart) was printed at 200°C. The same wash and sterilization steps were followed to prepare Thermoplastic-Polyurethane (T-PU) as with PETG. These samples were not tested with plasma etching.

3.3.6 **Drop test for measuring contact angle**

To measure contact angle, a drop test was performed on untreated and treated cell culture scaffold samples. A 2µL drop of MQ water was made using a micropipette, and the drop was slowly brought down to the surface being tested. The drop was allowed to contact the surface and stabilize for 10 seconds. A photograph was taken and uploaded to FIJI (ImageJ) for analysis. The analysis package used was drop_snake.[31] To do this the photograph was first converted to 8-bit black and white. Then using the software package the circumference was drawn, and vertexes of the angles noted. The software is then able to simulate the drop and calculate the contact angle of the drop. Hydrophobic surfaces are defined as having a contact angle greater than 90 degrees, and hydrophilic angles are less

than 90 degrees. Each treatment was measured three times and an average contact angle was calculated.

3.3.7 SEM imaging

PLA matrices were washed and prepared for electron microscopy. Using conductive double-sided copper tape samples were stuck to 1/2in slotted stages (TED PELLA 16111). Samples were imaged at 2kV using Hitachi SU-70 scanning electron microscope.

3.3.8 Confocal imaging

Cells were grown on various scaffolds and washed using Ca^{++} and Mg^{++} PBS. The cells were then fixed in place with 4% PFA for 15 minutes and washed again with PBS. Permeabilization was performed using 1% (W/V) Triton-X 100 in PBS for 30 minutes at 37°C. Cells were then washed and placed in 1% (W/V) Bovine Serum Albumin (BSA) and 0.1% (W/V) Triton-X 100 in PBS for 1 hour at room temperature. Cells were then stained with 1 drop per mL Phalloidin green (Invitrogen) and 2.3nM DAPI. To visualize viable cells on the matrix the same wash steps were followed, but cells were not fixed nor permeabilized. Calcein-AM (ab141420) was used instead of Phalloidin. 1μL of 1mM of Calcein solution was added to 1mL of Ca^{++} and Mg^{++} PBS and cells were incubated for 10 minutes at 37°C. Since Calcein-AM must be processed to fluoresce, no subsequent washing was performed.

3.3.9 Flow Cytometry

hMSCs were cultured in experimental conditions and lifted with TrypLE-Express to preserve cell surface receptors. Cells were first washed with PBS, then placed in TyrpLE for 15 minutes. After neutralization cells were fixed in 4% paraformaldehyde (PFA) for

15 minutes, washed twice, and blocked for 1 hour at room temperature. Blocking solution consisted of 1% (W/V) BSA (LONZA) and 0.1 % (W/V) Triton-X 100 in PBS. Cells were stained for the positive markers CD105 (Invitrogen MHCD10520) and CD73 (Abcam ab157335) and were negative for CD14 (Abcam ab91146) and CD19 (Abcam ab25510) at 1µL per 500,000 cells in 500µL following recommendations. Samples were then run at medium speed (35µl min^{-1}) on a BD Accuri C6 flow cytometer and analyzed using FlowJo V10 (Ashland, OR). Unstained controls were used to gate cells. Compensation was done through FlowJo and Fluorescence Minus One (FMO) techniques. Initial bioreactor studies were done using only CD105 and CD34.

3.4 RESULTS

3.4.1 Cultures

Cellulosic scaffold had very poor cell adhesion when un-gelatinized both with Bend3 (Figure 3-1 A) and with hMSCs (Figure 3-2 A). Without gelatin, cells were very spherical and pseudopodia can be seen unattached to cellulosic material. When gelatinized many more Bend3 cells can be seen on the cellulosic fibers (Figure 3-1 B). Furthermore, cell morphology is more similar to normal polystyrene T-flask culture, showing cell elongation running along the fiber (Figure 3-2 B).

Silk scaffolds showed some cell retention (Figure 3-3 A) but compared to cellulosic and PLA it performed very poorly. However, cells imaged on silk fabric showed some colonies forming by day seven. Because of poor growth and adhesion, it was not possible to run cells though flow to analyze resulting cells.

Polyethylene cultures visually show increased cell adhesion compared to silk fibers (Figure 3-3 B). However, when cells were lifted from scaffold and analyzed via two marker flow cytometry it was found that not only were there very few cells to count, but that cells did not maintain their CD105 marker expression indicating differentiation (Figure 3-4).

Contact angles were measured via software according to Figure 3-5. The only sample that showed statistically significant difference to other conditions tested was untreated PLA ($p<0.05$). Plasma treated PLA similar hydrophilicity ($p>0.05$) to PS dishes (Figure 3-6). Gelatin also resulted in similar contact angles as PS and plasma treated PLA ($p>0.05$). Because plasma treatment eliminates the use of animal derived products, we initially tested cell culture on plasma treated PLA prints. Cell adhesion and morphology of densely seeded hMSCs on day one appear very similar to polystyrene culture dishes (Figure 3-7 A). However, by day two very few cells were seen on the scaffold, and colonies were very sparse (Figure 3-7 B). Values are not reported, but when lifted cell number were far lower than expected. Gelatin coated PLA showed the same contact angle as control PS dishes. Because of this, gelatin treatment was used for all subsequent PLA cultures. Moreover, flow cytometry data showed that the cells that were lifted from gelatin coated PLA on day seven retained proper four marker cell surface profile (Figure 3-8).

Cells did not readily adhere to TPU, even when gelatinized. Its opacity also made it difficult to image. PETG scaffolds deformed in the autoclave and poor cell growth was seen. Because of this these scaffolds were omitted.

3.4.2 **PLA lattice**

Though testing of extrusion rates and speeds of the printer it was determined that between 20 and 30mm s^{-1} using 0.15mm layer height resulted in the best, most homogenous geometry (Figure 3-9). There were however some abnormalities in the print. At almost all tested printer speeds there is still a small extra filament crossing the lumen of the channel (Figure 3-9 A-D). As this would increase surface area and was rather predictable in printing it was not worrisome. Layer height and extrusion percent were also tested, and it was found that 0.15mm and 100% extrusion resulted in the most homogenous and optically clear PLA structures (Figure 3-10). To see surface nanotopology the lattices were imaged using SEM, which showed very similar surface modalities to polystyrene (Figure 3-11). However, after optimization it was found that the printer speed could be increased to 80mm s^{-1} at a layer height of 0.2mm. This was accomplished by slicing the object at 50% infill and printing at zero wall thickness. The resulting print was a grid pattern infill with very homogenous pores and no hanging extrusions or burrs (Figure 3-12).

3.4.3 **Bioreactor Culture**

Reactor cultures were step up and run according to Figure 3-13 A. The system is made of a polycarbonate tube and two stainless steel caps on either end to make a chamber. There is a small pass-through port capped with silicone on the front of the reactor, and four Luer lock ports on the top. Two ports handle liquids, while the remaining two are 0.2µm filter capped for gas exchange. Media is circulated by an external peristaltic pump and gas is overlaid into the chamber at a flow rate of 0.01VVM. Both cellulosic and gelatin coated PLA were tested in the system. Figure 3-13 B shows how the cellulosic swatch

was wrapped around a 15mL conical tube suspended in the center of the reactor. The growth area (PLA or cellulosic) is suspended to allow media to flow through it, creating a much smaller boundary layer of media above the cells. The media collects at the bottom and stays in the chamber to maintain humidity, where a drop tube from one of the top Luer lock ports can then continue recirculation via external peristaltic pump. Initial flow rates were 1mL min^{-1} and optimizing seeding procedure led to the largest increase in cells gained. Recirculating cell suspension resulted in little to no cell yields on day seven. Cellulosic based cultures supported cell adhesion (Figure 3-14 A) and growth, resulting in cell clusters within the fiber matrix (Figure 3-14 B). However, significant particulate collection at the base of the bioreactor reservoir, increasing particulates in solution and in turn making flow cytometry to quantify cell purity very difficult.

PLA reactor cultures performed better than cellulosic matrix. However, a different seeding strategy had to be adopted. To properly seed the lattice cells were suspended in small volumes and injected above the lattice. The cells in media were allowed one hour to settle and adhere without the reactor recirculating any media. Cells were easily lifted and characterized via four marker flow cytometry, which showed that cells maintained their stem cell phenotype (Figure 3-15). Dot-plot density also showed that much more cells had been harvested than previous runs. Confocal images using Calcein viability staining showed hMSCs adherent onto the PLA cross lattice in confluent layers of cells after seven days in culture (Figure 3-16).

Comparing PLA, PS and Cytodex we saw that cellulosic showed the best doubling time (

Table 3-1). It was found that the substrates and samples tested hade relatively similar doubling times after seven days in culture. The substrate that showed the most doublings was PLA in static culture, and the poorest performing was actually ungelatinized static PS. Unfortunately, this was not done in triplicate, and as such we could not calculate statistical difference.

3.5 DISCUSSION

TPU was optically opaque, making any cell visualization impossible. As such it was not pursued as a cell scaffold. Cell monitoring is necessary in reactor cultures, and since cells could not be easily seen on the substrate it was not used in bioreactor culture. It would be interesting to use optically clearer filament and test cells for differentiation. As softer materials have shown to induce chondrocyte differentiation, it may be a new dynamic culture method to differentiate hMSCs to chondrocytes in-situ.[4,7] This is especially true as polyurethane has been used in cartilage tissue engineering previously.[32]

PLA plasma treatment resulted in increased cell attachment, but also apoptosis. After treatment the polymer most likely retained reactive oxygen species on its surface, which while charging the surface and increasing wettability and adhesion, it also increased cell death. However, others have successfully used plasma to increase cell adhesion and have no effect on cell proliferation compared to untreated samples.[20] One difference was that the samples used in that study were ethylene oxide sterilized for four days post plasma treatment. What may be necessary for future plasma treatment steps is a PBS soak and time for surface species to dissipate. If cell death due to reactive species was mitigated

this would be a very scalable and cost-effective means of making a Xeno-free treatment for 3D cell culture.

Cellulosic scaffolds showed initial promise. Cellulosic is biocompatible and has already been tested as a drug delivery vehicle.[33–35] 3D printed cellulosic scaffolds have been proven to support cell growth.[36] However, in this case the cellulose may have been acting as a filter, catching cells as they passed through the material rather than promoting adhesion. Initially this was desirable, as cells would become stuck against the lattice through fluid movement, increasing final yield. However, untreated cellulosic did not show elongated cells indicative of cell adhesion, and thus cells did not proliferate. When cellulose was gelatinized the cells tended to grow in clusters, which has been shown to induce differentiation.[37] It has also been shown that aggregate culture decrease overall proliferation in MSCs, and as such cellulosic material was not pursued further.[38–40]

Thus, PLA was chosen for its cell adhesion, biodegradability, rigidity, and ease of manufacturing into 3D lattices.[41,42] Cells cultured for seven days retained their biomarker profile even on PLA in a dynamic culture environment. The decrease in doublings from static to dynamic culture is best explained by initial cell seating. Untreated PLA has a very high contact angle, and in dynamic culture would not catch the cells very well. In static culture though the cells would settle due to gravity, thus the initial seed would be far more efficient.

Even with this simplified small-scale reactor there were many problems. An Ishikawa diagram was used to highlight problem areas and possible causes during bioreactor culture (Figure 3-17). From this the main issues we saw that fittings were the main source of leakage and contamination. Once identified, the nylon fittings were exchanged for

polycarbonate Luer lock and stainless-steel barbed fittings, which stopped contamination and leaking problems.

3.6 CONCLUSION

Gelatinized PLA worked the best of the materials tested. Plasma treatment of the PLA led to increased hydrophilicity and better wetting. Initially cell cultures plated on plasma treated PLA showed better adhesion, however by day three cells were very sparse. This may be due to residual reactive species on the surface of the PLA. Gelatinized cellulosic also showed promise in cell culture, as cells were seeded in single cell suspension and colonies were observed by day seven. However, cell harvest was very sparse and contained degraded fragments of the matrix. Here we have shown that gelatinized 3D PLA scaffolds can support hMSC growth in a dynamic environment. Cells lifted also retained their biomarker profile.

3.7 ACKNOWLEDGEMENTS

I would like to thank Dr. Hal Van Ryswyk of Harvey Mudd College for his time and help with electron microscopy, and Dr. David Tanenbaum of Pomona College for allowing us to use the plasma cleaner. I would also like to Thank Dr. Anna Hickerson of Keck Graduate Institute for her permission to use the PrintrBot 3D printer.

1. Faiella W, Atoui R. Immunotolerant Properties of Mesenchymal Stem Cells: Updated Review. *Stem Cells Int*. 2016;2016:1-7. doi:10.1155/2016/1859567.

2. Abdallah BM, Kassem M. Human mesenchymal stem cells: from basic biology to clinical applications. *Gene Ther*. 2008;15(2):109-116. doi:10.1038/sj.gt.3303067.

3. Ortiz R, Moreno-Flores S, Quintana I, Vivanco M, Sarasua JR, Toca-Herrera JL. Laser induced topological cues shape, guide, and anchor human Mesenchymal Stem Cells. January 2018. http://arxiv.org/abs/1801.08635. Accessed March 22, 2019.

4. Park JS, Chu JS, Tsou AD, et al. The Effect of Matrix Stiffness on the Differentiation of Mesenchymal Stem Cells in Response to TGF-β. *Biomaterials*. 2011;32(16):3921-3930. doi:10.1016/j.biomaterials.2011.02.019.

5. Sun M, Chi G, Xu J, et al. Extracellular matrix stiffness controls osteogenic differentiation of mesenchymal stem cells mediated by integrin α5. doi:10.1186/s13287-018-0798-0.

6. Islam A, Younesi M, Mbimba T, Akkus O. Collagen Substrate Stiffness Anisotropy Affects Cellular Elongation, Nuclear Shape, and Stem Cell Fate toward Anisotropic Tissue Lineage. *Adv Healthc Mater*. 2016;5(17):2237-2247. doi:10.1002/adhm.201600284.

7. Olivares-Navarrete R, Lee EM, Smith K, et al. Substrate Stiffness Controls Osteoblastic and Chondrocytic Differentiation of Mesenchymal Stem Cells without Exogenous Stimuli. *PLoS One*. 2017;12(1):e0170312. doi:10.1371/journal.pone.0170312.

8. Li B, Moshfegh C, Lin Z, Albuschies J, Vogel V. Mesenchymal Stem Cells Exploit Extracellular Matrix as Mechanotransducer. *Sci Rep*. 2013;3(1):2425. doi:10.1038/srep02425.

9. Salzig D, Leber J, Merkewitz K, et al. Attachment, Growth, and Detachment of Human Mesenchymal Stem Cells in a Chemically Defined Medium. *Stem Cells Int*. 2016;2016:1-10. doi:10.1155/2016/5246584.

10. Davidenko N, Schuster CF, Bax D V, et al. Evaluation of cell binding to collagen and gelatin: a study of the effect of 2D and 3D architecture and surface chemistry. *J Mater Sci Mater Med*. 2016;27(10):148. doi:10.1007/s10856-016-5763-9.

11. Hynes RO. Integrins: Versatility, modulation, and signaling in cell adhesion. *Cell*. 1992;69(1):11-25. doi:10.1016/0092-8674(92)90115-S.

12. Chosa N, Ishisaki A. Two novel mechanisms for maintenance of stemness in mesenchymal stem cells: SCRG1/BST1 axis and cell-cell adhesion through N-cadherin. *Jpn Dent Sci Rev*. 2018;54(1):37-44. doi:10.1016/j.jdsr.2017.10.001.

13. Akitaya T, Bronner-Fraser M. Expression of cell adhesion molecules during initiation and cessation of neural crest cell migration. *Dev Dyn*. 1992;194(1):12-20. doi:10.1002/aja.1001940103.

14. De Wever O, Westbroek W, Verloes A, et al. Critical role of N-cadherin in myofibroblast invasion and migration in vitro stimulated by colon-cancer-cell-derived TGF- or wounding. *J Cell Sci*. 2004;117(20):4691-4703. doi:10.1242/jcs.01322.

15. Weber GF, Bjerke MA, DeSimone DW. Integrins and cadherins join forces to form adhesive networks. *J Cell Sci*. 2011;124(Pt 8):1183-1193. doi:10.1242/jcs.064618.

16. Curtis ASG, Forrester J V, Mclnnes C, Lawrie F, McInnes C, Lawrie F. Adhesion of cells to polystyrene surfaces. *J Cell Biol*. 1983;97(5 Pt 1):1500-1506. http://www.ncbi.nlm.nih.gov/pubmed/6355120. Accessed March 14, 2019.

17. Dominici M, Le Blanc K, Mueller I, et al. Minimal criteria for defining multipotent mesenchymal stromal cells. The International Society for Cellular Therapy position statement. doi:10.1080/14653240600855905.

18. Curtis ASG, Forrester J V, Clark P. *Substrate Hydroxylation and Cell Adhesion*. Vol 86.; 1986. http://citeseerx.ist.psu.edu/viewdoc/download?doi=10.1.1.828.4617&rep=rep1&type=pdf. Accessed March 21, 2019.

19. Ryan J. Evolution of cell culture surfaces. *Biofiles sigmaaldrich.com*. 2008. https://www.sigmaaldrich.com/china-mainland/zh/technical-documents/articles/biofiles/evolution-of-cell.html. Accessed March 26, 2019.

20. Jacobs T, Declercq H, De Geyter N, et al. Plasma surface modification of polylactic acid to promote interaction with fibroblasts. *J Mater Sci Mater Med*. 2013;24(2):469-478. doi:10.1007/s10856-012-4807-z.

21. Chuah YJ, Koh YT, Lim K, Menon N V., Wu Y, Kang Y. Simple surface engineering of polydimethylsiloxane with polydopamine for stabilized mesenchymal stem cell adhesion and multipotency. *Sci Rep*. 2016;5(1):18162. doi:10.1038/srep18162.

22. Tibbitt MW, Anseth KS. Hydrogels as extracellular matrix mimics for 3D cell culture. *Biotechnol Bioeng*. 2009;103(4):655-663. doi:10.1002/bit.22361.

23. Soares CP, Midlej V, Oliveira MEW de, Benchimol M, Costa ML, Mermelstein C. 2D and 3D-Organized Cardiac Cells Shows Differences in Cellular Morphology, Adhesion Junctions, Presence of Myofibrils and Protein Expression. Cordes N, ed. *PLoS One*. 2012;7(5):e38147. doi:10.1371/journal.pone.0038147.

24. Tappa K, Jammalamadaka U, Tappa K, Jammalamadaka U. Novel Biomaterials Used in Medical 3D Printing Techniques. *J Funct Biomater*. 2018;9(1):17. doi:10.3390/jfb9010017.

25. Szivek JA, Gonzales DA, Wojtanowski AM, Martinez MA, Smith JL. Mesenchymal stem cell seeded, biomimetic 3D printed scaffolds induce complete bridging of femoral critical sized defects. *J Biomed Mater Res Part B Appl Biomater*. 2019;107(2):242-252. doi:10.1002/jbm.b.34115.

26. Wurm MC, Möst T, Bergauer B, et al. In-vitro evaluation of Polylactic acid (PLA) manufactured by fused deposition modeling. *J Biol Eng*. 2017;11:29. doi:10.1186/s13036-017-0073-4.

27. Feng K-C, Pinkas-Sarafova A, Ricotta V, et al. The influence of roughness on stem cell differentiation using 3D printed polylactic acid scaffolds. *Soft Matter*. 2018;14(48):9838-9846. doi:10.1039/C8SM01797B.

28. Xue R, Qian Y, Li L, Yao G, Yang L, Sun Y. Polycaprolactone nanofiber scaffold enhances the osteogenic differentiation potency of various human tissue-derived mesenchymal stem cells. *Stem Cell Res Ther*. 2017;8(1):148. doi:10.1186/s13287-017-0588-0.

29. Biazar E, Ahmadian M, Heidari K S, et al. Electro-spun Polyethylene Terephthalate (PET) Mat as a Keratoprosthesis Skirt and Its Cellular Study. *Fibers Polym*. 2017;18(8):1545-1553. doi:10.1007/s12221-017-7345-y.

30. Whitely M, Cereceres S, Dhavalikar P, et al. Improved in situ seeding of 3D printed scaffolds using cell-releasing hydrogels. *Biomaterials*. 2018;185:194-204. doi:10.1016/J.BIOMATERIALS.2018.09.027.

31. Stalder A. *DropSnake and LB-ADSA User Manual*. www.epfl.ch/demo/dropanalysis. Accessed March 20, 2019.

32. Grad S, Kupcsik L, Gorna K, Gogolewski S, Alini M. The use of biodegradable polyurethane scaffolds for cartilage tissue engineering: potential and limitations. *Biomaterials*. 2003;24(28):5163-5171. http://www.ncbi.nlm.nih.gov/pubmed/14568433. Accessed March 30, 2019.

33. Furst T, Piette M, Lechanteur A, Evrard B, Piel G. Mucoadhesive cellulosic derivative sponges as drug delivery system for vaginal application. *Eur J Pharm Biopharm*. 2015;95:128-135. doi:10.1016/J.EJPB.2015.01.019.

34. de Lucena MT, de Melo Júnior MR, de Melo Lira MM, et al. Biocompatibility and cutaneous reactivity of cellulosic polysaccharide film in induced skin wounds in rats. *J Mater Sci Mater Med*. 2015;26(2):82. doi:10.1007/s10856-015-5410-x.

35. Nugraha B, Hong X, Mo X, et al. Galactosylated cellulosic sponge for multi-well drug safety testing. *Biomaterials*. 2011;32(29):6982-6994. doi:10.1016/J.BIOMATERIALS.2011.05.087.

36. Sultan S, Siqueira G, Zimmermann T, Mathew AP. 3D printing of nano-cellulosic biomaterials for medical applications. *Curr Opin Biomed Eng*. 2017;2:29-34. doi:10.1016/J.COBME.2017.06.002.

37. Sart S, Tsai A-C, Li Y, Ma T. Three-dimensional aggregates of mesenchymal stem cells: cellular mechanisms, biological properties, and applications. *Tissue Eng Part B Rev*. 2014;20(5):365-380. doi:10.1089/ten.TEB.2013.0537.

38. Muraglia A, Corsi A, Riminucci M, et al. Formation of a chondro-osseous rudiment in micromass cultures of human bone-marrow stromal cells. *J Cell Sci*. 2003;116(Pt 14):2949-2955. doi:10.1242/jcs.00527.

39. Wang W, Itaka K, Ohba S, et al. 3D spheroid culture system on micropatterned substrates for improved differentiation efficiency of multipotent mesenchymal stem cells. *Biomaterials*. 2009;30(14):2705-2715. doi:10.1016/J.BIOMATERIALS.2009.01.030.

40. Hildebrandt C, Büth H, Thielecke H. A scaffold-free in vitro model for osteogenesis of human mesenchymal stem cells. *Tissue Cell*. 2011;43(2):91-100. doi:10.1016/J.TICE.2010.12.004.

41. Lesage F, Roman S, Pranpanus S, et al. Modulation of the Early Host Response to Electrospun Polylactic Acid Matrices by Mesenchymal Stem Cells from the Amniotic Fluid. *Eur J Pediatr Surg*. 2018;28(03):285-292. doi:10.1055/s-0037-1603522.

42. Santoro M, Shah SR, Walker JL, Mikos AG. Poly(lactic acid) nanofibrous scaffolds for tissue engineering. *Adv Drug Deliv Rev*. 2016;107:206-212. doi:10.1016/J.ADDR.2016.04.019.

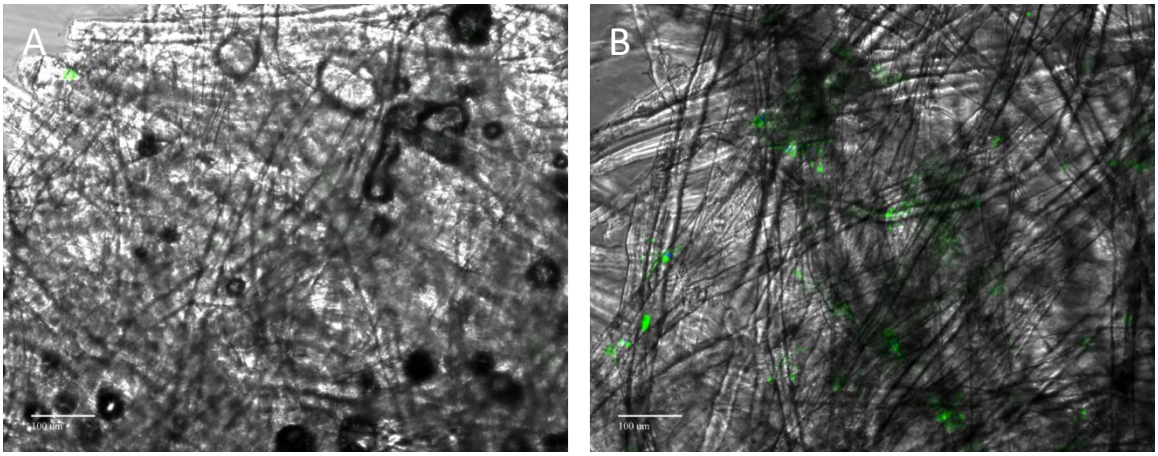

Figure 3-1: Bend3 Cultures on A) untreated control and B) gelatinized cellulosic material in static culture conditions. Cells were seeded statically by overlaying cell containing media onto scaffolds and culturing for 24 hours. Green is actin staining.

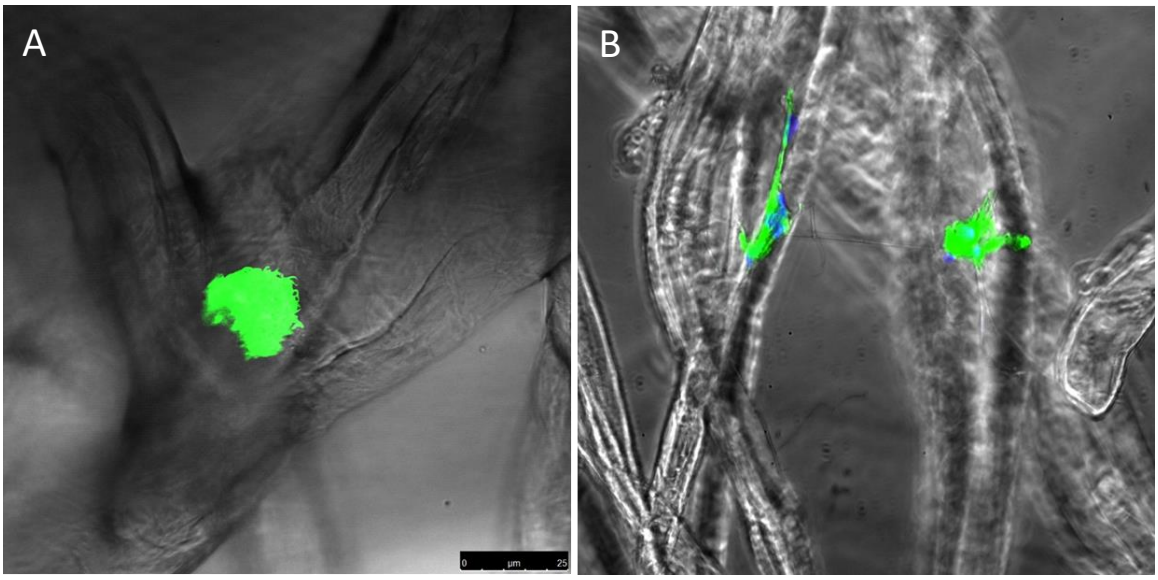

Figure 3-2: hMSCs culture on cellulosic fibers after 24 hours. A) Single cell on ungelatinized control and B) Gelatin coated cellulosic material in seeded statically. Green is actin and blue are the nuclei. Nuclear staining was not seen in A because of issues with UV laser on the confocal.

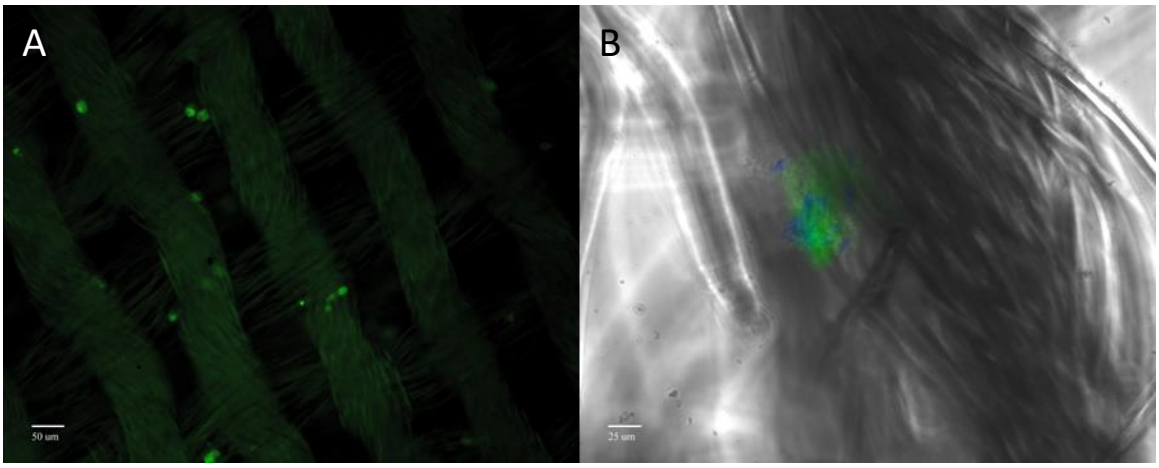

Figure 3-3: hMSCs grown on other fiber lattices for seven days. A) Gelatin coated silk fibroin and B) gelatin coated Polyethylene. Green is actin and blue are the nuclei.

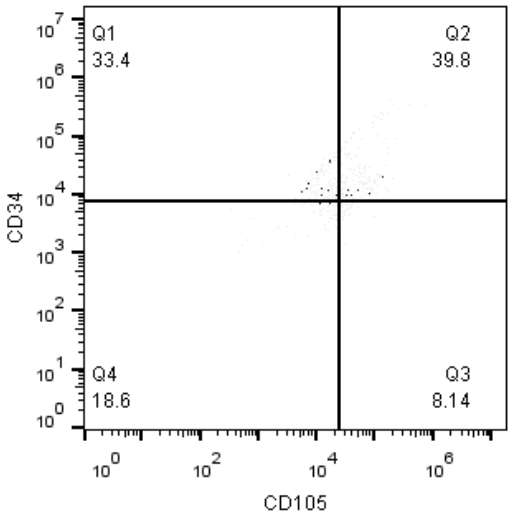

Figure 3-4: Flow cytometry of hMSCs grown for seven days on Polyethylene in static culture. Very few cells recovered from PE fiber swatch, so very few cells were tested for flow cytometry.

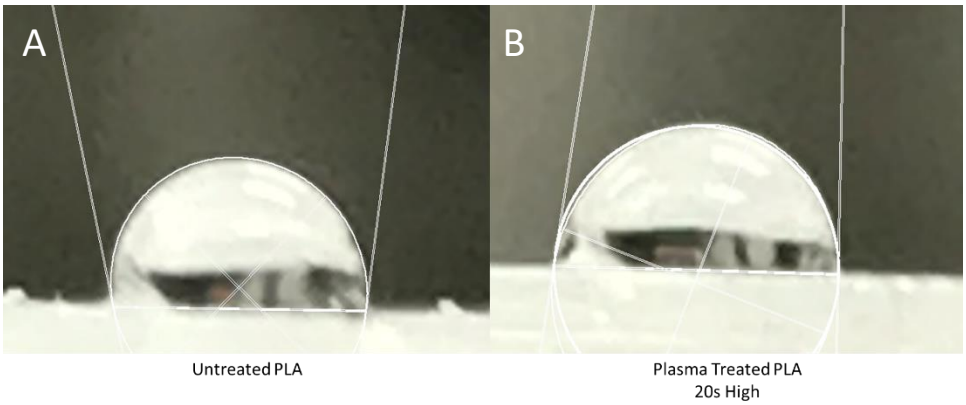

Figure 3-5: Contact angle measurements of PLA. Vertical lines overlaid onto picture of 2µl droplet created using drop_snake software. The circumference of the drop is outlined through the software, which then calculates the angle from normal. A) Untreated PLA from printer. B) Three-minute plasma treated PLA.

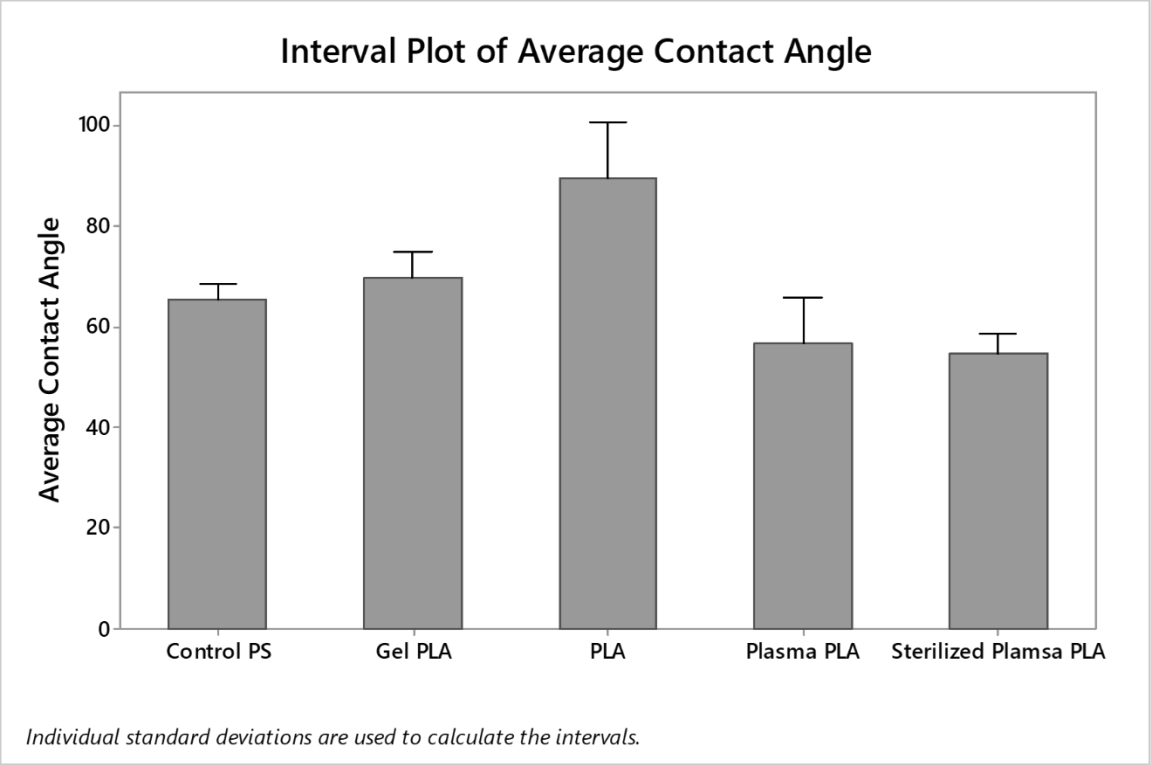

Figure 3-6: Contact angles of plastics and treatments calculated via the drop_snake method in FIJI.

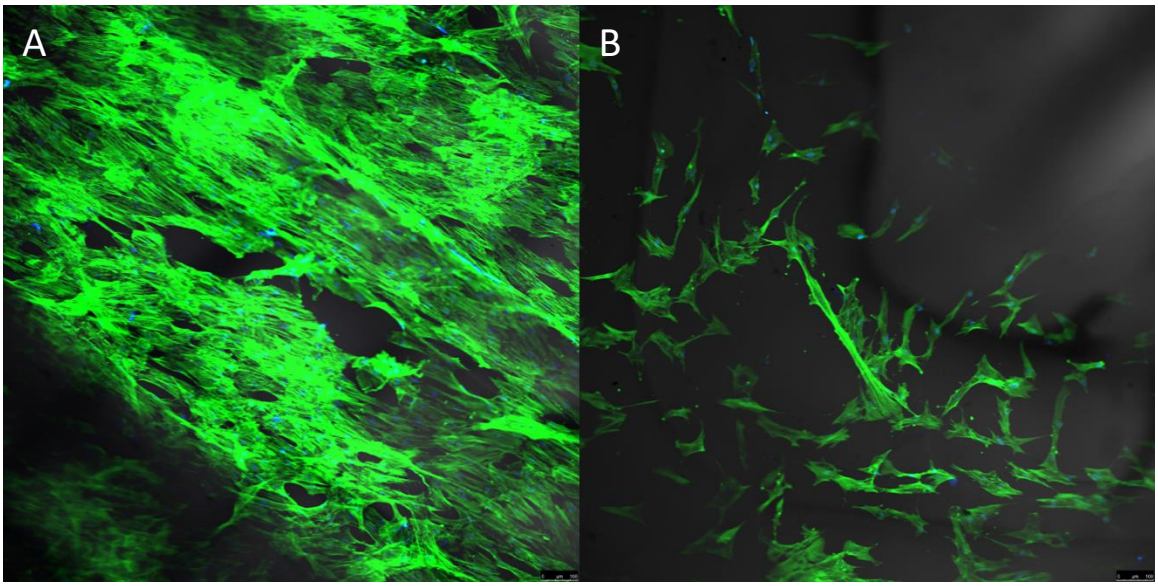

Figure 3-7: hMSCs statically seeded onto plasma treated PLA 2D sheets. A) hMSCs show adhesion to PLA surface after 24 hours. B) After 48 hours hMSCs appear more sparse on the surface of the plasma treated PLA. Green is actin and blue are the nuclei.

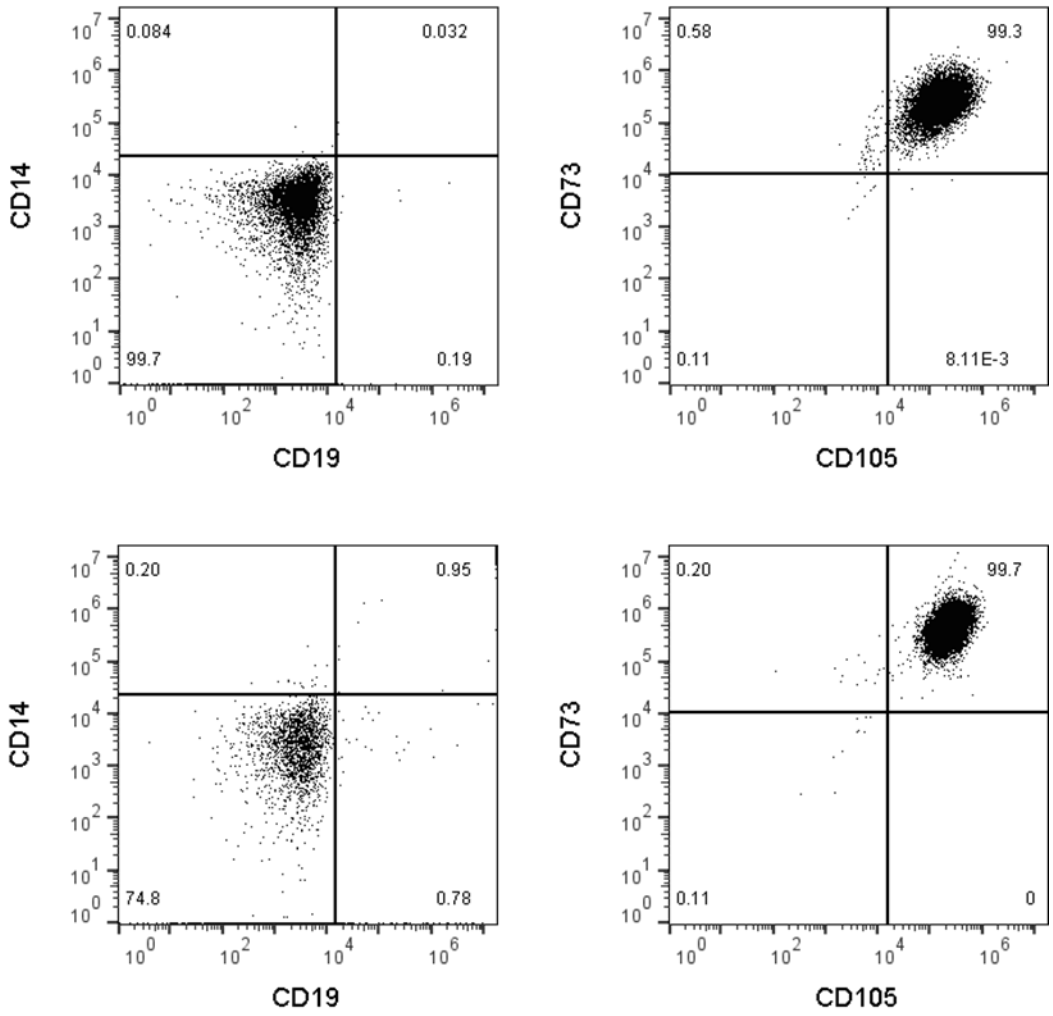

Figure 3-8: Static culture of hMSCs on PLA static controls. Cells were fixed, blocked, and stained for surface markers CD105 CD73 CD19 and CD14. Rows correspond to two different samples.

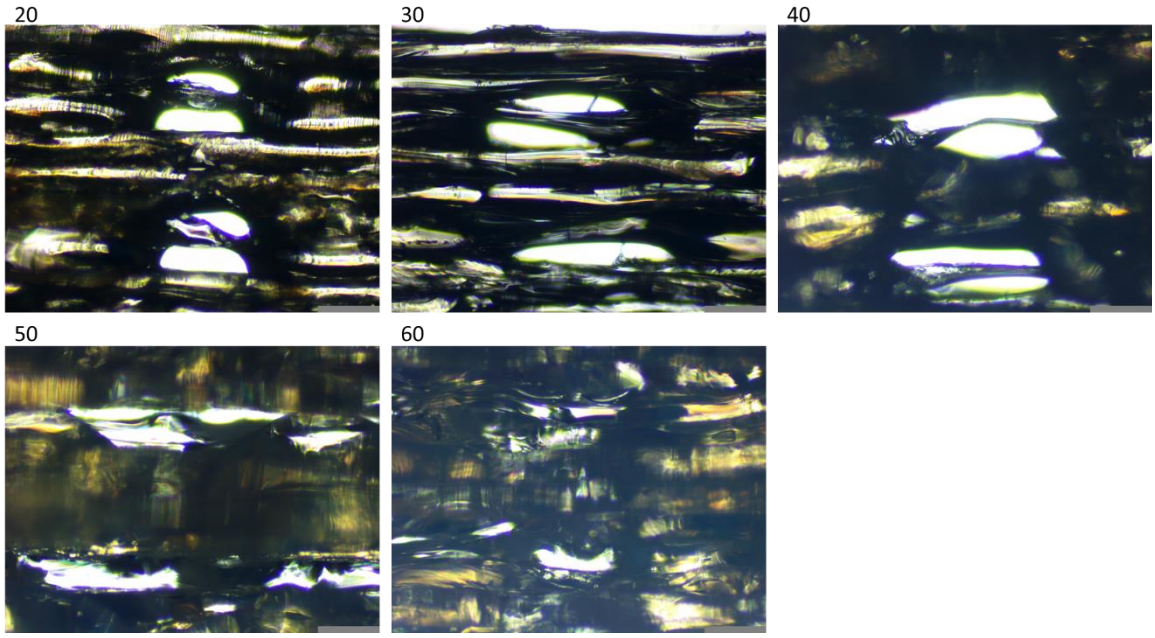

Figure 3-9: Printer speed effect on 3D printed PLA lattice pore geometry. Scale bars are 200 microns and values above images are the printer speed in mm s^{-1}. Viewed from the side (XZ).

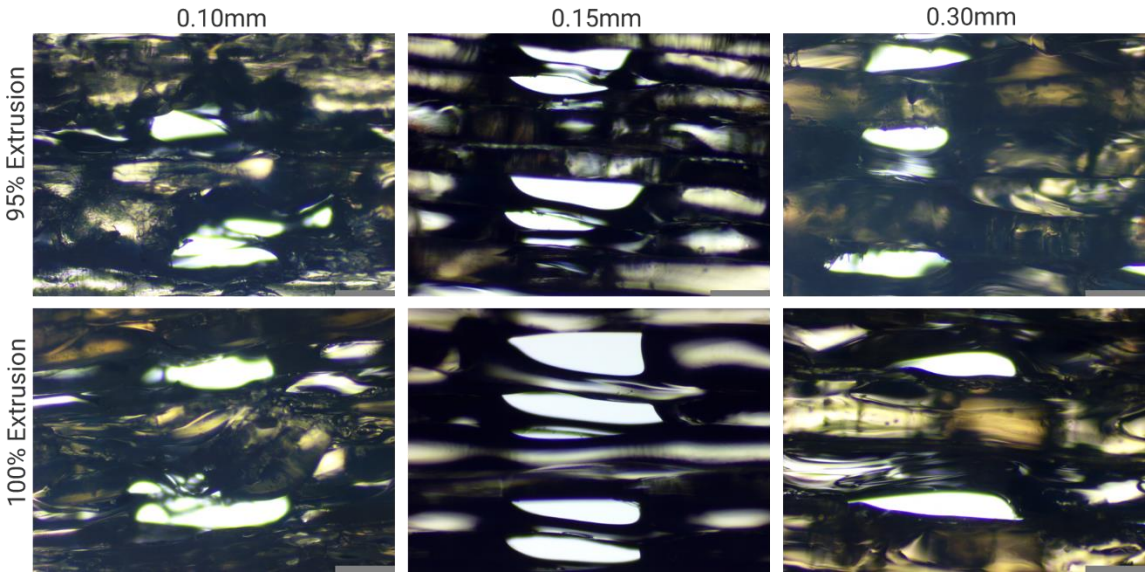

Figure 3-10: Printer setup. Extrusion percent vs layer height. Viewed from the side (XZ). Scale bars are 200 microns.

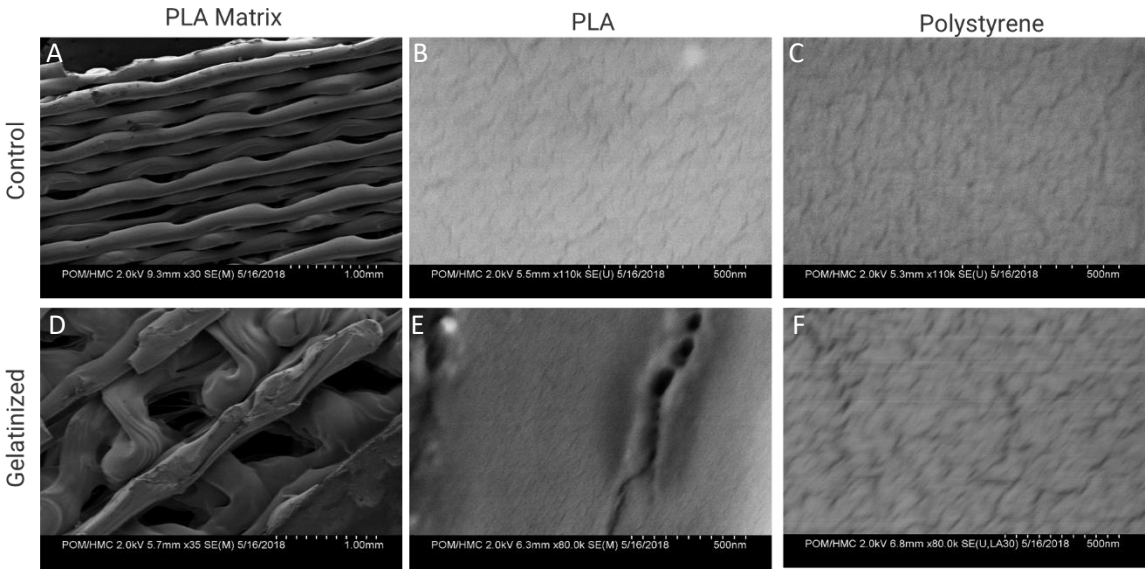

Figure 3-11: SEM images of Polystyrene and PLA lattice. Top row shows ungelatinized controls and bottom are gelatin treated. A) Low magnification image of the side of ungelatinized PLA lattice. B) High magnification of ungelatinized PLA. C) Ungelatinized PS control culture dish at high magnification. D) Low magnification of gelatinized PLA lattice from the top view. E) High magnification image of gelatinized PLA. F) High magnification of gelatinized polystyrene culture plate control.

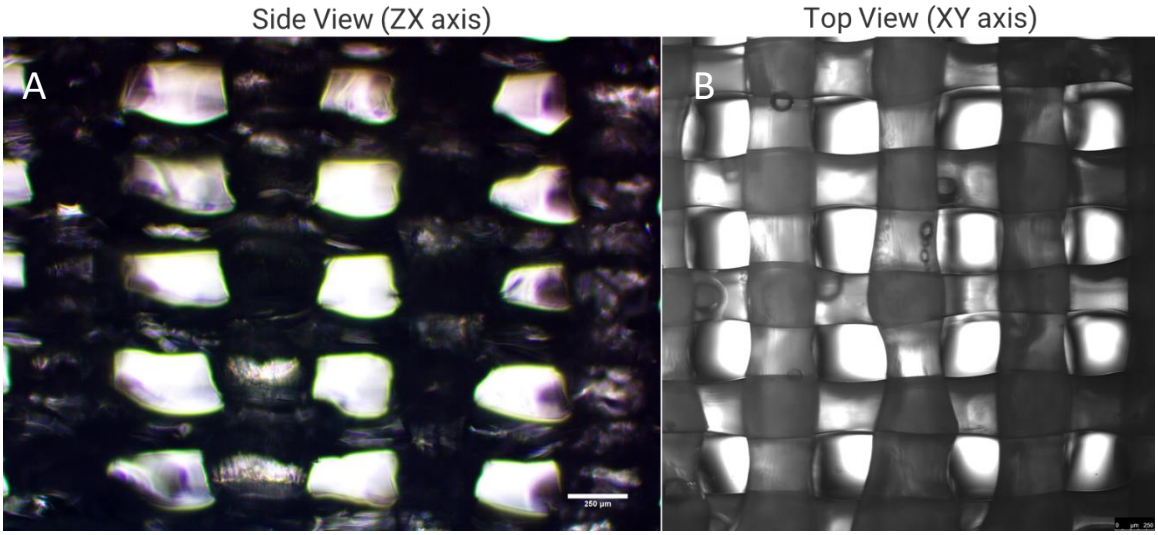

Figure 3-12: Improved printing of lattice. By altering G-code 3D printer more homogenous prints were achieved with less burning and distortion of filaments. A) shows a ZX plane of the print and B) shows a XY plane.

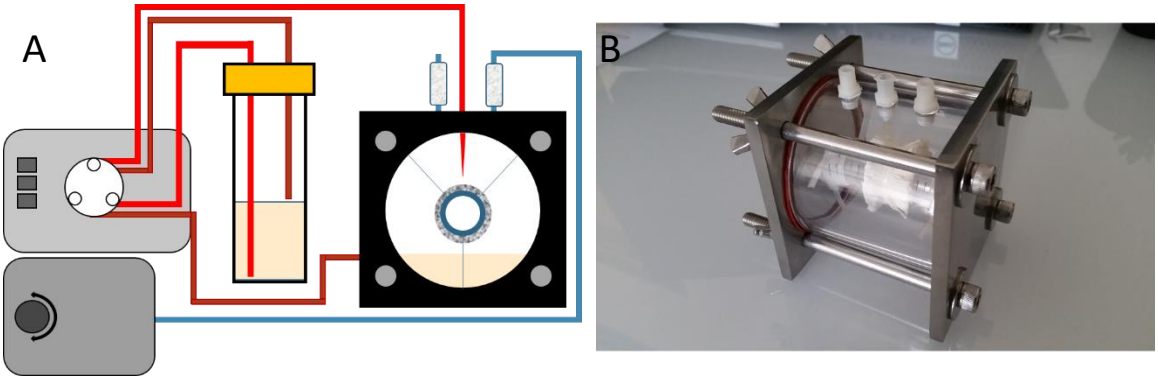

Figure 3-13: Bioreactor design using cellulosic scaffold. A) Cartoon diagram showing reactor, reservoir, peristaltic pump and air pump. B) Assembled cellulosic scaffold-based reactor. Reactor comprised of two 316 stainless steel capping a polycarbonate chamber sealed with high temperature silicone O-rings sealed. Four threaded Luer loc connectors allow media circulation and gas exchange.

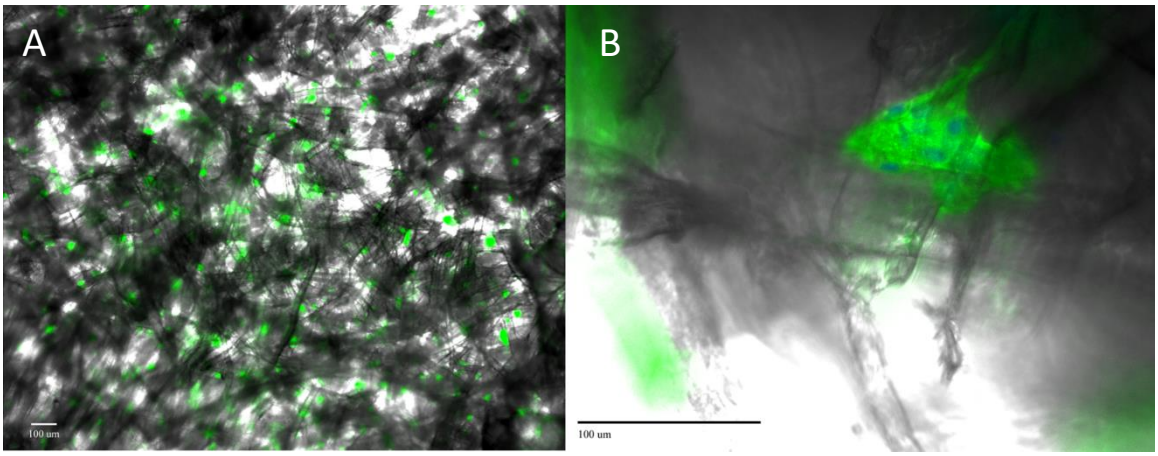

Figure 3-14: hMSCs cultured for seven days on gelatin treated cellulosic scaffold in dynamic bioreactor culture. A) Low magnification picture of seeded lattice. B) High magnification of cell cluster grown from single cell. Green is actin and blue are the nuclei.

.

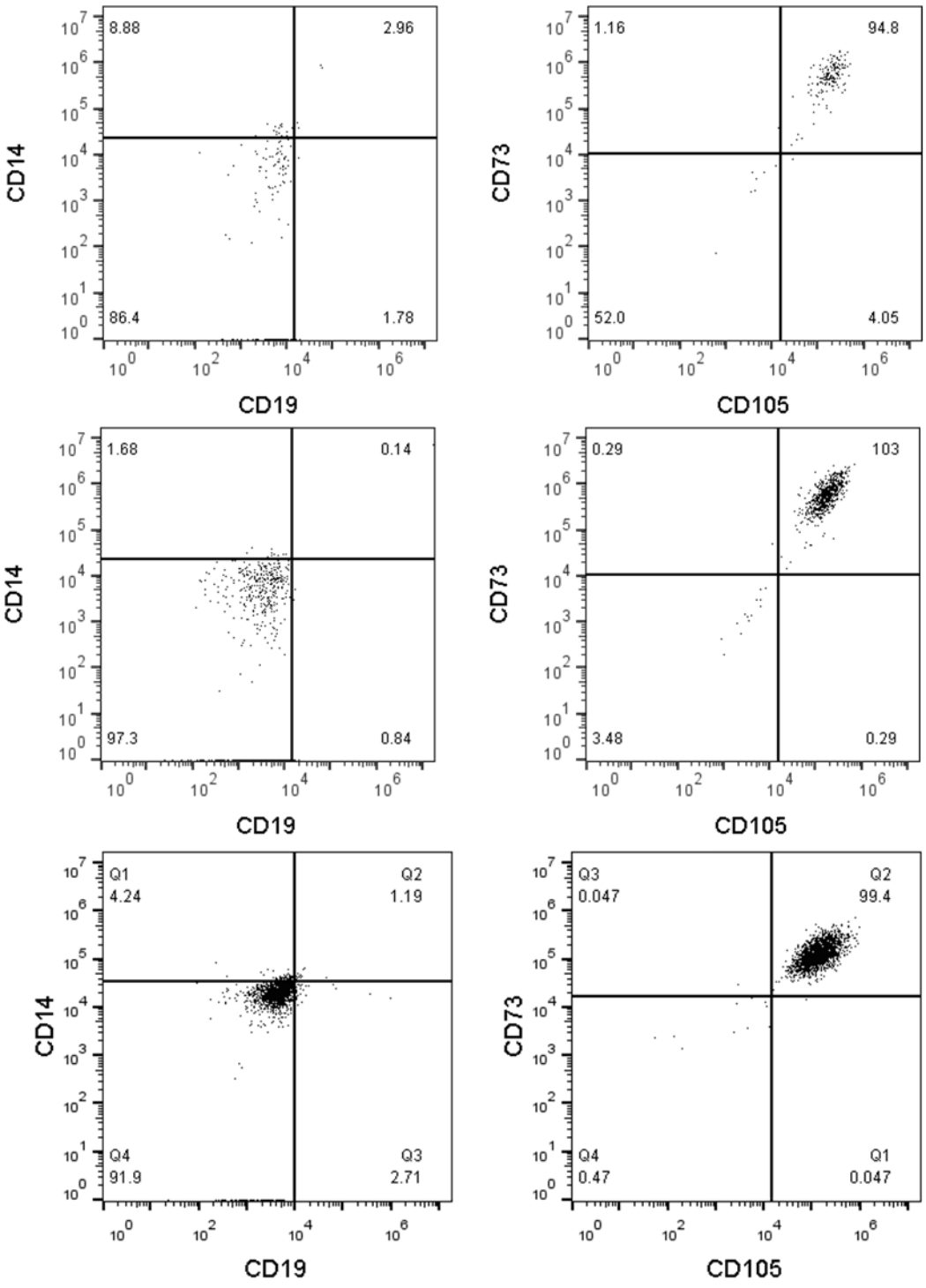

Figure 3-15: F Flowcytometry of hMSCs from PLA Bioreactor lifted on day 7. Cells were cultured in normoxic conditions in the PLA lattice for seven days prior to lifting and staining. Cells were fixed, blocked and stained for CD105 and CD34. Each row is one sample.

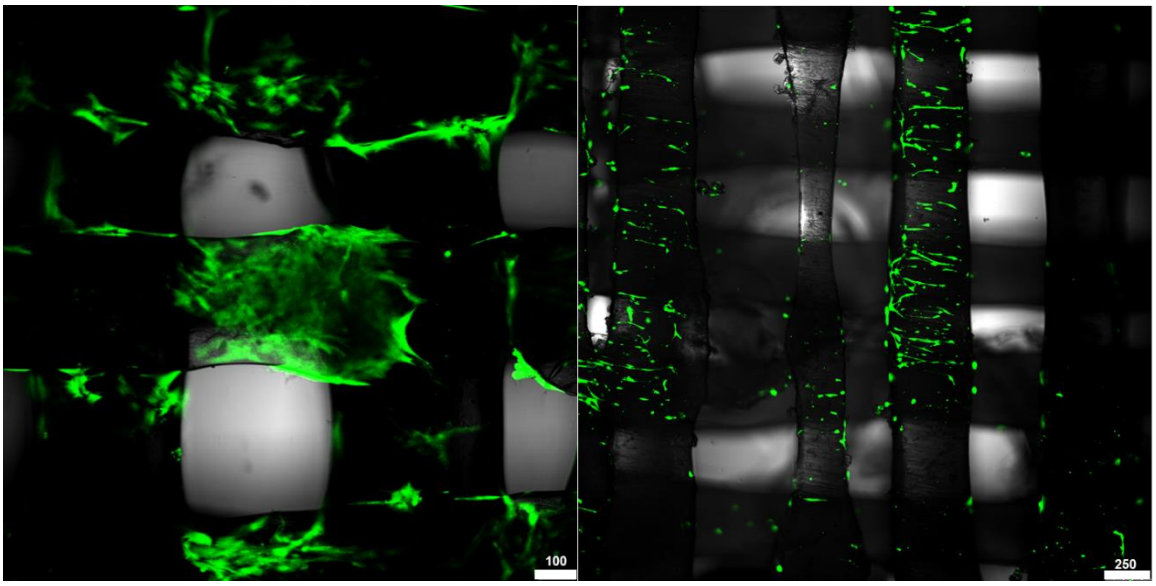

Figure 3-16: Cells on improved PLA Lattice. hMSCs were cultured for seven days on the PLA scaffolds in the bioreactor, then stained for viability. Green is Calcein viability staining.

Table 3-1 Doubling statistics of hMSCs on various culture substrates

Condition	Doublings	Doubling Time (hr)	μ (1/hr)	Fold Increase
PS Static	1.37	124	0.006	2.93
PS Static 0.1% Gelatin	1.56	109	0.006	-
Cellulosic Matrix	1.81	93	0.007	3.00
PLA Static	2.08	80	0.009	2.69
PLA Dynamic	1.42	120	0.006	2.72

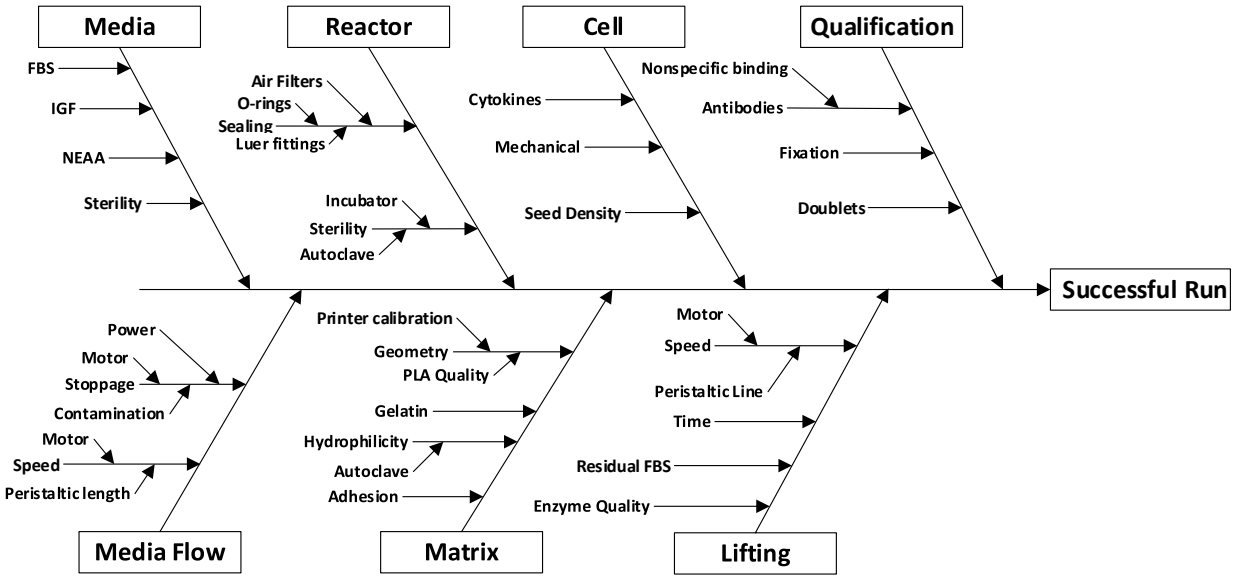

Figure 3-17: Ishikawa diagram of sensitive processes and problem areas in stem cell culture.

4 STEM CELL REACTOR CULTURE

4.1 ABSTRACT

Bone marrow derived human Mesenchymal Stem Cell (hMSC) harvest is invasive, painful, and expensive, which makes it difficult to supply the enormous amount of pure hMSCs needed for future allogenic therapies. Because of this, a robust method of scaled bioreactor culture must be designed to supply the need for high purity, high density hMSC yields. Here we test a scaled down model of a novel bioreactor consisting of a 3D printed PLA lattice matrix suspended outside of its culture media. The growth matrix is a uniform and replicable biocompatible 3D printed polylactic acid lattice matrix, which enables homogenous cell culture in three dimensions. The system tested resulted in comparable stem cell yields to other cell culture systems using bone marrow derived hMSCs, while maintaining high purity (>98% expression of combined positive markers), high viability (96.54% ±2.82), and differentiation ability into functional cell types.

4.2 INTRODUCTION

Stem cells are a major component of regenerative medicine that show promise of curing chronic diseases and organ regeneration.[1] What defines this cell type and cements its usefulness in regenerative therapies is that stem cells can both self-renew and differentiate into functional cell types. Stem cells are generally classified into three main types: embryonic, induced pluripotent, and adult stem cells. Human Mesenchymal Stem Cells (hMSCs) are a type of adult multipotent stem cell which can differentiate into many

useful cell types for regenerative medicine including osteocytes, adipocytes, chondrocytes, myocytes, and cardiomyocytes.[2] hMSCs have been widely researched, and hMSC derived stem cell therapies are currently under clinical trials for cardiovascular, neurologic, bone and cartilage, lung, kidney, liver, and autoimmune diseases.[3] They also show immunotolerant and immunomodulatory properties in allogenic transplants.[2,4] However, bone marrow derived hMSC harvest is invasive, relatively low yield, and painful, making allogenic therapies difficult and expensive.[5]

The challenges of creating therapeutic dosages lies in both the number of cells needed for a successful therapy, and the sensitive nature of hMSCs. It is estimated that a therapeutic dose of 10^6 to $15x10^6$ stem cells per kilogram are needed to treat diseases such as diabetes and myocardial infarction.[6–9] These high estimates are due to apoptosis, unwanted differentiation, and cell attrition after implantation.[10–12] Furthermore, dosing strategies may require multiple doses, further inflating estimates. This may explain the lack of phase three clinical trials.[12] Scaled bioproduction of hMSCs is one way to supply such a large number of stem cells. However, conventional scalable culture procedures are difficult since hMSCs are anchorage dependent and sensitive to mechanical and chemical stresses.[13–15] Exposure to high shear stress, media gradients, unfavorable surface treatments, improper cytokine mixtures, or nanotopologies can lead to differentiation and apoptosis.[15–18] In scalable systems aimed at producing hMSCs, any of these factors would decrease purity and result in lost yield. Per the International Society for Cellular Therapy (ISCT), tested stem cell populations must be greater than 95% positive for CD105, CD73, and CD90, while being negative (less than 2% positive) for CD45, CD34, CD19 and CD14 via flow cytometry in order to be considered pure.[19] hMSCs must also maintain

their ability to differentiation into adipocytes, chondrocytes, and osteocytes. Any decrease in purity would increase downstream purification, further decreasing cell yield and increasing cost.

To meet the high hMSC yields and purities needed, specialized bioreactors have been developed to optimize culture conditions. Systems used for stem cell bioprocessing vary but fall into three general categories: stacked two-dimensional surfaces, microcarrier or aggregate based, and fixed bed reactors. A brief comparison of various adherent cell culture methods can be seen in Table 4-1. Stacked systems such as the Xpansion Multiplate parallel plate bioreactor (Pall) combine multiple 2D culture surfaces into one unit analogous to multiple T-flasks.[20] Media can then be flowed laterally across the cells to supply nutrients and exchange gases. Though the most similar to flask culture, it is difficult to visualize for in-process tests and may produce more shear than desired.[21,22] Microcarriers have been used for 3D suspension culture of adherent stem cells. They can be made from a variety of materials including inorganic plastics, sugars, and digestible materials.[12,23,24] The microcarriers are suspended via mechanical mixing while cells adhere to the surface of the microcarriers. Because mixing is usually impeller driven, cells can be exposed to high shear.[22,25] Using microcarriers also involves more downstream processes to purify the cells from the carriers, and lifting procedures can involve multiple steps.[7,26] Fixed bed reactors use fiber mesh as their culture surface and provide nutrient and gas exchange by flowing media through the mesh. Examples of this type of bioreactor include the iCELLis (Pall), hollow fiber membranes such as Quantum (Terumo BCT), and the Express (Sepragen) reactor. Like the multiplate systems

mentioned, it is difficult to visualize the cells during culture. A summary of cell yield and reported values of various cell culture systems can be seen in Table 4-2.

Here we investigate a scaled down model of the Express bioreactor. The variant tested works much like the parent reactor, using gravity and wicking of media to provide nutrients and gas exchange to a growth matrix suspended above culture media. This geometry and media circulation strategy results in low shear fluid movement. Instead of cellulosic, a 3D printed lattice made of Polylactic Acid (PLA) lattice matrix is suspended outside of the liquid media, providing a biocompatible culture surface with similar stiffness to plastics used in conventional culture. Small sampling shelves are integrated into the lattice matrix, which can be easily removed for cell sampling and imaging. By combining this dynamic culture method with a hypoxic conditioning, stem cell proliferation was significantly increased while maintaining stem cell biomarker expression.

4.3 METHODS

4.3.1 Stem cell culture

hMSCs were cultured according to guidelines provided from American Type Culture Collection (ATCC). Briefly, cells were cultured in hMSC media (ATCC PCS-500-030) supplemented with the bone marrow derived hMSC bullet kit (ATCC PCS-500-041) at 37°C and 5% CO_2 on T-75 treated tissue culture flasks. A ¾ media exchange was performed on day 3, and cells were passaged at 80% confluency, usually on days 6 or 7. Cells were lifted using 3.5mL of 0.25% trypsin and 0.53 mM EDTA solution (ATCC 30-2101) for regular passaging of T-75 flasks, and cells were re-plated at 5,000 cm^{-2}. Cell

pelleting was performed by centrifugation at 270 x g for 5 minutes. Working cell bank was created from passage 4 hMSCs and stored in liquid nitrogen. Experiments using hMSCs were conducted on cells between passage 5 and 9. Specific growth rate and doubling time were calculated to compare culture success.

$$T_d = (T_2 - T_1) * \frac{\ln(2)}{\ln\left(\frac{q_2}{q_1}\right)}$$

Equation 4-1: Doubling time. Where T_d is the doubling time in days, q_2 is the final cell count, and q_1 is the initial cell seeding quantity.

$$\mu = \frac{\ln\left(\frac{q_2}{q_1}\right)}{t}$$

Equation 4-2: Specific growth rate. Where μ is the specific growth rate in hours, q_2 is the final cell yield and q_1 is the initial cell seeding quantity.

4.3.2 Oxygen tension studies

To induce low oxygen states, cells were placed in a hypoxia chamber (billups-rothenberg) and gas flushed for 6 minutes with the regulator set at 5PSI and 10L min^{-1}. Gas composition varied but was mixed based on PSI. For reactor cultures the mixed gasses were introduced at 100mL min^{-1} for 5 minutes to exchange the head space and oxygen from the media. At first tri-gas mixture including 5% CO2 was used, but hMSCs preferred basic conditions and as such $CO_2$was excluded from later bioreactor runs with negligible impact on yield and purity.

4.3.3 Reactor construction

The chamber of the reactor is made of a 9cm long polycarbonate tube with an ID of 2.25in and an OD of 2.50in. Four 316 stainless steel barbed hose adapters are tapped into

the top of the polycarbonate, two for media circulation and two for gas exchange through 0.2µm filters. Size 14 silicone hose was used for main liquid handing loop, with a Tygon Pharmed section for peristaltic pumping. The headplate and backplate are made of 316 Stainless steel. The interior reactor components include the 3D printed matrix, which is suspended out of the media using two brackets. Media pumped to the top of the lattice is perfused through the lattice design via gravity, providing gas exchange and nutrients to the cells. Gas control is highly tunable, as there is less liquid for gas to diffuse through to be available to the cells. The front plate of steel has a pass-through port for access to removable sampling scaffolds to monitor cell confluency. Both the lattice matrix and the holding parts were printed from PLA. Minimum and maximum working volumes used were 20 and 30mL.

4.3.4 Lattice design and bioreactor culture

PLA matrices were 3D printed using a PrintrBot Simple printer and Cura 3D (V3.2.1) printing software. A 0.4mm nozzle diameter was used. PLA was chosen as it has been used for cell culture, is both biocompatible and biodegradable, and is a thermoplastic commonly used in 3D printing.[27,28] The lattice is constructed in such a way that the smallest features are printable with a conventional 3D printer, and allow ample space for cells to culture into monolayers. For this extruder the lower limit of resolution was 400 microns in the XY plane. The lumen between fibers was made to be the same width as the fiber itself. Also included into the design are two inserts for non-destructive means of visualization of cell confluence and viability via calcein staining. To sterilize parts before culture, the matrix and supports are assembled and placed into reactor and steam sterilized at 121°C for 15 minutes under a dry cycle. After sterilization the matrix is

washed and wetted with filtered and autoclave-sterilized 1x PBS (VWR VE404) and gelatinized with filtered and autoclave-sterilized 0.1% (W/V) gelatin (Fisher 9000-70-8) in MQ water for 45 minutes at 37°C, or overnight at 4°C. The matrix is then rinsed with PBS to remove excess gelatin, and cells are seeded at 2,500 cells cm^{-2}. Approximate surface area was calculated using Solidworks (Waltham, MA) analysis function. To allow cells to adhere only in the lattice the desired number of cells were resuspended first in a total of 2mL, as this volume was found to be the holding volume of the matrix. Cells were allowed to settle in the matrix for 45 minutes before starting the recirculation loop. Recirculation was run between 0.25mL min^{-1} and 0.5mL min^{-1}. A range is noted because as the peristaltic tube relaxed during use, the peristaltic pump tended to speed up, slightly increasing the overall rate. This was the allowable flow rate range because it was the slowest rate that still allowed complete matrix wetting. A ¾ media exchange was performed on day 3, and cells were harvested on day 7 using a lifting cocktail comprised of a 2:1 mixture of Cell Dissociation Buffer (CDB) (Gibco 13151014) and TrypLE-Express (Gibco 12604021). Lifting was accomplished by aspirating media out and cycling 10mL of PBS through system at 1ml min^{-1} to remove residual media. PBS was then aspirated and cell lifting cocktail was added. The reactor was then cycled at 0.25ml min^{-1} for 30 minutes, or later at 1.5mL min^{-1} for 15 minutes. Viability and cell counting were performed using hemocytometer and trypan blue staining.

4.3.5 Microcarrier culture in spinner flask

Cytodex-1 microcarriers were weighed and autoclaved at 121°C for 15 minutes. Microcarriers were then hydrated in hMSC media. Cells were seeded at 5,000 cells cm^{-2} in 50mL of media in a 250mL spinner flask (Wheaton). For the first 24 hours, the spinner

flask was set to 15RPM to allow hMSCs time to adhere to the microcarriers, after which agitation was increased to 30RPM and volume increased to 80mL. A ½ media change was performed on day 3. Samples were drawn each day and fixed in 4% paraformaldehyde (PFA) for 15 minutes. Cells were then prepared for cell counting via DRAQ5 (Abcam ab108410), staining in a 5mMol solution overnight. Samples were then washed twice with PBS, allowing microcarriers to gravity settle between washes. Samples were imaged on Leica SP5. The culture was run for a total of 7 days. On day 7 media containing microcarriers was split into 50 falcon tubes and microcarriers allowed to settle for 20 minutes. Media was aspirated and microcarriers washed twice with PBS. When settled again, TryplE (Gibco 12604021) was added and mixture was put back into the incubator for one hour to lift cells for counting and characterization.

4.3.6 Confocal microscopy

Cells were cultured on lattice matrices in the bioreactor for seven days. Cells were washed using Ca^{++} and Mg^{++} PBS and fixed in place with 4% PFA for 15 minutes and washed again with PBS. Permeabilization was performed using 1% (W/V) Triton-X 100 in PBS for 30 minutes at 37°C. Cells were then washed and placed in 1% (W/V) Bovine Serum Albumin (BSA) and 0.1% (W/V) Triton-X 100 in PBS for one hour at room temperature. Cells were then stained for 30 minutes with 1 drop mL^{-1} Phalloidin green (Invitrogen) and 1µl mL^{-1} DRAQ 5 (Abcam) resulting in a 5mMol solution in the blocking solution. Cells were washed with Ca^{++} and Mg^{++} PBS and imaged on a Leica SP5 confocal microscope.

4.3.7 SEM imaging

PLA matrices were washed and prepared for electron microscopy. Samples were stuck to 0.5in slotted stages (TED PELLA 16111) using conductive double-sided copper tape. Samples were imaged at 2kV using Hitachi SU-70 scanning electron microscope.

4.3.8 Flow cytometry

hMSCs were cultured in experimental conditions and lifted with a 2:1 mixture of Cell Dissociation Buffer (CDB) (Gibco 13151014) and TrypLE-Express (Gibco 12604021) lifting cocktail to preserve cell surface markers. Cells were washed in PBS and placed in lifting cocktail for 15 minutes. After neutralization with fresh media, cells were fixed in 4% PFA for 15 minutes, washed twice with PBS, and blocked for 1 hour at room temperature. Blocking solution consisted of 1% (W/V) BSA (LONZA) and 0.1% (W/V) Triton-X 100 in PBS. Cells were stained for the positive markers CD105 (Invitrogen MHCD10520) and CD73 (Abcam ab157335) and were negative markers CD14 (Abcam ab91146) and CD19 (Abcam ab25510) at 1µL per 500,000 cells in 500µL following recommendations. Samples were then run at medium speed (35µl/min) on a BD Accuri C6 flow cytometer and analyzed using FlowJo (Ashland, OR). Unstained controls were used to gate cells. Fluorophore compensation was done through FlowJo and Fluorescence minus one (FMO) techniques.

4.3.9 hMSC Differentiation and staining

For both adipocyte and osteocyte differentiation, hMSCs were seeded at 12,000 cells cm^2 and cultured for three days in hMSC media following ATCC Toolkit protocols. ATCC differentiation toolkits for Osteocyte (PCS-500-052) and Adipocyte (PCS-500-050)

differentiation were used. On the third day media was completely exchanged. For Adipocyte differentiation a conditioning pre-differentiation media was used, and every third day a ½ media change was performed with Adipocyte maintenance media. Osteocyte differentiation did not require a conditioning media and was maintained with only osteocyte toolkit media. On day 20 cells were washed with calcium magnesium free PBS and fixed by 4% PFA at room temperature for 15 minutes. Cells were washed, stained following respective protocols explained below, washed with MQ water, and visualized on a phase contrast Olympus IX microscope.

Chondrocyte induction was performed according to a combination of ATCC protocols and previous research. Briefly, hMSCs were lifted from reactor using lifting cocktail, and counted. Cells were resuspended in chondrocyte differentiation toolkit (ATCC PCS-500-051) at 125,000 cells mL^{-1}. 200µl of cell laden media was put into 15ml polypropylene falcon tubes and centrifuged at 270 x g for 5 minutes and placed into incubator without resuspending cell pellet. When placed into incubator the tops of the tubes were loosened to allow gas exchange. After 24 hours the pellet was gently suspended via pipetting. Media was changed every 3 days for 21 days total. On day 21 cell aggregates were sliced into 8µm thick samples using a HM 500 cryostat (Microm) and OTC compound (Tissue Tek 4583) and place onto glass slides. Samples were then stained and visualized on a phase contrast Olympus IX microscope.

4.3.9.1 Oil red O

Oil Red O was used to stain adipogenic differentiation of hMSCs. A working solution was prepared by mixing 3ml of Oil Red solution (#O-1391, Sigma) 2ml of MQ water

immediately before. Cells were covered with oil red working solution and stained for 30 minutes at room temperature. Cells were washed twice with MQ water and visualized.

4.3.9.2 Alizarin red

Alizarin Red stain was used to stain osteogenic differentiation of hMSCs. It arrived in working concentration at the proper pH, so no extra formulation was necessary. After fixation cells were washed twice with MQ water, then Alizarin red staining was overlaid onto the cells and left for 15 minutes. Cells were then washed three times with MQ Water and visualized.

4.3.9.3 Alcian blue

Alcian blue was used to stain for chondrogenic differentiation of hMSCs. After cryostat slicing the samples were washed in Ca^{++} Mg^{++} PBS to preserve attachments while removing OTC compound, and fixed for 15 minutes in 4% PFA. The slides were then washed gently in DI water and alcian blue stain was overlaid onto the samples for 30 minutes. After 30 minutes the slides were rinsed with DI water, and then washed with 3% (V/V) glacial acetic acid solution in MQ water to remove excess dye. The cells were then gently rinsed again with DI water and visualized.

4.3.10 Computational fluid dynamic modeling

A simplified model was created in ANSYS 8.1 using a multiphase Volume of Fluid model in ANSYS FLUENT 18.2 (ANSYS Inc., Canonsburg, PA). The model consists of an inlet, the lattice made of crossing 0.4mm square flow channels, a center void where the lattice would be anchored to its support in the system, and an outlet. The object was meshed with 28,530 quadrilateral elements. Viscosity was modeled using Naiver-stokes

equations and simulated using Standard K epsilon. Both energy and species transport were included. The SIMPLE pressure-velocity coupling scheme was used to run a transient model. Momentum convergence was set to 10^{-8}. The inlet velocity was calculated by taking volumetric flow and dividing it by the diameter of the simulated inlet to give velocity. The model was validated comparing velocity in the model to dye experiments. Shear stress was calculated by equation 3 using reported strain rate.

$$\tau = \eta\gamma$$

Equation 4-3: Shear Stress. Where τ is the shear stress in dynes cm^{-2}, γ is the strain rate (s^{-1}), and η is the viscosity of the liquid in dynes cm^{-2}.

This value was used in conjunction with the lowest flow rate needed to keep the lattice wetted.

4.3.11 Statistics

Graphs and statistics were done using Minitab 17 (Minitab Inc., PA). Error bars on graphs show 2 standard errors. Student's two-tailed t-test was used to determine significance for two data sets. Significance of multiple data sets was performed via one-way ANOVA and Tukey test.

4.4 RESULTS

4.4.1 Scaled System

The aim of this work was to show high purity, high yield stem cell culture on a 3D biocompatible lattice. To do this a scaled model of the system of the Express bioreactor

was engineered, conserving the main geometry of the reactor chamber and method of media handling. PLA was used in leu of cellulosic, as cells tended to grow in clusters on cellulosic fibers (data not shown). To accommodate the PLA in an unobtrusive way, two stands were also made using 3D printing. To decrease shear from the falling water droplet, a 316 stainless steel tip was added to allow seamless flow from the recirculation loop to the lattice growth matrix. The full reactor assembly and photo of the system can be seen in Figure 4-1. As an easy means of visualizing cells, sampling shelves were built into the lattice. This allowed for simple sample harvest and preparation for fluorescent microscopy. This sample shelf was constructed in the same geometry as the lattice itself. From 3D modeling in Solidworks it was calculated that the 30mm diameter lattice used has a theoretical surface area of 225cm^2. As a comparison, each 30mm diameter repeating layer provides 23.5cm^2, which equates to a 32-fold increase in surface area when comparing the 3D lattice to the equivalent 2D culture area.

4.4.2 **CFD Modeling**

To demonstrate the principle of the reactor and extrapolate hydrodynamic forces in the lattice, ANSYS FLUENT was used with a simplified model of the growth lattice. SEM images (Figure 4-2) of the scaffold were taken to understand the printed geometries and properly model the system in FLUENT (Figure 4-3). A dye tracer benchtop experiment was used to validate the model. As mentioned, media is cycled to the top of the circular lattice and pulled by gravity through the pores. Because mixing is accomplished through passive means rather than an impeller, the system is inherently very low shear. This was proven by testing a range of flow rates to estimate shear vs flow rate (Figure 4-4). All prospective flow rates fell well below 0.4 dynes cm^{-2}. As 0.25mL min^{-1} resulted in the

lowest shear while keeping the matrix well wetted, it was the tested flow rate for hMSC culture. At this flow rate CFD modeling reported a maximum of 0.0054 dynes cm^{-2} (Figure 4-3) and an average of 0.00031 dynes cm^{-2} (Figure 4-4). The areas of highest shear were at the top and bottom center of the matrix insert, where the media was entering and exiting the lattice respectively.

4.4.3 Spinner flask control

As a comparison hMSCs growth was also investigated on Cytodex-1 microcarriers in small scale spinner flasks. Static cultures (n=6) showed an average doubling time and specific growth rate of 119.07hrs ±11.23 and 0.0062 hr^{-1} ±0.0013 respectively (Figure 4-5 A). Cells cultured in spinner flasks showed an average doubling time of 113.6hrs ±23.75 and a specific growth rate of 0.0062hr^{-1} ±0.0013 (n=3) (Figure 4-5 B). Both are significantly longer (p=0.002) compared to lattice reactor (n=5) results, which are discussed later.

4.4.4 Cell viability on PLA Lattice

Cell viability was compared between culture substrates and static vs dynamic cultures as previous studies with fibrous matrices exhibited increased cytotoxicity. On day 7 of cultures, cells were enzymatically lifted and viability was tested via trypan blue staining. PLA lattices were removed from culture wells to isolate only cells adherent to the PLA lattice. Dynamic PLA cultures from the bioreactor had an average viability of 96.54% ±2.82. Cells grown in dynamic bioreactor culture on PLA showed no statistically significant difference (p=0.98) from static PLA culture plates, with an average viability of 96.76% ±3.84. Dynamic PLA showed no difference (p=0.45) from Static PS, which had an average viability of 95.13% ±1.07. This is also in agreement with the fact that

static PLA and PS showed no statistical difference in viability (p=0.38). Therefore, PLA showed no detrimental effects on cell viability in both static and dynamic cultures compared to conventual culture on treated polystyrene flasks.

4.4.5 **Dynamic seeding**

Because of the larger channel sized and homogeneity of the lattice, a new seeding protocol was developed to increase seeding efficiency. The method that yielded the best results was through static settling of the cells. The volume of media the lattice could hold was found to be 2mL. Thus, 500,000 cells were resuspended in 2mL of hMSC media. This cell rich media was then slowly injected through a Luer lock until liquid had cleared the lines. The reactor was then placed into the incubator for 45 minutes to allow cells to settle onto lattice and adhere. Hypoxic gas was then overlaid into the system though the filter ports and the peristaltic pump was then started. Cells formed confluent monolayers towards the top center of the lattice sampling shelf (Figure 4-6).

4.4.6 **Reactor Culture**

Normoxic reactor culture resulted very similar doubling time as PS control cultures (Figure 4-7 A). Because hMSCs normally grow in more comparatively more hypoxic conditions in vivo, oxygen tension was investigated as a means of increasing cell proliferation. It was found that 1.5% O_2 resulted in a four-fold increase in cell yield; double that of conventional flask culture methods tested ($p<0.001$) (Figure 4-7 B). Normalized yield to surface area was 13,725 cells cm^{-2} at 1.5% O_2 (Figure 4-7 C).This in-situ conditioning resulted in the significant increase in specific growth rate (O.0085hr^{-1} ±0.0005) (Figure 4-7 D). When lifted and analyzed via flow cytometry it was found that cells cultured in the bioreactor retained their biomarker phenotype regardless of gas

composition used for hypoxic treatment (CD105+ CD73+ CD14- CD19-); ANOVA showed no significant difference in CD105 ($p=0.309$), CD73 ($p=0.347$), CD19 ($p=0.676$), and CD14 ($p=0.523$) biomarker expression (Figure 4-8). Thus, oxygen tension had a drastic effect on cell proliferation, and no effect on biomarker profile. Cultures primed at 0% and 1% ($n=3$ for both conditions) produced statistically similar cell yields, and cultures primed at 5% and 21% oxygen showed no statistically significant difference via Tukey test at 95% CI. Compared to control cultures on static tissue treated PS, the dynamic bioreactor culture on PLA produced a higher purity MSCs according to ISCT standards, Lifted cells were over 98% dual CD105 and CD73 positive cells in reactor culture compared to 94% in static normoxic polystyrene culture ($p=0.005$) (Figure 4-9 A). There was no significant difference in the negative markers CD14 and CD19 under normoxic ($n=9$) or 1.5% hypoxic conditioning ($n=6$) (Figure 4-9 A), and single populations of cells were harvested from bioreactors (Figure 4-9 B). Again, cells formed monolayers on the PLA filaments much like control cultures on PS dishes (Figure 4-6).

4.4.7 **Differentiation potential**

As previously discussed, ISCT standards for stem cell purity and identification include differentiation ability. To test stemness, osteocyte, adipocyte, and chondrocyte inductions were performed stem cells harvested from seven-day bioreactor culture. For inductions cells were cultured between 15 to 20 days in their respective, defined ATCC differentiation media, after which cells were washed, fixed and stained. After seven days in bioreactor culture and hypoxic conditioning the cells retained their ability to differentiate into Adipocytes, Chondrocytes, and Osteocytes (Figure 4-10). Control cultures were also done in parallel with the inductions and stained with the same dyes.

Control cultures showed no staining of uninduced cells cultured for 21 days in hMSC media.

4.5 DISCUSSION

By culturing hMSCs in this scaled down bioreactor, we were able to increase cell yield four-fold over conventional flask culture methods. It was found that cells cultured in this manner maintained high expression (>97% combined CD105+ and CD73+) of positive stem cell markers. PLA did not impact cell viability compared to cultures on polystyrene in both static and dynamic culture conditions. CFD modeling shows very low velocities, and subsequently low shear inside the lattice matrix. The computational modeling of this lattice reactor reports maximum values of 0.0054 dynes cm^{-2} (Figure 4-3). CFD of stirred tank reactors utilizing microcarriers report values of approximately 1 to 5 dynes cm^{-2}, and packed bed Fibracell systems report an average shear of dynes cm^{-2} (Table 4-2). Tubular systems with similar laminar flow patterns report average values of 0.98 dynes cm^{-2}.[29] These values all fall within 0.02 to 9 dynes cm^{-2}, a range shown to upregulate osteogenic genes and differentiation in hMSCs.[15,30,31] The system tested at the parameters determined was two orders of magnitude lower than this reference range.

Surface profile of hMSCs did not change with oxygen percentage, as ranges tested were within physiological normoxia and treatment times were comparatively short to other hypoxic culturing.[32] These findings follow previous findings of oxygen tension promoting stem cell proliferation and stemness.[33–36] As mentioned previously, cells were most concentrated on the top of the fibers. In reality, the cells seem to utilize only the top

portion of the fibers, which would be a product of their static seeding. This would make cell-seeding density closer to 5,000 cells cm^{-2}.

This combination of hypoxic conditioning and gentle fluid movement may be mimicking their niche more closely than static cultures. PLA printed by filament deposition has a modulus of elasticity of 3.2, which falls in the range of elasticity of trabecular bone.[37,38] BM-hMSCs are normally harvested from the trabeculae of the iliac crest or head of the femur. When these three factors are combined, it creates the normal niche for these stem cells, which would explain why the cells perform much better in the dynamic culture condition of the reactor compared to static flask culture.

As a benchmark, hMSCs were cultured on Cytodex 1 microcarriers. The doubling time for this cell line grown in spinner flasks was significantly longer compared to culture in the lattice reactor. Cells were not characterized via flow cytometry, as even after an hour in TrypLE they did not lift from the Cytodex 1 beads. This problem of inadequate cell lifting has been noted before.[26] Whereas cells cultured in this system had no issue dissociating from matrix using CDB and TrypLE.

Another benefit of this system is the comparative ease of downstream purification compared to microcarriers. Microcarrier base culture of stem cells requires extra steps to purifying the cells from the beads. Some beads require cell detachment using trypsin, resulting in an extra step of straining the microcarriers from the lifted cells. Some microcarriers are themselves digested by enzymes, eliminating the need of straining or filtering. However, depending on the enzyme cell-cell junction may remain, resulting in cell clusters in final product. Furthermore, the byproducts of digestion of these microcarriers is still a concern for final formulation and patient administration.[39] Per UPS

<788> removal of microcarriers as particulate matter is recommendation for injected products.[7] Thus systems using microcarriers for hMSC therapies would require either inertial steps or straining and filtration steps to remove microcarriers from cells after dissociation, adding complication and potentially decreasing overall yield through shear.[40,41] Centrifugation of the cells can cause cell clumping and exposes the cells to high shear, resulting in product loss.[12] Also, filtration and straining have been shown to decrease viability of harvested cells.[41] In our system this purification step is more robust, as cells can be washed in place and lifted with a reduced process related impurities after lifting. By using recombinant TrypLE we have shown optimal cell lifting within 15 minutes. Another avenue of cell lifting in this system is via thermoresponsive polymers. P(NIPAM) could be coated into the stationary PLA lattice, and cell lifting would be completed by only dropping the temperature.[42] This would eliminate the need for exogenous enzymes and washes, easing downstream processes and subsequently increasing yield. Unlike particulate from microcarriers, the degradation product of the PLA lattice dissolves into solution as lactic acid.[43] This byproduct can easily be removed through buffer exchange, but it is also biocompatible and broken down in the body naturally.

Because of its biocompatibility, cell detachment may not be necessary depending on the application. As PLA is biocompatible and similar in rigidity to cancellous bone, hMSCs can be expanded and differentiated in-situ. Polymer rigidity can be either avoided or exploited for tailored stem cell differentiation. Harder polymers like PLA, polystyrene, or polycarbonate (PC) can be printed using high temperature 3D printers, and can be easily treated for cell adhesion. Softer, more elastic materials like polyurethane have been used

for stem cell culture and are also readily available materials for 3D printing.[44] Culture on more elastic scaffolds, such as alginate encapsulation, can direct hMSCs to differentiate into chondrocytes and has been used in established differentiation protocols[45,46]

Here we have shown a system for high purity stem cell culture. The system resulted in above normal yields for tested systems, while maintaining high expression of stem cell biomarkers. The cells lifted from the system were easily dissociated with minimal open-air steps and required no extra purification. When tested for stemness, the cells readily differentiated into osteocytes and were able to differentiate into adipocytes.

Another possible use of this system is for the production of secreted product, as cells are adherent to a stationary scaffold. This system is ideal for secreted proteins and vesicles. The cells are bound to the substrate and will release cytokines and exosomes of therapeutic interest into circulating media. Research into exosomes has shown their usefulness in wound healing and inflammatory diseases.[47–49] These vesicles are secreted by hMSCs and contain mRNA, cytokines, growth factors, and other signaling molecules involved in healing, and are a major interest for regenerative medicine.[49] The proposed lattice system can be run in perfusion, allowing simple harvest of the secretome while cells are held stationary in the reactor.

4.6 CONCLUSION

Here we show the successful use of a scale down model of a novel suspended matrix bioreactor for the culture of hMSCs. Cells adhered well to PLA lattice and grew as monolayers similar to conventional culture techniques. A combinatory effect of low oxygen tension and slow recirculation rate of 0.25mL min^{-1} through the lattice based

culture resulted in higher than average cell yields compared to conventional expansion systems, including static T-flasks and spinner flask with microcarriers. 1.5% O_2 gas had the best cell growth, resulting in a four-fold increase in overall cell yield. The cells lifted from the reactor showed excellent stem cell biomarker expression through flow cytometry, showing significant increase over conventional flask culture. hMSCs also retained their ability to differentiate into bone, cartilage, and fat cells. Further work into scaling this system up needs further investigation. Nonetheless we have shown the validity of suspended matrix reactor systems for high purity hMSC production.

4.7 ACKNOWLEDGEMENTS

I would like to Thank Dr. Anna Hickerson of Keck Graduate Institute for allowing me to use the PrintrBot 3D printer. I would like to thank Dr. David Tanenbaum at Pomona College and Dr. Van Ryswyk at Harvey Mudd College for their time training me on scanning electron microscopy. I would like to thank Hardy Richardson of Pomona College and Hsiang Wei for their help in machining the reactors. I would like to thank Vinit Saxena and Sepragen for allowing me to test their system for the cultivation of stem cells. I would also like to thank Dr. Dennis Fenton, whose generous Graduate Institute funded this research.

1. Department of Health and Human Services. *Regenerative Medicine*.; 2006. https://stemcells.nih.gov/sites/all/themes/stemcells_theme/stemcell_includes/Regenerative_Medicine_2006.pdf. Accessed April 9, 2019.

2. Faiella W, Atoui R. Immunotolerant Properties of Mesenchymal Stem Cells: Updated Review. *Stem Cells Int*. 2016;2016:1-7. doi:10.1155/2016/1859567.

3. Squillaro T, Peluso G, Galderisi U. Clinical Trials with Mesenchymal Stem Cells: An Update. *Cell Transplant*. 2016;25(5):829-848. doi:10.3727/096368915X689622.

4. Balikov DA, Crowder SW, Boire TC, et al. Tunable Surface Repellency Maintains Stemness and Redox Capacity of Human Mesenchymal Stem Cells. *ACS Appl Mater Interfaces*. 2017;9(27):22994-23006. doi:10.1021/acsami.7b06103.

5. Hass R, Kasper C, Böhm S, Jacobs R. Different populations and sources of human mesenchymal stem cells (MSC): A comparison of adult and neonatal tissue-derived MSC. *Cell Commun Signal*. 2011;9(1):12. doi:10.1186/1478-811X-9-12.

6. Jossen V, Schirmer C, Mostafa Sindi D, et al. Theoretical and Practical Issues That Are Relevant When Scaling Up hMSC Microcarrier Production Processes. *Stem Cells Int*. 2016;2016:1-15. doi:10.1155/2016/4760414.

7. Schnitzler AC, Verma A, Kehoe DE, et al. Bioprocessing of human mesenchymal stem/stromal cells for therapeutic use: Current technologies and challenges. *Biochem Eng J*. 2016;108:3-13. doi:10.1016/j.bej.2015.08.014.

8. Kempf H, Andree B, Zweigerdt R. Large-scale production of human pluripotent stem cell derived cardiomyocytes. *Adv Drug Deliv Rev*. 2016;96:18-30. doi:10.1016/j.addr.2015.11.016.

9. Kebriaei P, Isola L, Bahceci E, et al. Adult Human Mesenchymal Stem Cells Added to Corticosteroid Therapy for the Treatment of Acute Graft-versus-Host Disease. doi:10.1016/j.bbmt.2008.03.012.

10. Xu J-Y, Cai W-Y, Tian M, Liu D, Huang R-C. Stem cell transplantation dose in patients with acute myocardial infarction: A meta-analysis. *Chronic Dis Transl Med*. 2016;2(2):92-101. doi:10.1016/j.cdtm.2016.09.006.

11. Houtgraaf J, den Dekker W, van Dalen B, et al. First Experience in Humans Using Adipose Tissue-Derived Regenerative Cells in the Treatment of Patients With ST-Segment Elevation Myocardial Infarction. *JAC*. 2012;59:539-540. doi:10.1016/j.jacc.2011.09.065.

12. Jossen V, van den Bos C, Eibl R, Eibl D. Manufacturing human mesenchymal stem cells at clinical scale: process and regulatory challenges. *Appl Microbiol Biotechnol*. 2018;102(9):3981-3994. doi:10.1007/s00253-018-8912-x.

13. Glaser DE, Turner WS, Madfis N, et al. Multifactorial Optimizations for Directing Endothelial Fate from Stem Cells. Rajasingh J, ed. *PLoS One*. 2016;11(12):e0166663. doi:10.1371/journal.pone.0166663.

14. Park J, Kim P, Helen W, Engler AJ, Levchenko A, Kim D-H. Control of stem cell fate and function by engineering physical microenvironments. https://www.ncbi.nlm.nih.gov/pmc/articles/PMC3476065/pdf/nihms404576.pdf. Accessed March 19, 2018.

15. Yourek G, McCormick SM, Mao JJ, Reilly GC. Shear stress induces osteogenic differentiation of human mesenchymal stem cells. *Regen Med*. 2010;5(5):713-724. doi:10.2217/rme.10.60.

16. Ross JJ, Hong Z, Willenbring B, et al. Cytokine-induced differentiation of multipotent adult progenitor cells into functional smooth muscle cells. *J Clin Invest*. 2006;116. doi:10.1172/JCI28184.

17. Kulangara K, Yang Y, Yang J, Leong KW. Nanotopography as Modulator of Human Mesenchymal Stem Cell Function. 2012. doi:10.1016/j.biomaterials.2012.03.053.

18. Kawano T, Sato M, Yabu H, Shimomura M. Biomaterials Science www.rsc.org/biomaterialsscience Honeycomb-shaped surface topography induces differentiation of human mesenchymal stem cells (hMSCs): uniform porous polymer scaffolds prepared by the breath figure technique † ‡. *Biomater Sci*. 2014;2:52. doi:10.1039/c3bm60195a.

19. Dominici M, Le Blanc K, Mueller I, et al. Minimal criteria for defining multipotent mesenchymal stromal cells. The International Society for Cellular Therapy position statement. doi:10.1080/14653240600855905.

20. Lechanteur C, Baila S, Janssens ME, et al. Stem Cell Large-Scale Clinical Expansion of Mesenchymal Stem Cells in the GMP-Compliant, Closed Automated Quantum ® Cell Expansion System: Comparison with Expansion in Traditional T-Flasks Large-Scale Clinical Expansion of Mesenchymal Stem Cells in the GM. *J Stem Cell Res Ther Lechanteur*. 2014;4(8):222. doi:10.4172/2157-7633.1000222.

21. Jossen V, Pörtner R, Kaiser SC, Kraume M, Eibl D, Eibl R. Mass Production of Mesenchymal Stem Cells — Impact of Bioreactor Design and Flow Conditions on Proliferation and Differentiation. In: *Cells and Biomaterials in Regenerative Medicine*. InTech; 2014. doi:10.5772/59385.

22. Rodrigues C, Fernandes T, Diogo M, da Silva C, Cabral J. Bioreactors for Stem Cell Expansion and Differentiation. In: *Stem Cell Engineering*. CRC Press; 2012:1-28. doi:10.1201/b12942-11.

23. Hewitt CJ, Lee K, Nienow AW, Thomas RJ, Smith M, Thomas CR. Expansion of human mesenchymal stem cells on microcarriers. *Biotechnol Lett*. 2011;33(11):2325-2335. doi:10.1007/s10529-011-0695-4.

24. Caracci SJ, Henry D, Walerack C, Zhou Y. Digestible substrates for cell culture. June 2016. https://patents.google.com/patent/US20180179489A1/en. Accessed March 16, 2019.

25. Liu N, Zang R, Yang S-T, Li Y. Stem cell engineering in bioreactors for large-

scale bioprocessing. *Eng Life Sci*. 2014;14(1):4-15. doi:10.1002/elsc.201300013.

26. Timmins NE, Kiel M, Günther M, et al. Closed system isolation and scalable expansion of human placental mesenchymal stem cells. *Biotechnol Bioeng*. 2012;109(7):1817-1826. doi:10.1002/bit.24425.

27. Jin J, Jeong SI, Shin YM, et al. Transplantation of mesenchymal stem cells within a poly(lactide- *co* -ε-caprolactone) scaffold improves cardiac function in a rat myocardial infarction model. *Eur J Heart Fail*. 2009;11(2):147-153. doi:10.1093/eurjhf/hfn017.

28. Zong X, Bien H, Chung C, et al. Electrospun fine-textured scaffolds for heart tissue constructs. *Biomaterials*. 2005;26(26):5330-5338. doi:10.1016/j.biomaterials.2005.01.052.

29. Yeatts AB, Fisher JP. Tubular Perfusion System for the Long-Term Dynamic Culture of Human Mesenchymal Stem Cells. *Tissue Eng Part C Methods*. 2011;17(3):337-348. doi:10.1089/ten.tec.2010.0172.

30. McBride SH, Falls T, Knothe Tate ML. Modulation of Stem Cell Shape and Fate B: Mechanical Modulation of Cell Shape and Gene Expression. *Tissue Eng Part A*. 2008;14(9):1573-1580. doi:10.1089/ten.tea.2008.0113.

31. Kim KM, Choi YJ, Hwang J-H, et al. Shear Stress Induced by an Interstitial Level of Slow Flow Increases the Osteogenic Differentiation of Mesenchymal Stem Cells through TAZ Activation. Eddington DT, ed. *PLoS One*. 2014;9(3):e92427. doi:10.1371/journal.pone.0092427.

32. Spencer JA, Ferraro F, Roussakis E, et al. Direct measurement of local oxygen concentration in the bone marrow of live animals. *Nature*. 2014;508(7495):269-273. doi:10.1038/nature13034.

33. Abdollahi H, Harris LJ, Zhang P, et al. The Role of Hypoxia in Stem Cell Differentiation and Therapeutics. *J Surg Res*. 2011;165(1):112-117. doi:10.1016/j.jss.2009.09.057.

34. Estrada JC, Albo C, Benguría A, et al. Culture of human mesenchymal stem cells at low oxygen tension improves growth and genetic stability by activating glycolysis. *Cell Death Differ*. 2011;19:743-755. doi:10.1038/cdd.2011.172.

35. Shearier E, Xing Q, Qian Z, Zhao F. Physiologically Low Oxygen Enhances Biomolecule Production and Stemness of Mesenchymal Stem Cell Spheroids. doi:10.1089/ten.tec.2015.0465.

36. Ahmed Mohyeldin, Tomas Garzon-Muvdi AQ-H. Oxygen in Stem Cell Biology: A Critical Component of the Stem Cell Niche. *Cell Stem Cell*. 2010;7. doi:10.1016/j.stem.2010.07.007.

37. Wurm MC, Möst T, Bergauer B, et al. In-vitro evaluation of Polylactic acid (PLA) manufactured by fused deposition modeling. *J Biol Eng*. 2017;11:29. doi:10.1186/s13036-017-0073-4.

38. Jacobs CR, Cowin SC. *Bone Mechanics Handbook (Second Edition)*. Vol 35. Bone Mecha. (Cowin S, ed.). Boca Raton: CRC Press; 2002. doi:10.1016/s0021-9290(01)00251-2.

39. Rafiq QA, Masri F. *Downstream Processing Challenges and Opportunities for Cell-Based Therapies*. http://discovery.ucl.ac.uk/1557536/1/Rafiq_Harvest paper Final.pdf. Accessed February 28, 2019.

40. Moloudi R, Oh S, Yang C, et al. Inertial-Based Filtration Method for Removal of Microcarriers from Mesenchymal Stem Cell Suspensions. *Sci Rep*. 2018;8(1):12481. doi:10.1038/s41598-018-31019-y.

41. Rodrigues AL, Rodrigues CA V., Gomes AR, et al. Dissolvable Microcarriers Allow Scalable Expansion And Harvesting Of Human Induced Pluripotent Stem Cells Under Xeno-Free Conditions. *Biotechnol J*. 2019;14(4):1800461. doi:10.1002/biot.201800461.

42. Nash ME, Healy D, Carroll WM, Elvira C, Rochev YA. Cell and cell sheet recovery from pNIPAm coatings; motivation and history to present day approaches. *J Mater Chem*. 2012;22(37):19376. doi:10.1039/c2jm31748f.

43. Elsawy MA, Kim K-H, Park J-W, Deep A. Hydrolytic degradation of polylactic acid (PLA) and its composites. *Renew Sustain Energy Rev*. 2017;79:1346-1352. doi:10.1016/J.RSER.2017.05.143.

44. Fromstein JD, Zandstra PW, Alperin C, Rockwood D, Rabolt JF, Woodhouse KA. Seeding Bioreactor-Produced Embryonic Stem Cell-Derived Cardiomyocytes on Different Porous, Degradable, Polyurethane Scaffolds Reveals the Effect of Scaffold Architecture on Cell Morphology. *Tissue Eng Part A*. 2008;14(3):369-378. doi:10.1089/tea.2006.0410.

45. Singh N, Rahatekar SS, Koziol KKK, et al. Directing Chondrogenesis of Stem Cells with Specific Blends of Cellulose and Silk. *Biomacromolecules*. 2013;14(5):1287-1298. doi:10.1021/bm301762p.

46. ATCC. Chondrocyte Differentiation Tool ATCC ® PCS-500-051™. https://www.atcc.org/products/all/PCS-500-051.aspx#culturecconditions. Accessed March 2, 2019.

47. Hu L, Wang J, Zhou X, et al. Exosomes derived from human adipose mensenchymal stem cells accelerates cutaneous wound healing via optimizing the characteristics of fibroblasts. *Nat Publ Gr*. 2016. doi:10.1038/srep32993.

48. Kim SH, Bianco NR, Shufesky WJ, Morelli AE, Robbins PD. Effective treatment of inflammatory disease models with exosomes derived from dendritic cells genetically modified to express IL-4. *J Immunol*. 2007;179(4):2242-2249. http://www.ncbi.nlm.nih.gov/pubmed/17675485. Accessed March 2, 2019.

49. Vishnubhatla I, Corteling R, Stevanato L, Hicks C, Sinden J. The Development of Stem Cell-derived Exosomes as a Cell-free Regenerative Medicine. 2014. doi:10.5772/58597.

50. Kumar A, Starly B. Large scale industrialized cell expansion: producing the critical raw material for biofabrication processes. *Biofabrication*. 2015;7(4):044103. doi:10.1088/1758-5090/7/4/044103.

51. Osiecki MJ, Michl TD, Kul Babur B, et al. Packed Bed Bioreactor for the Isolation and Expansion of Placental-Derived Mesenchymal Stromal Cells. *PLoS One*. 2015;10(12):e0144941. doi:10.1371/journal.pone.0144941.

52. Mizukami A, de Abreu Neto MS, Moreira F, et al. A Fully-Closed and Automated Hollow Fiber Bioreactor for Clinical-Grade Manufacturing of Human Mesenchymal Stem/Stromal Cells. *Stem Cell Rev Reports*. 2018;14(1):141-143. doi:10.1007/s12015-017-9787-4.

53. Chaudhuri J, Al-Rubeai M. *Bioreactors for Tissue Engineering : Principles, Design and Operation*. Springer; 2005.

54. Martin I, Wendt D, Heberer M. The role of bioreactors in tissue engineering. doi:10.1016/j.tibtech.2003.12.001.

55. Jones ME, Nankervis BJ, Fuerst KE, Dodd JA. Cell Growth with Mechanical Stimuli. May 2018. http://www.freepatentsonline.com/y2018/0142199.html. Accessed February 20, 2019.

56. Lawson T, Kehoe DE, Schnitzler AC, et al. Process development for expansion of human mesenchymal stromal cells in a 50 L single-use stirred tank bioreactor. *Biochem Eng J*. 2017;120:49-62. doi:10.1016/J.BEJ.2016.11.020.

57. Tsai A-C, Liu Y, Ma T. Expansion of human mesenchymal stem cells in fibrous bed bioreactor. *Biochem Eng J*. 2016;108:51-57. doi:10.1016/j.bej.2015.09.002.

58. Singh V. Disposable bioreactor for cell culture using wave-induced agitation. *Cytotechnology*. 1999;30(1/3):149-158. doi:10.1023/A:1008025016272.

59. Giroux D, Wesselschmidt R, Hashimura Y, et al. *Development of Scalable Manufacturing Processes for Bone-Marrow Derived Mesenchymal Stem Cells in a Low Shear, Single Use Bioreactor System*.; 2014. https://www.pbsbiotech.com/uploads/1/7/9/9/17996975/chi_poster-final_v.140817.pdf. Accessed May 5, 2018.

60. Pall Corporation. *ICELLis ® Single-Use Fixed-Bed Bioreactor System Productivity and Reduced Footprint for Virus Production in Adherent Cell Growth*. https://biotech.pall.com/content/dam/pall/biopharm/lit-library/non-gated/Brochures/17.06955_USD3262_iCELLis_Bioreactor_DS-EN.pdf. Accessed May 7, 2018.

61. Weber C, Freimark D, Pörtner R, et al. *Expansion of Human Mesenchymal Stem Cells in a Fixed-Bed Bioreactor System Based on Non-Porous Glass Carrier-Part A: Inoculation, Cultivation, and Cell Harvest Procedures*. http://krex.ksu.edu. Accessed February 19, 2019.

Table 4-1: Reactor Advantages and Disadvantages for hMSC Culture. Adapted from Liu et al.[23] *and Kumar and Starly.*[43]

Type	Advantages	Disadvantages
Microcarrier	Support high-density cell culture; regulate cell growth and differentiation; serve as cell delivery systems. Easy to scale up. Easy sampling and cell visualization	Difficult to harvest cells. Purification from microcarriers. Still some possible shear issues due to energy required for suspension. Limited growth area on microcarriers.
Plate	Very similar to flask culture; easy to translate. Low shear stress because no impellor needed	Difficult to visualize cells. environment is inhomogeneous due to the nutrient and oxygen gradient
Packed bed	Provide 3D microenvironment; allow cell spatial organization; regulate proliferation, differentiation and tissue formation. Large SA:V	Difficult to harvest cells. Difficult to visualize cells. Concentration gradients. Indirect cell measurements

Table 4-2: Comparison of Culture Systems. Volume, available surfaces areas, cell types used, total stem cell yield normalized to volume and surface area, total overall yield, doubling time and reported shear rates of various systems.

Name	Type	Classification	Vendor	V (mL)	SA (cm^2)	SA: V	Cell type	SC/mL $x10^6$	SC/cm^2 $x10^4$	Total SCs $x10^6$	Td (hr^{-1})	Shear (dynes cm^{-2})	Source
-	PDMS Matrix	Immobilized	-	110	2,800	25.5	hP-MSC	0.509	2.00	56	30.2	1-5	[44]
Quantum	Hollow Fiber	Immobilized	TERUMO BCT	1,440	21,000	14.6	hAd-MSC	0.167	1.14	240	34.1	0.3-0.7	[45–48]
Mobius	STBR	Suspension	Milipore Sigma	50,000	300,000	6	hBM-MSC	2.00	1.67	5,000	54.0	2-40	[46,49,50]
Applifle x	Wave Bag	Suspension	Applikon	1,500	7,360	4.91	hAd-MSC	0.190	3.87	285	31.2	0.1-0.5	[5,51]
Mag 3	Paddle	Suspension	PBS	3,000	-	-	hBM-MSC	1.90	-	5,700	63.0	-	[52]
Xpansion Multiplate	Parallel Plate	Immobilized	Pall	1600	6,120	3.83	hAd-MSC	0.111	5.4	334	34.1	0.1-0.5	[18]
iCellis	Random Fiber Matrix	Immobilized	Pall	1000 - 5000	40,000	40	hBM-MSC	2.93	16	-	67.2	1-5	[50,53,54]
In House	Lattice	Immobilized	-	20	122	6.1	hBM-MSC	0.2	2	1.8	82	0.0048	-

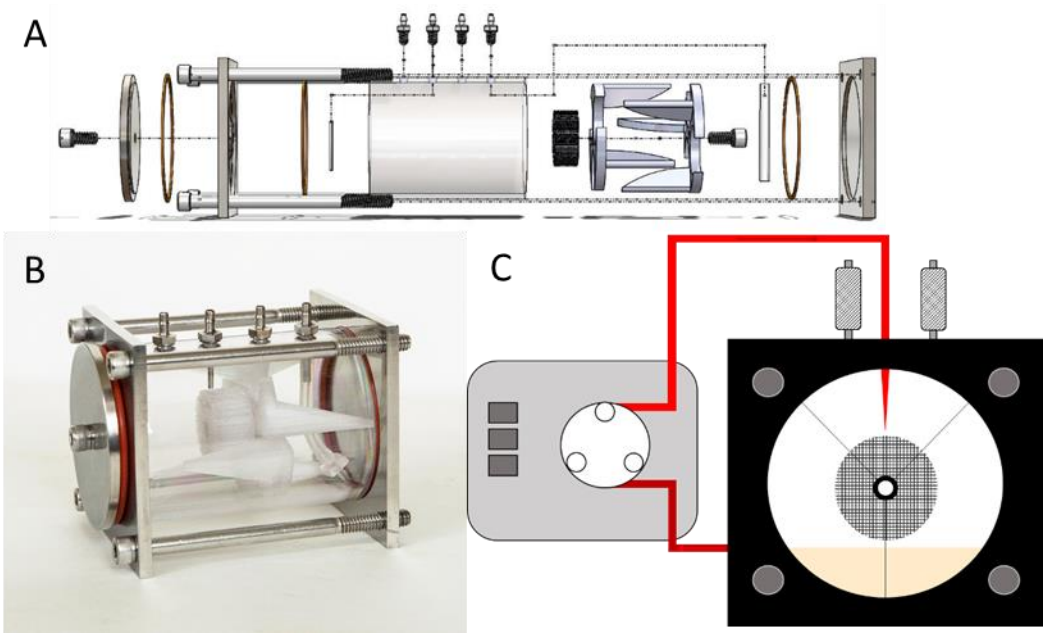

Figure 4-1: Schematic and picture of reactor. A) Exploded diagram of components and how they are pieced together. B) Image of assembled reactor. C) Cartoon front-on schematic of how lattice is suspended out of media and fluid is recirculated through system.

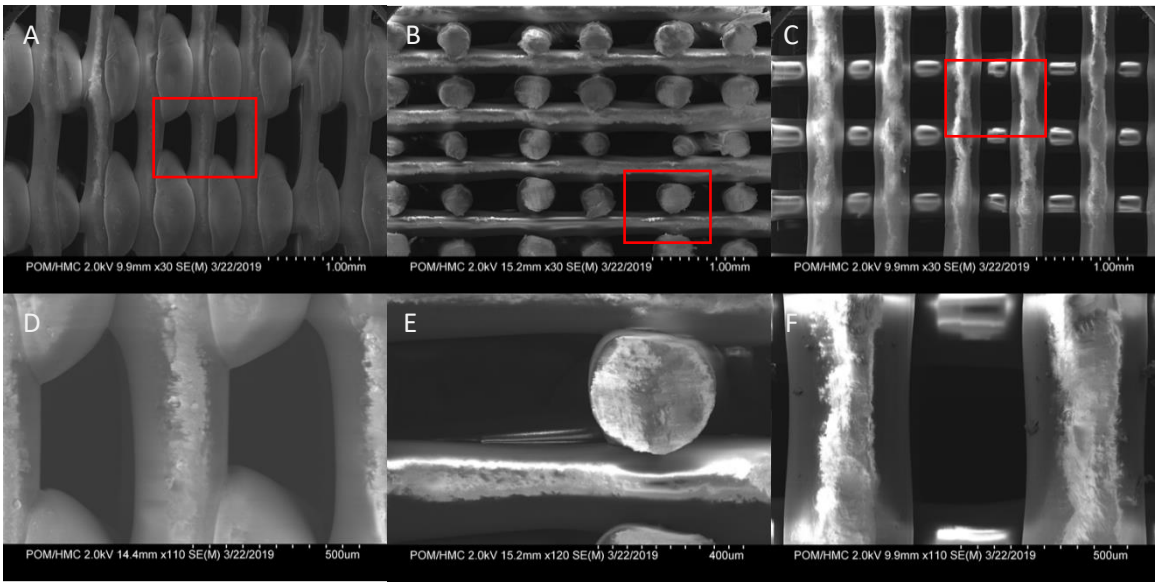

Figure 4-2: Scanning Electron Microscopy images of 3D Printed PLA. A) Outside side orientation. B) Cut interior orientation. C) Top down view of PLA lattice. E) High zoom of Outside side F) Cut interior, and G) top-down views. Red red squares denote zoom seen in second row.

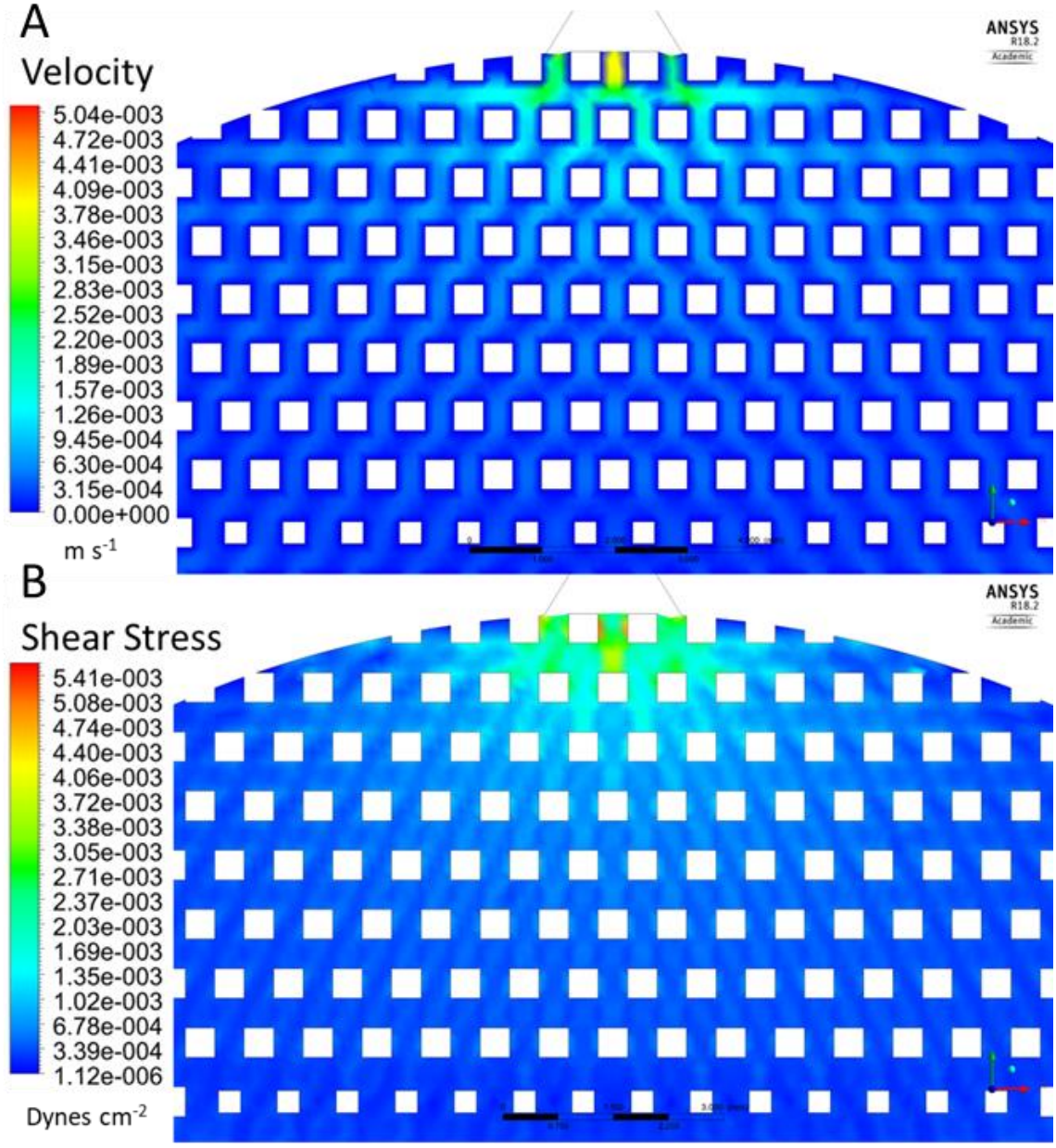

Figure 4-3: CFD modeling of lattice matrix. A) Velocity contour and B) shear stress. Maximum velocity of 0.0039m s^{-1} and maximum shear stress of 0.0056 dyne s cm^{-2} measured inside the lattice, excluding the inlet and outlet. Shear was calculated by multiplying strain rate by the viscosity of the fluid.

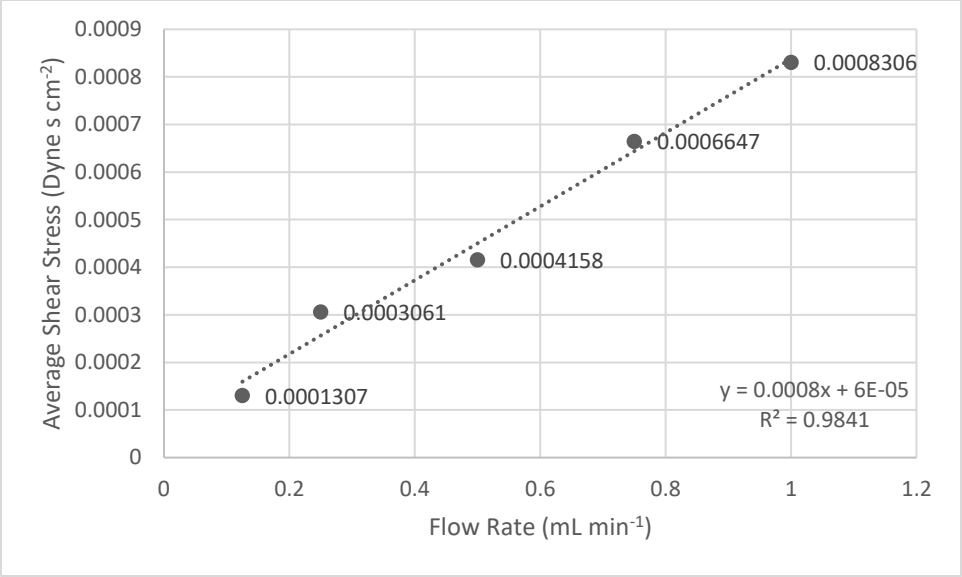

Figure 4-4: Inlet Flow Rate vs Average Wall Shear. The lattice matrix was modeled in ANSYS and tested at various flow rates using Fluent. Strain rate was converted into shear stress using Equation 4-3.

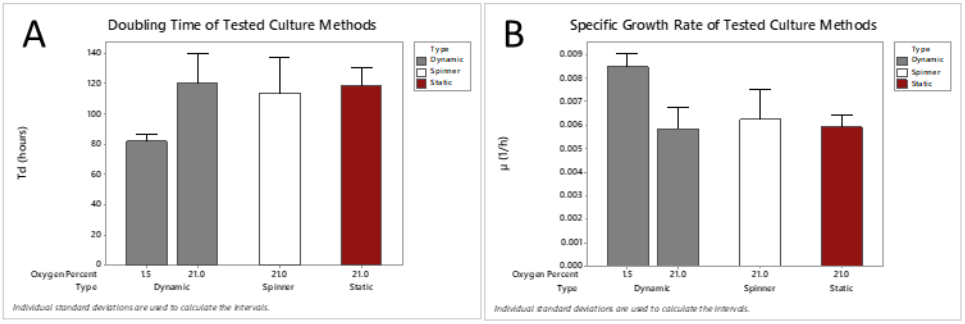

Figure 4-5: Culture method on A) doubling time and B) specific growth rate of hMSCs. Static cultures grown in t75 flasks according to ATCC guidelines. Spinner cultures used Cytodex-1 microcarriers in spinner flask. Dynamic culture used PLA lattice as per method

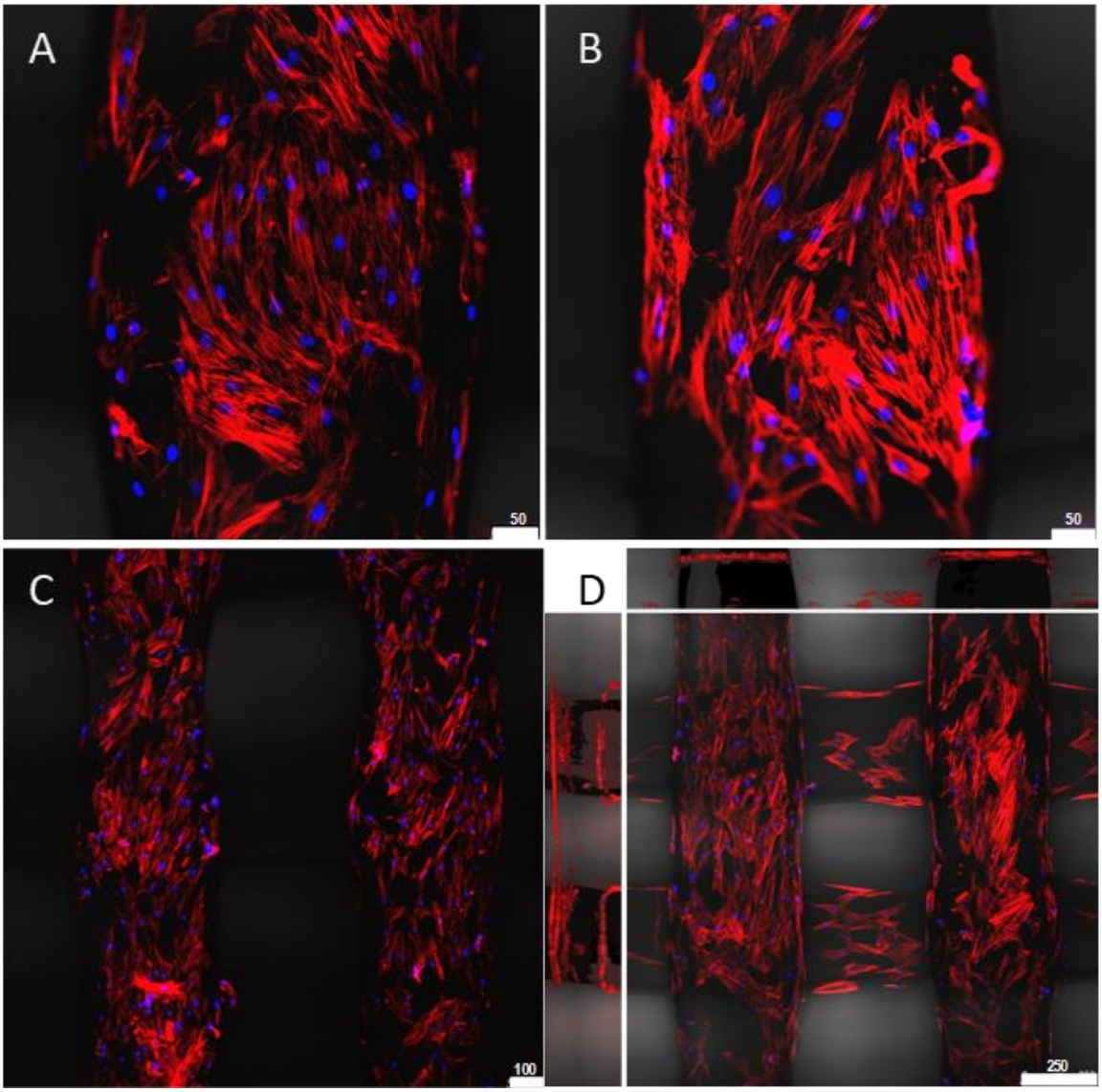

Figure 4-6: hMSCs imaged on PLA Scaffold from bioreactor. Cells underwent a three-day prime at 1.5% oxygen and were then cultured out for seven days. Stained with phalloidin (red) and DRAQ5 (blue). A) and B) show hMSC on single fiber. C) Low magnification showing hMSC coverage among parallel fibers. D) Projected Z-stack of fibers showing cell coverage. Center image shows top view (XY projection). Top and side bars show sideways projection (ZX and ZY)

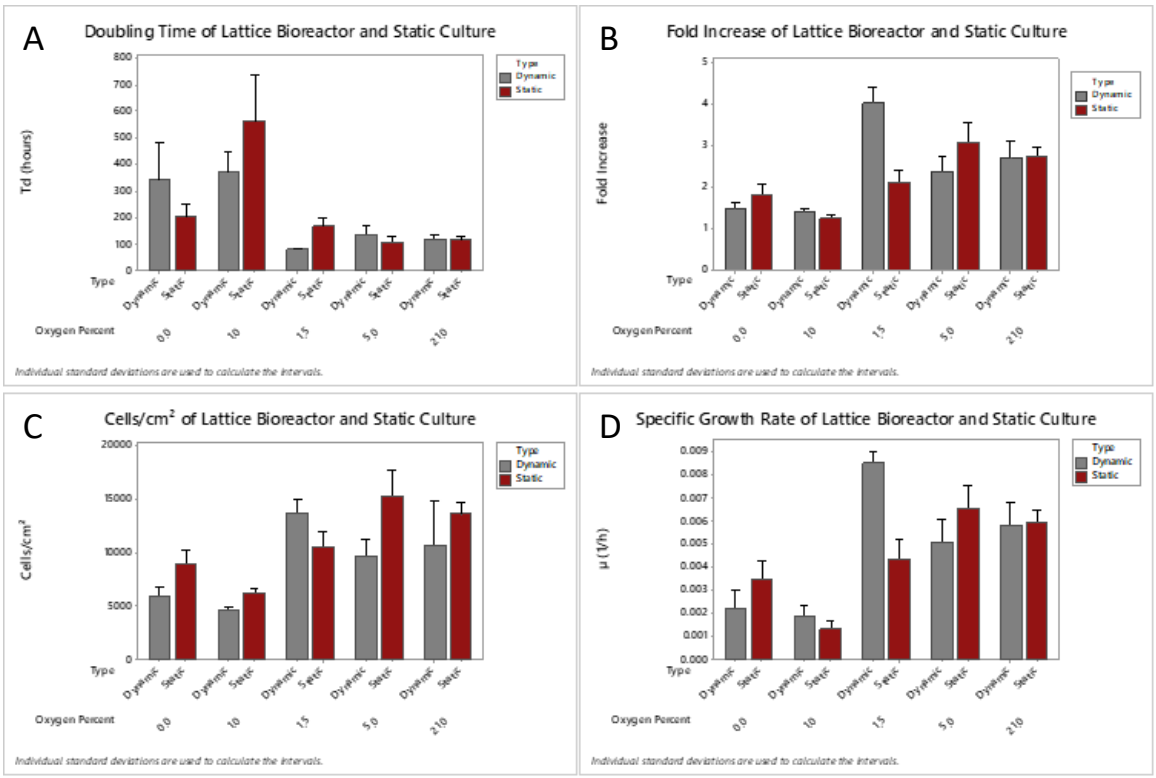

Figure 4-7: hMSC bioreactor culture of varying oxygen tension compared to static culture of same oxygen amounts harvested on day 7. A) Doubling time, B) Fold increase, C) Cells per cm² D) Specific growth rate, and doubling times of hMSC. Day seven cell harvested from reactors

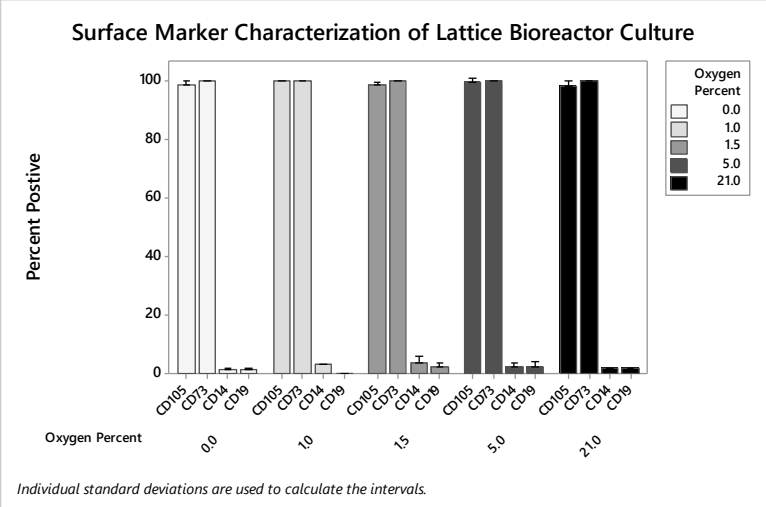

Figure 4-8: Flow Cytometry of hMSC from Reactors harvested Day seven from varying oxygen tension. CD105, CD73, CD19 and CD14 stained cells were analyzed using flow cytometry. No significant difference was found in marker expression vs hypoxic preconditioning.

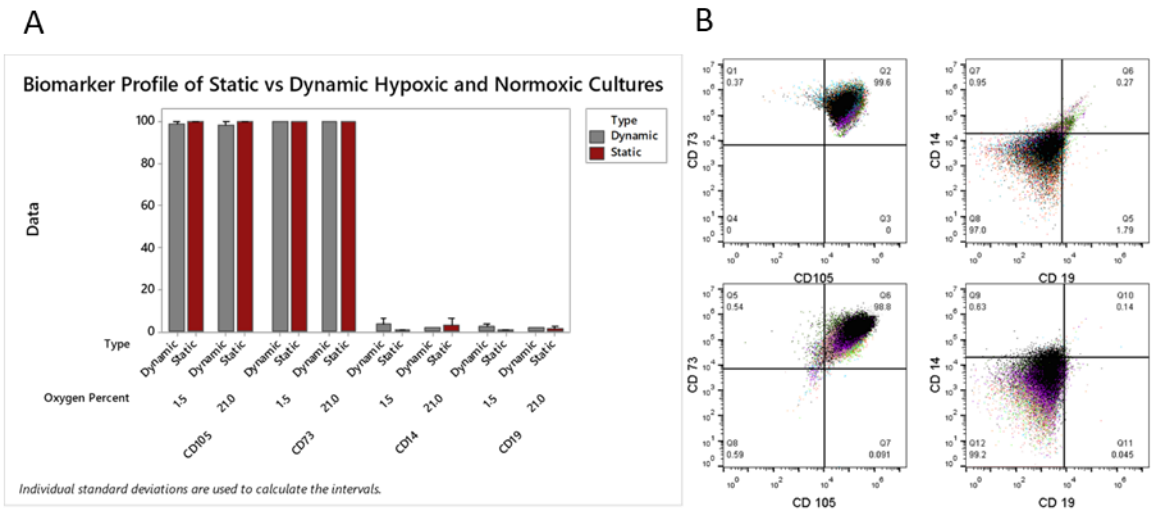

Figure 4-9: hMSC biomarker characterization using flow cytometry. Cells were cultured in both static and in bioreactor and compared using CD105, C73, CD19, and CD14 staining. B) Overlaid flow cytometry image of 1.5% O2 primed hMSC cultures from D7 bioreactors.

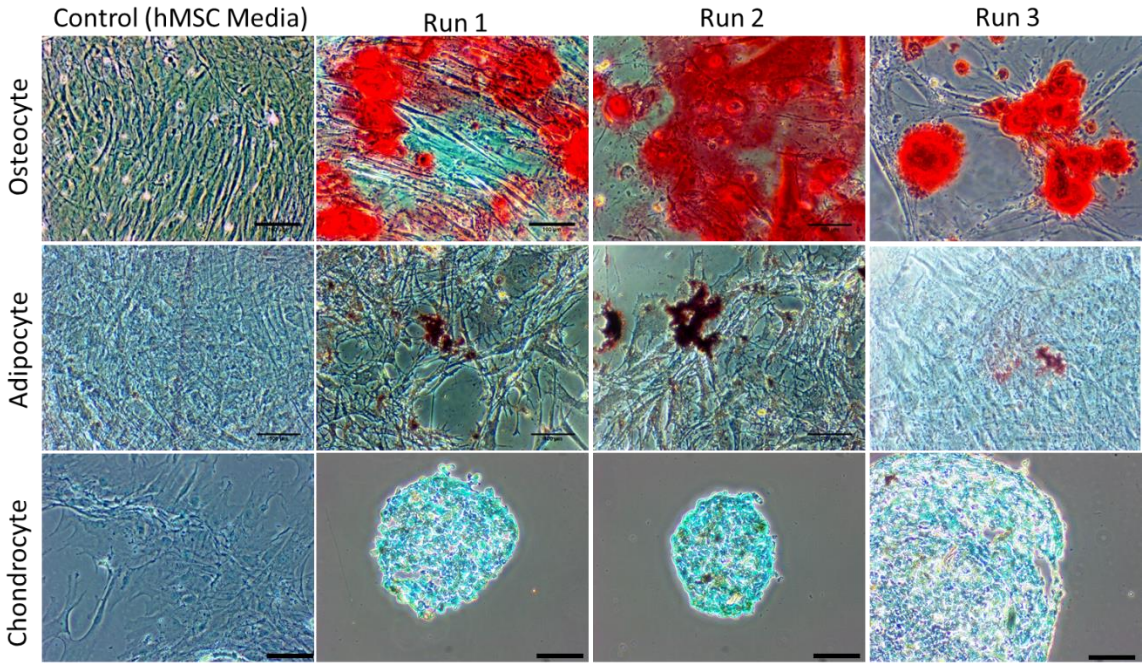

Figure 4-10: Stem Cell induction. Cells harvested day seven from bioreactor and cultured out in in respective differentiation media following specialized protocols. After allotted time cells were fixed, stained, and imaged using light microscopy. Scale bars are 100 microns.

5 COMPUTATIONAL FLUID DYNAMICS

5.1 ABSTRACT

Computational Fluid Dynamics (CFD) is a method of modeling fluid flow and energy transfer in silico. In bioprocessing this technique is used both to optimize and characterize cell culture systems. In this study we use CFD to better understand hydrodynamic forces and flow regimes within the lattice of the bioreactor. For this we modeled flow in a 2D model of the scaffold insert of reactor. This was accomplished by alternating 400µm by 400µm squares representing the cross sections of the polylactic acid fibers. Alternating the fibers made the model match flow patterns seen in benchtop dye experiments, bring 3D flow patterns into the 2D simulation. We found that laminar flow through the channels of the PLA lattice is predicted to only produce a maximum of $8.0x10^{-4}$ dynes cm^{-2}. We also calculated the KLa to be 2.14 hr^{-1}, very similar to other un-sparged culture vessels for stem cell bioproduction. This prediction confirms laboratory testing of the system were sensitive cell types cultured well in the scaffold.

5.2 INTRODUCTION

In this work we use CFD and fluidic validation techniques to characterize a novel low shear bioreactor for use with sensitive cell types. We accomplish this by using a simplified model in ANSYS 18.2 Fluent and show that when run within certain boundaries will provide an acceptable environment for the culture of human Mesenchymal Stem Cells (hMSCs). This type of adult stem cell is found in many tissues,

but is mainly sourced from adipose, bone marrow, or umbilical cord blood.[1] hMSCs have been shown to react to shear stresses, often differentiating into osteocytes and decreasing overall stem cell yield when bioproducing this cell type for regenerative medicine.[2] Thus, being able to model a system aimed at producing pure hMSCs as a product allows researchers to characterize the shear stresses the cells may be exposed too, moving design from long and expensive benchtop studies to relatively faster and cheaper in silico modeling.

CFD is a field of applied mathematics aimed at computing fluid flow and forces. CFD works by numerically calculating fluid flow and resulting forces. It does this by solving Navier-Stokes equations for mass, momentum, and energy conservation. To accurately and timely solve for these values the area of fluid flow is broken down into smaller geometries called elemental volumes. The discretization of a geometry into elemental volumes is a process known as meshing. The solver can then calculate desired equations for these cells based on methods including Finite Difference Modeling (FDM), Finite Volume Modeling (FVM), and Finite Element Modeling (FEM), with FEM being the most common.[3]

CFD is a valuable tool for the characterization of bioreactor design and operation.[4,5] does not eliminate benchtop experiments, but it can decrease the amount of time and cost of designing systems. It can also be used to characterize existing stir tank bioreactor systems, with a common application being to test impeller speeds vs mixing and shear.[6] CFD modeling for adherent stem cell bioreactors can be used to determine shear stress where media flow can affect cells. In the system tested here it allows the user to understand fluid flow patterns through a porous matrix. It can also be used as a means of

ensuring that concept reactors will operate as intended, elucidating problem areas, such as in concept reactors before mass production. It has also been very helpful in designing scale models for cell culture, much like the system tested within.[7,8] the ability to rapidly test shear, mixing, pressure, and other parameters important in culture make CFD modeling very useful when developing systems for sensitive cells, such as stem cells. With regards to bioreactor culture specifically to these cells, CFD is invaluable for quantifying how the geometry of the scaffold and supplementation of media impacts fluid patterns and flow, velocity distribution and shear, as well as liquid mixing and related gas transfer coefficients. As stated previously, CFD can also reduce the burden of benchtop experiments, cutting cost of testing and increasing speed of development. All these factors combined make CFD an ideal tool when developing and testing systems designed to meet the high demand of biologically produced drugs and whole cell therapies.

The objective of this study was to utilize CFD to model fluid flow in the scaffold in a similar fashion to other fixed bed systems.[9] Flow regimes in such reactors are usually lamiar due to the slow speed of media flow. Laminar flow is defined by Reynolds Number (Re), where a system with a Re less than 2300 is considered laminar. For a pipe, or through channels like in this system, a Re less than 1000 is laminar flow. This means that there is no turbulence in the system and flow move steadily with little mixing. While turbulence drives mixing in many systems, it is important with stem cells to keep strong hydrodynamic forces to a minimum. To accomplish this, systems for stem cell culture often operate at much slower flow rates, but this can lead to media gradients and low oxygen diffusion. To compensate for this special geometries can be used to drive mixing

in a way that does not increase the amount of shear the cells are exposed to. Reynolds number though a pipe is calculated following the equation:

$$Re = \frac{\rho V d}{\eta}$$

Equation 5-1: Reynolds Number. Where ρ is the density of the fluid, V is the velocity of the fluid moving through the pipe, d is the diameter of the pipe, and η is the viscosity of the fluid at a given temperature.

The oxygen transfer rate into the system is also a valuable tool to determine bioreactor performance, usually reported as the transfer coefficient K_La. This value can be calculated in CFD by modeling turbulence, or is some small cases through laminar modeling.[10,11] K_La is incredibly important for bioreactor culture. In most systems oxygen is the limiting factor for cell growth.[12] A system with higher K_La can provide more oxygen to cells. It is because of this that constant K_La has become a standard value to use when scaling systems, from clonal selection to large scale culture.[13]

Mass transfer regimes can also be calculated using CFD. Péclet number is a dimensionless number and is the ratio of advection rate to the diffusion rate. Using Péclet number one can deduce whether the movement of gasses and nutrients in the media are diffusing through mechanical mixing via fluid flow, or through molecular diffusion. Regarding mass transfer it is calculated by the equation:

$$Pe = \frac{Lu}{D} = Re_L\, Sc$$

Equation 5-2: Péclet Number. Where L is the characteristic length, u is the local velocity and D is the mass diffusion coefficient.

Péclet Number is also the product of the Reynold number and the Schmitt number. In water, the diffusion coefficient of air is $2.0x10^{-5}$cm s^{-1}.[14,15] Using this information the Schmidt number can be obtained by:

$$Sc = \frac{\mu}{\rho D}$$

Equation 5-3: Schmidt Number. Where μ is the dynamic viscosity of the fluid, ρ is the density of the fluid, and D is the mass diffusivity.

In our system the shear stress is a byproduct of the velocity gradient of the fluid flowing parallel to a surface, and is a property of the viscosity of the fluid. Velocity will be slower closer to the wall of a pipe, and faster towards the center. This leads to a velocity gradient, and near the walls where shear is the highest known as the boundary layer. Shear stress can be calculated from the strain rate following the equation:

$$\tau = \eta\gamma$$

Equation 5-4: Shear Stress. Where τ is the shear stress, γ is the strain rate, and η is the viscosity of the liquid.

As strain rate in the system is calculated spatially, this accounts for the distance from the walls of the lattice. Thus, a wholistic map of shear stress can be obtained using this equation.

5.3 METHODS

5.3.1 **Computer rendering and machining**

Solidworks Computer Aided Design (CAD) software was used to generate three dimensional designs of the bioreactor scaffold for in silico simulations and experimental

studies. This allowed model with behavior of flow for multiple geometries to optimize both scaffold and reactor designs prior to 3D printing and machining. The scaffold, comprising of fibers forming a homogenous lattice, was then 3D printed in PLA using Printrbot Simple Metal printer.

The reactor tested here is a scaled system of the Express bioreactor manufactured by Sepragen. To produce a quality model parts were modeled in Solidworks and physical fits were tested via 3D printing, allowing easy design changes prior to machining the system from stainless steel. After test fitting and addition of a sampling port and various adapters the files were organized in Fusion 360 and milled on a CNC adapted Bridgeport milling machine in 316 stainless steel.

5.3.2 **ANSYS Modeling**

A simplified 2D cross-sectional model of the scaffold geometry was rendered using Design Modeler within ANSYS 18.1. A 2D model was used and was adequate to capture the flow dynamics of the reactor due to the scale and repetition of the scaffold geometries. The scaffold itself is comprised essentially of one unit that is repeated in a lattice pattern. Designing the model like this reduced the computation time required while providing and accurate characterization of fluid flow through the lattice. The scaffold was prioritized, as it would be where the cells reside while culturing, and because it is the narrowest point of the system and would theoretically result in the highest shear. FLUENT was used to model fluid flow through the system. Turbulence was modeled using k-epsilon in a VOF model using SIMPLE. Convergence was set to 10^{-8}.

A 2D model was used to monitor tracer infiltration into the modeled lattice. The pressure-velocity coupling solution method used SIMPLE, gradient of lease squares cell based,

pressure of PRESTO!, Second order upwind for momentum, geo reconstruct for volume fraction, first order upwind for turbulent kinetic energy and for turbulent dissipation rate, and second order upwind for energy. First order implicit was used for transient formulation. A tracer with the same properties as water was modeled into the system. After initialization the tracer was patched into the inlet and the simulation run for simulated three minutes. This was chosen because of the time it took for dye to flow through the entire system in the benchtop model.

5.3.3 **Benchtop Dye testing**

To validate CFD modeling the velocity and fluid movement was visualized using dye flowing through the PLA scaffold. The lattice was first wetted with MilliQ water and set up with the same nozzle as in the bioreactor. Fluid was handled via a peristaltic pump. The media line above the inlet to the lattice matrix was teed to allow a pulse of water-based dye into the loop. After the system had run long enough to purge air from the lines and reach a steady state flow the pump was temporarily paused and the dye pushed into the inlet until the color was seen beading on the tip of the inlet. The pump was then reinitialized, and the matrix was filmed until it was saturated with color. Time points of the video were then clipped and used as a visual comparison for CFD validation of velocity and liquid movement.

5.3.4 **$K_l a$ and Oxygen Transfer**

To determine the coefficient of oxygen transfer of the bioreactor the system was filled with 30mL of PBS and heated to 30°C and run at 0.5mL min^{-1}. Pyroscience FireStingO_2 dissolved oxygen (DO) system was used in conjunction with their small-scale flow through sensor. Air was bubbled into the water inside the reactor until DO reading

stabilized, at which point the probe was set to 100% DO. The media was then bubbled with nitrogen to strip the system of oxygen until the reading stabilized, at which point the probe was zeroed. Gas was pumped into the headspace for 3 minutes to strip nitrogen and DO was measured over time. Oxygen percent [C] was correlated to concentrations and a plot of ln(C*-C) vs time to obtain the $K_L a$. The maximum Oxygen Transfer Rate was then calculated using the equation:

$$OTR = K_L a(C^* * C)$$

Equation 5-5: Oxygen Transfer Rate (OTR). Where OTR is in mMol $O_2 L^{-1}$ hr^{-1}, KLa is the oxygen transfer coefficient in hr^{-1}, C^* is maximum oxygen saturation of media at that given temperature and pressure in mMol $O_2 L^{-1}$, and C is recorded saturation. For OTR_{max} C is zero, making OTR a function of $K_L a$ and 100% saturation of the media.

5.4 RESULTS

Early 2D modeling in CFD were not matching dye testing. The PLA lattice tested showed good dye infiltration across the lattice insert, while initial models showed tracer moving straight through. This was because when the geometry was converted to 2D, there were direct channels for the fluid to move down, which was highly favored over horizontal tracer movement. To fix this and better match the model to the fluid dye movement seen in benchtop experiments, alternating fiber “holes” were patterned into the modeled 2D lattice. This led to higher fidelity between the model and benchtop testing. The modeled fibers were left as square due to the deposition method of printing. While the body of the fibers are more rounded, there is compression of the layers at the joints, causing those intersections to be more angular. This also helped to make meshing easier, resulting in a more uniform mesh (Figure 5-1). Located halfway between the center and the top of the

reactor are two rows of larger channels running horizontally. This is to mimic the gap left in the lattice from the removable insert that resides there (Figure 5-2).

The simplified model agreed very well with actual tests at calculated equivalent flow rate. The dye test in Figure 5-3 shows dye infiltration and dispersion in the model and the tested scaffold. After model validation through dye testing Figure 5-3 a range of shear values vs the flow rate of the pump was tested. Flow rates tested were between 0.125 and 1.00mL. Shear stress values in dynes cm^{-2} were calculated by multiplying the strain rate by the viscosity of the fluid according to Equation 5-4. The calculated minimum and maximum rates were $1.3x10^{-3}$ and $8.0x10^{-3}$ dynes cm^{-2}. Average and maximum shear values vs flow rates can be seen in Table 5-1.

The simplified model run at 0.25mL min^{-1} showed expected velocity profile through fibers. Velocity was highest at the inlet and the outlet where fluid was concentrated. The velocity slows as the lattice expands in the middle and the fluid disperses through many channels. Strain rate mirrors the velocity profile (Figure 5-5).

By graphing the log difference in oxygen saturation of the media over time we were able to calculate the K_La of the system to be $2.14hr^{-1}$ (Figure 5-6). From this OTR_{max} was found to be 16.26mMol L^{-1} hr^{-1}.

Flow was characterized as laminar by calculating Reynolds number. Using the average fluid velocity of 0.000172m s^{-1} through a 0.4mm diameter opening the Reynolds number was found to be $2.88x10^{-3}$ Via Equation 5-1. This indicates very laminar flow through the channels of the PLA lattice. Average Péclet number in the channels was calculated and found to be 21 via Equation 5-2. When horizontal velocity was used to calculate Péclet

the result was 0.01, meaning that mass transfer within horizontal channels is mainly through diffusion. Thus, mass transport of oxygen through the channels differ via the direction. In vertical channels transport is driven though advection.

By using cell specific oxygen uptake rate, we can calculate under equilibrium what the gas dependent maximum cell density achievable would be. Researchers report that bone marrow derived hMSCs have a cell specific OUR of $9.8x10^{-11}$ mMol $cell^{-1}$ hr^{-1}.[16]

5.5 DISCUSSION

Initial flow rates were based on values found in literature, where researchers were culturing shear sensitive mammalian cells in dynamic flowing system.[17] All tested flow rates resulted in shear values less than reported shear stresses shown to drive differentiation in mesenchymal stem cells (0.02 -22 dynes cm^{-2})[2,18] (Figure 5-4). However, because shear is a source of impurities in cell yields the system was still operated at the lowest feasible flow rate. This meant that the reactor was circulated at 0.25mL min^{-1}, as it was the slowest rate that still wetted the surface of the lattice.

Velocity was high at the inlet because a fully developed fluid flow is entering narrowed channels (Figure 5-5). The velocity quickly dissipates through the lattice as the fluid becomes more dispersed through the structure. As these individual velocities begin to combine in the bottom half of the reactor, we see fluid velocity begin to increase. This is similar to other rigid lattice systems tested using similar fluidics modeling techniques.[19] However, since fluid was moving freely though the system and not forcedly pumped across the matrix, there is no pressure drop in this system and shear is comparably much less in. As expected, strain rate mirrored velocity contours; shear was highest at the inlet

and outlet of the matrix. However, even the maximum shear stress values within the lattice where cells are attached fall well below reported values of 0.4-9 dynes cm^{-2} that have resulted in stem cell differentiation.[2] This is important as it has been shown that exposure even as low as 0.02 dynes cm^{-2} can lead to upregulation of osteocyte markers.[18]

The calculated K_La is similar to the approximate $2.00hr^{-1}$ reported in stirred systems using gas overlay without sparging.[20,21] It is also within the range of 1.59-$3.00hr^{-1}$ reported in a specialized system using gyroscopic mixing. [22] The lattice system tested here also had higher K_La values compared to spinner flasks which, were reported to be between 1.00-$1.91hr^{-1}$.[22] This rough similarity in K_La is likely due to the fact that gas exchange in all of these systems is happening passively at the interface of the media and the gas in the chamber. Since all methods mentioned are run with the intention of decreasing shear, and consequently do not used forced oxygenation of the media, it is reasonable that the K_La would be similar. It is also well above the reported K_La value theoretically needed to sustain hMSC proliferation in a reactor.[23]

Using K_La we can calculate the theoretical maximum cell density. In steady state the maximum oxygen transfer rate of the tested lattice system was calculated to be $16.264hr^{-1}$. Dividing this by cell specific OUR obtained from literature, we were able to determine that gas exchange is not the limiting factor of the system. Furthermore, we can calculate the theoretical maximum cell density. Using reported values, the maximum OTR of this system could sustain up to $1.66x10^{11}$ bone marrow derived hMSCs. Knowing this, scaling of the system is very possible, and the limiting factors would be surface area and nutrients in media rather than oxygen transfer.

Using Péclet number we can conclude that mass transfer varies slightly within the lattice based on the channel orientation. In horizontal connecting channels mass transfer of air is mainly accomplished through passive diffusion, while vertically oriented channels are predicted to have more transfer through advection.

5.6 CONCLUSION

Here we have successfully modeled the 3D PLA lattice used to culture hMSCs. This modeling allows us to better characterize and understand the forces at play in this system. For future experiments CFD will be invaluable for scaling the system. In silico modeling of larger matrix inserts and smaller fiber diameters will allow rapid testing without using consumables.

The system shows marginally better K_La than comparable systems, including stirred systems commonly used with microcarrier culture of stem cells. This increase may be due in part to the unique way the cell culture scaffold is suspended outside of the media, resulting in only a very thin layer of media between the cells and atmosphere.

5.7 ACKNOWLEDGEMENTS

I would like to thank Hardy Richardson and Hsiang-Wei for helping to machine my reactor and allowing me access to the proper tools for this project. I would also like to thank Kevin Vehar and Corinna Doris for their help with the CFD modeling of the reactor.

1. Hass R, Kasper C, Böhm S, Jacobs R. Different populations and sources of human mesenchymal stem cells (MSC): A comparison of adult and neonatal tissue-derived MSC. *Cell Commun Signal*. 2011;9(1):12. doi:10.1186/1478-811X-9-12.

2. Yourek G, McCormick SM, Mao JJ, Reilly GC. Shear stress induces osteogenic differentiation of human mesenchymal stem cells. *Regen Med*. 2010;5(5):713-724. doi:10.2217/rme.10.60.

3. Rapp BE, Rapp BE. Computational Fluid Dynamics. *Microfluid Model Mech Math*. January 2017:609-622. doi:10.1016/B978-1-4557-3141-1.50029-0.

4. Hutmacher DW, Singh H. Computational fluid dynamics for improved bioreactor design and 3D culture. *Trends Biotechnol*. 2008;26(4):166-172. doi:10.1016/J.TIBTECH.2007.11.012.

5. Ram N, Sinha K, Wang Y, Subramanian K, Nere N. Improving bioreactor design through pH mapping of bioreactors employing Computational Fluid Dynamics coupled with equilibrium calculations. *Cell Cult Eng XVI*. May 2018. http://dc.engconfintl.org/ccexvi/174. Accessed April 2, 2019.

6. Liu X, Wang Y, Shi Y, et al. CFD modelling of uneven flows behaviour in flat-sheet membrane bioreactors: From bubble generation to shear stress distribution. *J Memb Sci*. 2019;570-571:146-155. doi:10.1016/J.MEMSCI.2018.10.040.

7. Li X, Scott K, Kelly WJ, Huang Z. Development of a Computational Fluid Dynamics Model for Scaling-up Ambr Bioreactors. *Biotechnol Bioprocess Eng*. 2018;23(6):710-725. doi:10.1007/s12257-018-0063-5.

8. Tajsoleiman T, Mears L, Krühne U, Gernaey K V., Cornelissen S. An Industrial Perspective on Scale-Down Challenges Using Miniaturized Bioreactors. *Trends Biotechnol*. February 2019. doi:10.1016/J.TIBTECH.2019.01.002.

9. Jafari A, Zamankhan P, Mousavi SM, Pietarinen K. Modeling and CFD simulation of flow behavior and dispersivity through randomly packed bed reactors. *Chem Eng J*. 2008;144(3):476-482. doi:10.1016/J.CEJ.2008.07.033.

10. Zhang H, Lamping SR, Pickering SCR, Lye GJ, Shamlou PA. Engineering characterisation of a single well from 24-well and 96-well microtitre plates. *Biochem Eng J*. 2008;40(1):138-149. doi:10.1016/J.BEJ.2007.12.005.

11. Salek MM, Sattari P, Martinuzzi RJ. Analysis of Fluid Flow and Wall Shear Stress Patterns Inside Partially Filled Agitated Culture Well Plates. *Ann Biomed Eng*. 2012;40(3):707-728. doi:10.1007/s10439-011-0444-9.

12. Hu WS, Meier J, Wang DIC. Use of surface aerator improve oxygen transfer in cell culture. *Biotechnol Bioeng*. 1986;28(1):122-125. doi:10.1002/bit.260280120.

13. Wutz J, Steiner R, Assfalg K, Wucherpfennig T. Establishment of a CFD-based kLa model in microtiter plates to support CHO cell culture scale-up during clone selection. *Biotechnol Prog*. 2018;34(5):1120-1128. doi:10.1002/btpr.2707.

14. Mostinsky IL. DIFFUSION COEFFICIENT. In: *A-to-Z Guide to*

Thermodynamics, Heat and Mass Transfer, and Fluids Engineering. Begellhouse. doi:10.1615/AtoZ.d.diffusion_coefficient.

15. Allen JW, Bhatia SN. Formation of steady-state oxygen gradients in vitro:Application to liver zonation. *Biotechnol Bioeng*. 2003;82(3):253-262. doi:10.1002/bit.10569.

16. Pattappa G, Heywood HK, de Bruijn JD, Lee DA. The metabolism of human mesenchymal stem cells during proliferation and differentiation. *J Cell Physiol*. 2011;226(10):2562-2570. doi:10.1002/jcp.22605.

17. Zhao F, Chella R, Ma T. Effects of shear stress on 3-D human mesenchymal stem cell construct development in a perfusion bioreactor system: Experiments and hydrodynamic modeling. *Biotechnol Bioeng*. 2007;96(3):584-595. doi:10.1002/bit.21184.

18. McBride SH, Falls T, Knothe Tate ML. Modulation of Stem Cell Shape and Fate B: Mechanical Modulation of Cell Shape and Gene Expression. *Tissue Eng Part A*. 2008;14(9):1573-1580. doi:10.1089/ten.tea.2008.0113.

19. Kumar A, Lau W, Starly B. Human Mesenchymal Stem Cells Expansion on Three-Dimensional (3D) Printed Poly-Styrene (PS) Scaffolds in a Perfusion Bioreactor. *Procedia CIRP*. 2017;65:115-120. doi:10.1016/J.PROCIR.2017.04.012.

20. Connon CJ. *Bioprocessing for Cell Based Therapies*. https://books.google.com/books?hl=en&lr=&id=AhdCDgAAQBAJ&oi=fnd&pg=PA35&dq=kla+hmsc+bioreactor&ots=fY1aNWyDtM&sig=ToHvjvXahr9R5cgL67BFgBcn0pA#v=onepage&q=kla hmsc bioreactor&f=false. Accessed April 1, 2019.

21. Weber C, Freimark D, Pörtner R, et al. Expansion of Human Mesenchymal Stem Cells in a Fixed-Bed Bioreactor System Based on Non-Porous Glass Carrier – Part B: Modeling and Scale-up of the System. *Int J Artif Organs*. 2010;33(11):782-795. doi:10.1177/039139881003301103.

22. Shah R, Shah C, Park H-S. Proposed design model of single use bioreactor for mesenchymal stem cells proliferation. *Procedia CIRP*. 2016;41:382 – 386. doi:10.1016/j.procir.2015.12.127.

23. Petry F, Weidner T, Czermak P, Salzig D. Three-Dimensional Bioreactor Technologies for the Cocultivation of Human Mesenchymal Stem/Stromal Cells and Beta Cells. *Stem Cells Int*. 2018;2018:1-14. doi:10.1155/2018/2547098.

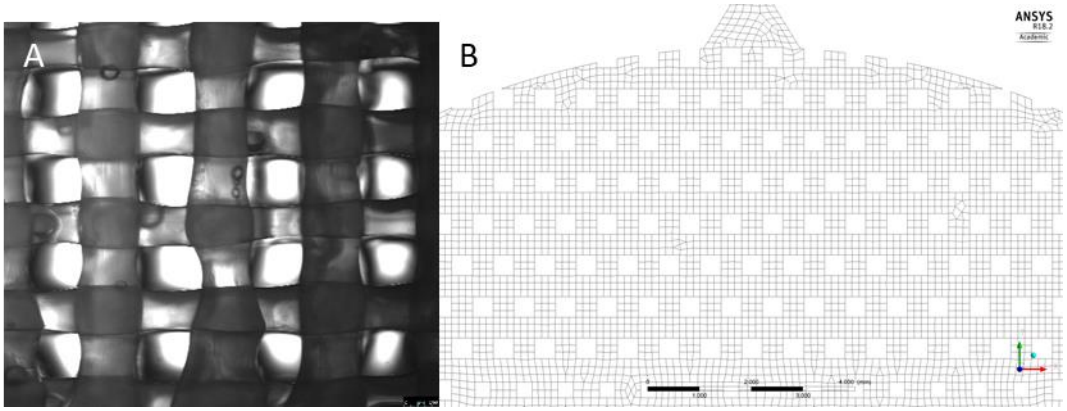

Figure 5-1: Scaffold Modeling used for CFD. A) Image of 3D printed PLA lattice. B) design of 2D model and mesh comprised of nodes and quadrilaterals used to solve for fluid motion and forces.

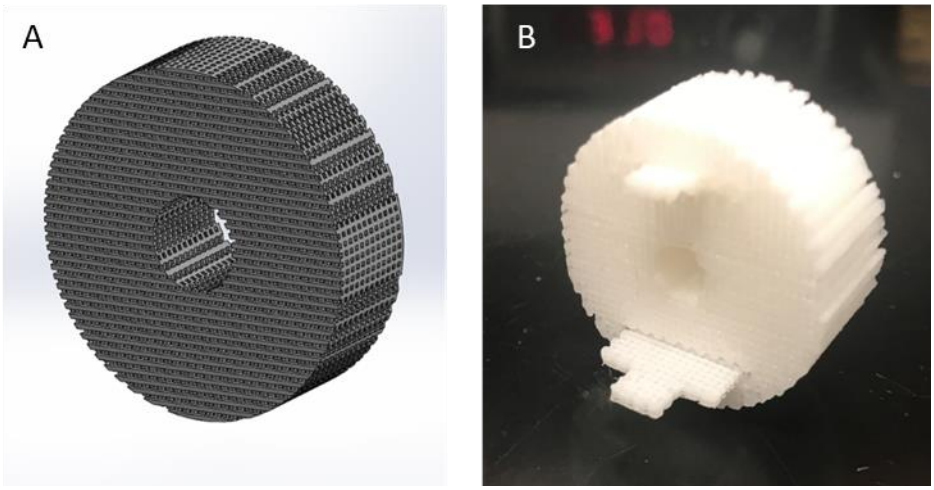

Figure 5-2: PLA Lattice used in bioreactor culture. A) Solidworks mock-up of lattice. B) 3D printed lattice showing removable piece halfway retracted from the lattice body.

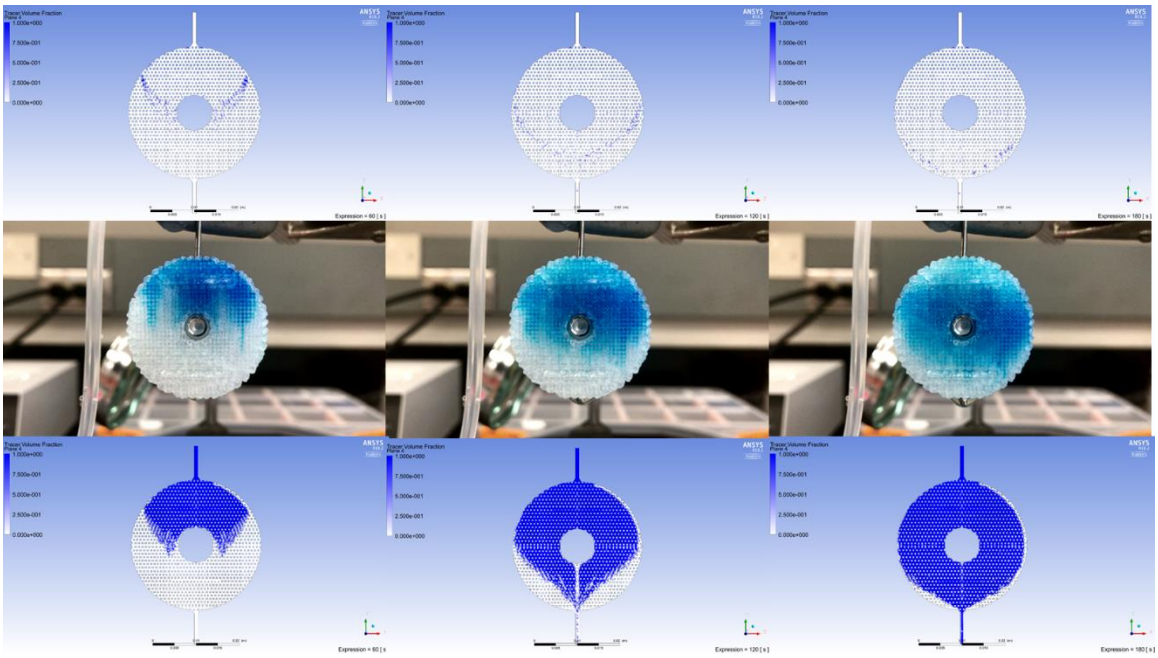

Figure 5-3: Dye testing of flow through lattice matrix. Fluid velocity calculated to me 0.00368m s^{-1} was tested using transient modeling on FLUENT in Ansys 18.2 as an inlet patch. This was compared to dye tests at the same flow rate (Middle row). Bottom row is the same as top row, only dye is provided continuously.

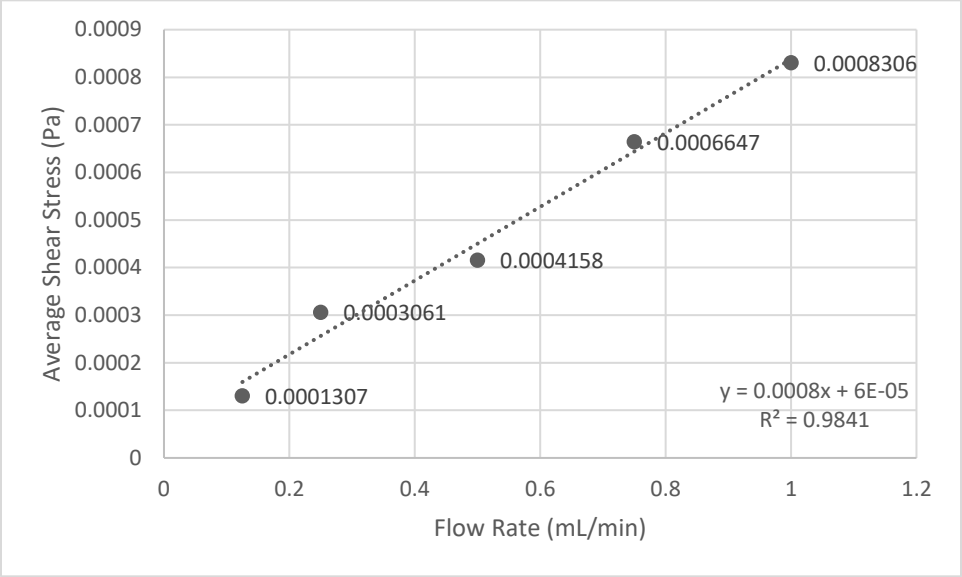

Figure 5-4: Inlet Flow Rate vs Average Wall Shear. Modeled in ANSYS Fluent and graphed in Excel.

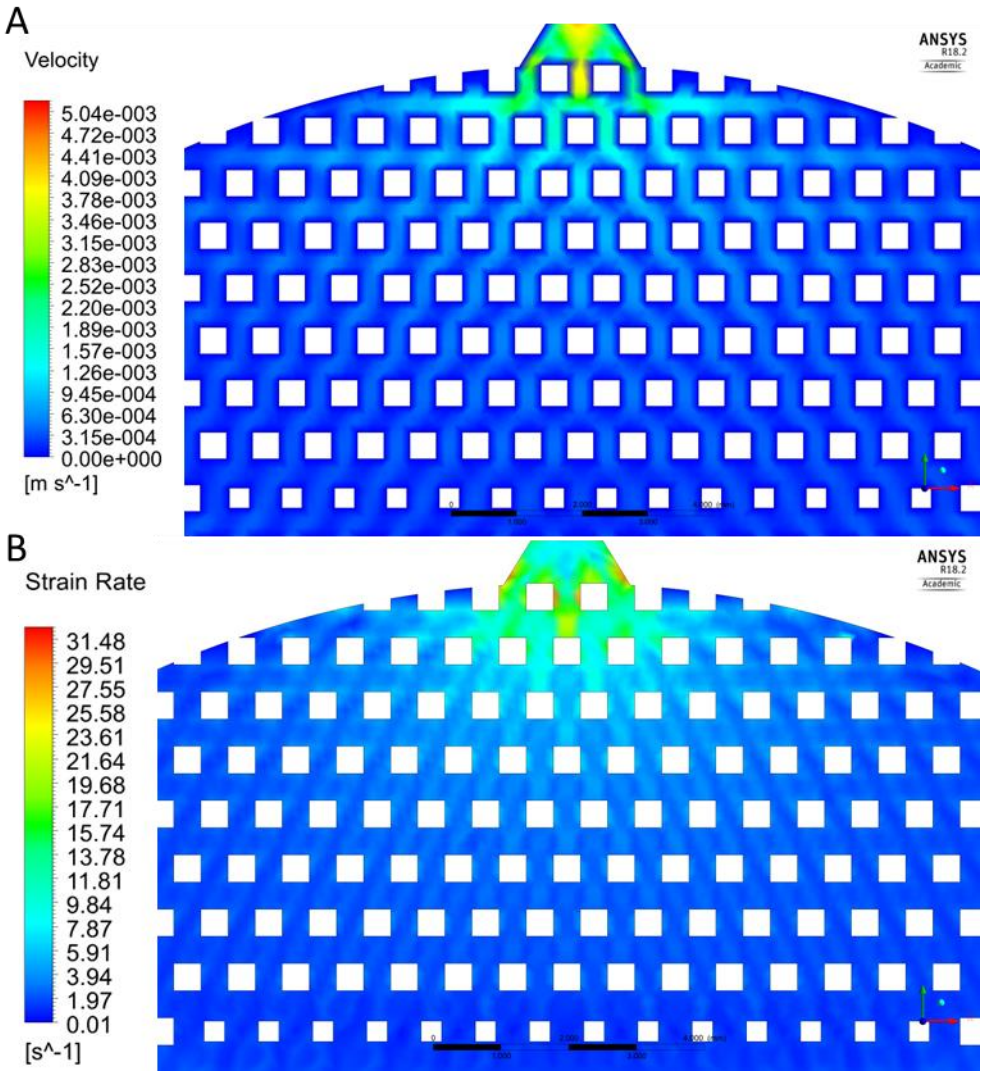

Figure 5-5: CFD modeling of lattice matrix. A) Velocity contour and B) wall shear stress. Maximum velocity of 0.0039m/s and maximum shear stress of 0.0056 dynes cm^{-2} measured inside the lattice, excluding the inlet and outlet. Shear was calculated by multiplying strain rate by the viscosity of the fluid.

Table 5-1: Flow rate vs average and maximum shear stress

Flow Rate mL min^{-1}	Average Shear Stress Dynes cm^{-2}	Maximum Shear Stress Dynes cm^{-2}
0.125	0.00131	0.00252
0.25	0.00306	0.00589
0.5	0.00416	0.00799
0.75	0.00665	0.01274
1	0.00831	0.01591

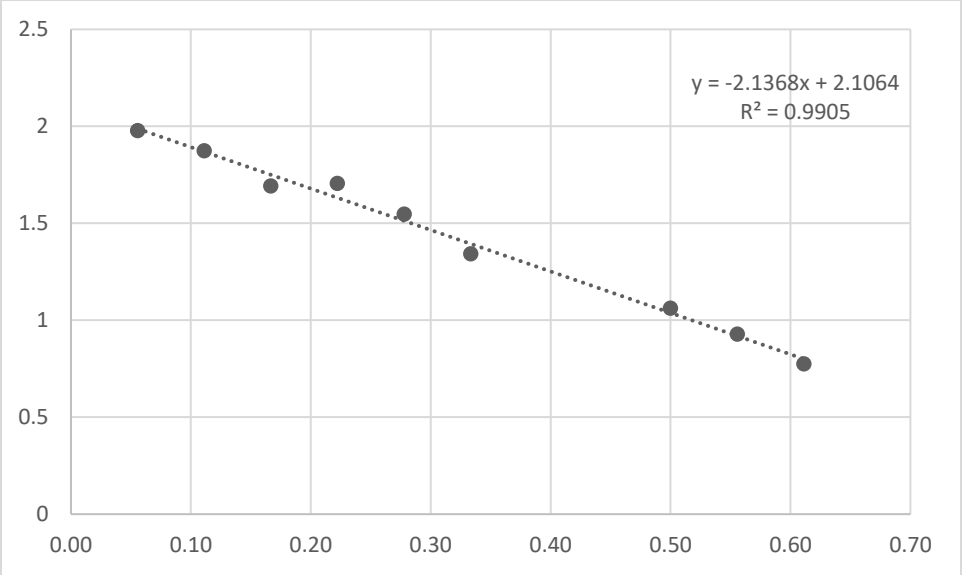

Figure 5-6: Kla calculation plot showing ln(C-C) vs flow rate vs time. Resulting slope is the Kla hr^{-1}.*

6 CONCLUSION

In this work we have designed and characterized a novel 3D culture system for the proliferation of mesenchymal stem cells (hMSCs). The system consists of a cylindrical body made of clear polycarbonate. It is capped by two plates on either side, with a passthrough port to allow sampling of the scaffold. The system allowed for media circulation through external peristaltic pumping.

The scaffold area chosen for studies was a 3D printed polylactic acid (PLA) thermoplastic lattice printed on a hobbyist printer. The lattice was made as a crosshatching grid, increasing surface area substantially. PLA was chosen for its special properties, including: ease of printing, similar rigidity to cancellous bone, biocompatibility and biodegradability. Cells readily adhered to the polymer and were easily removed from it as well, a key consideration when the cell is the product of the system.

The system worked better for hypoxic priming of the cells compared to a conventional static hypoxia chamber. And overall this hypoxic preconditioning of the hMSCs resulted in increased yields, averaging 4-fold over seeding density without detrimentally impacting stemness. After seven days of culture the stem cells retained their cell surface biomarker (CD105+ CD73+ CD19- CD14-) and could still give rise to adipocytes, chondrocytes, and osteocytes after 21-day induction in specified medias. Of the oxygen mixes used, we found a 1.5% O_2 in nitrogen worked best when exposure was kept to a 3 days and the recirculation was kept at 0.25mL $min^{-1.}$ This resulted in the best and most reproducible results.

To understand the reactor better we employed CFD to elucidate flow and hydrodynamic forces. This allowed us to simulate fluid movement through the small geometries of the lattice. What we saw was that fluid was moving uniformly and slow through the lattice, resulting in very low shear. The K_La of the system matched other reported values for other passively aerated systems. Overall, a lattice of this design suspended out of the media lead to an ideal low shear environment for stem cell culture while retaining high cell purity and viability.

7 FUTURE DIRECTION

Testing of other coatings should be performed on the PLA. With gelatin we were able to form monolayers very easily, but it is till derived from animal sources. What I suggest is to revisit the plasma treatment on PLA combined with a xeno-free coating. The plasma treatment drastically increases the wettability of the scaffold, which would help combat the drying of the lattice and allow better seeding. It would also eliminate animal sources from the system if combined with serum free media. To do this I would treat the lattice in the plasma cleaner as described before, but instead of PBS washing and plating the cells directly onto the scaffold I would use the resulting charge to coat the PLA with another polymer. The two that come to mind are poly-lysine and PNIPAAM. Poly-lysine has been used to coat tissue culture plastics, which hMSCs will ready adhere to and grow on. It is not derived from animals, a huge benefit if any hMSC based product is to go to the FDA. PNIPAAM is a thermoresponsive polymer and would allow non-enzymatic lifting of cells. This would eliminate the use of enzymes, which are either animal derived, or recombinant and not very scalable due to price.

I also suggest scaling of the matrix. As a next step the lattice matrix diameter should be increased and tested. CFD would be very helpful in finding the limit of diameter both for fluid infiltration in the horizontal, and for oxygen diffusion. What I see happening is having a larger diameter matrix with more sampling shelves, but also some larger 5.0mm through channels running in the horizontal axis for gas exchange. To better understand the fluid mechanics in such a system a more complete 3D model would have to be made.

This would better elucidate lateral and horizontal movement of the media inside of the lattice.

Lastly, I would have liked to harvest the secretome of the cells grown in this system. Exosomes have shown much promise in wound healing and have great potential in treating diseases. The regulator pathway for a product like this would be much clearer than with a whole cell therapy. What I suggest is seeding and culturing the cells as previously described, but omitting the cell lifting strategies. Instead, a tangential flow filter or alternating flow filter should be placed in the line with pores ranging from 50 to 500nm. A secondary peristaltic pump could control permeate, meaning that the flow rate of the reactor itself would not have to be adjusted. This would allow controlled passage of cell exosomes, which could be collected very easily. As cells are immobilized on the scaffold, there should theoretically be very little cell debris reaching the filter. As the only byproduct of PLA degradation is lactic acid, as long as pH is monitored well there should be low scaffold-based cytotoxicity resulting in undamaged exosomes.

8 BIOSKETCH

Born and raised in the San Francisco Bay Area, Andrew Burns was interested in science from a young age. As a child he often passed the time looking at his parents' dental anatomy books, and as he got older, he consistently gravitated towards all things science. As a hobby, he spent the majority of his teenage years at his uncle's car shop where he refurbished his Datsun 280z from a shell of a car to a 1970's classic. Tinkering with the parts and learning the mechanics of the car cultivated his inclination towards problem solving, which later developed into his fervor for stem cell engineering.

Andrew was first exposed to stem cell culture in college when he worked in Dr. Kara McCloskey's research lab to induce human and murine embryonic stem cell differentiation. This undergraduate research paved a path for his master's degree, and later his Ph.D. Under the guidance of Dr. M. Ian Phillips, his Ph.D. focused on the design, development, and operation of a scalable, novel stem cell bioreactor for potential allogeneic cell therapies. Going forward, Andrew is excited about developing novel technologies and processes for generating stem cells to positively impact medical research in emerging therapeutics.

9 SUPPLEMENTAL DATA

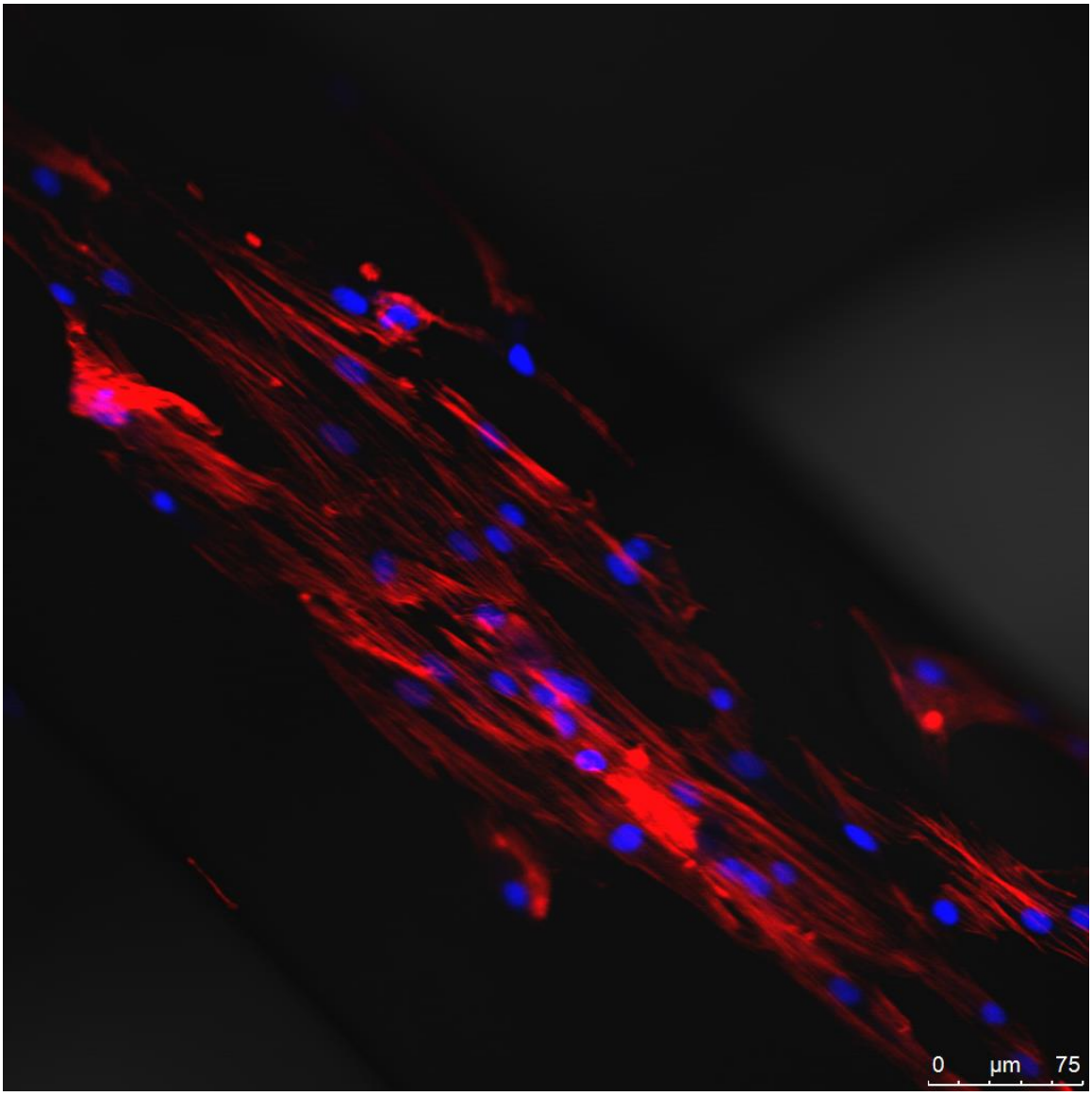

Figure 9-1: hMSC on 3D printed 3D filament. Cells cultured in bioreactor at 0.25mL min^{-1} for 7 days with a 3 day 1.5%O_2 prime. Actin is in red and nuclei are in blue. Note actin filament alignment running diagonal following the length of the PLA structure.

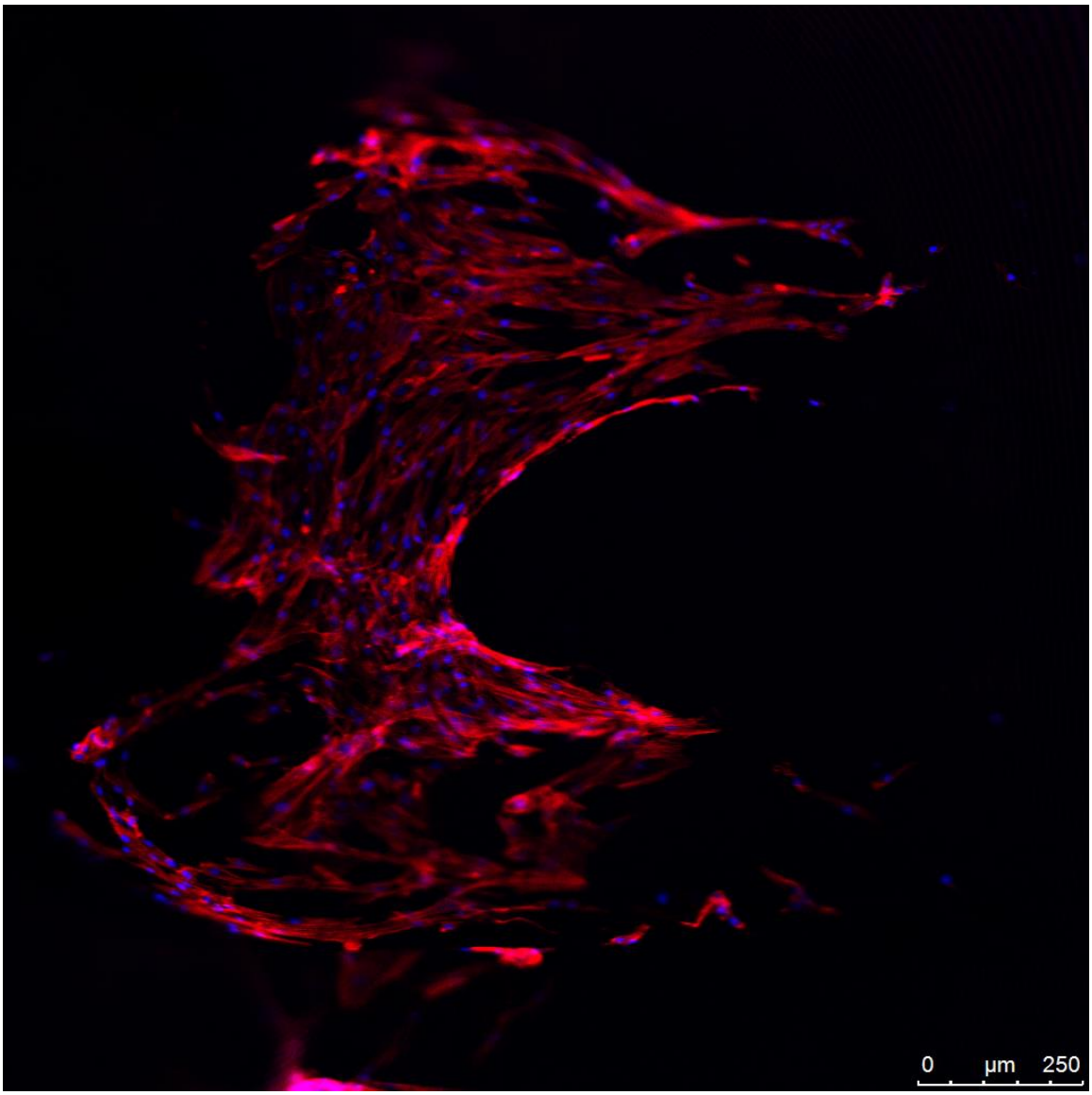

Figure 9-2: hMSC on 3D printed 3D filament. Cells cultured in bioreactor at 0.25mL min^{-1} for 7 days with a 3 day 1.5%O_2 prime. Actin is in red and nuclei are in blue. Note actin aligns with the bend of the PLA structure.

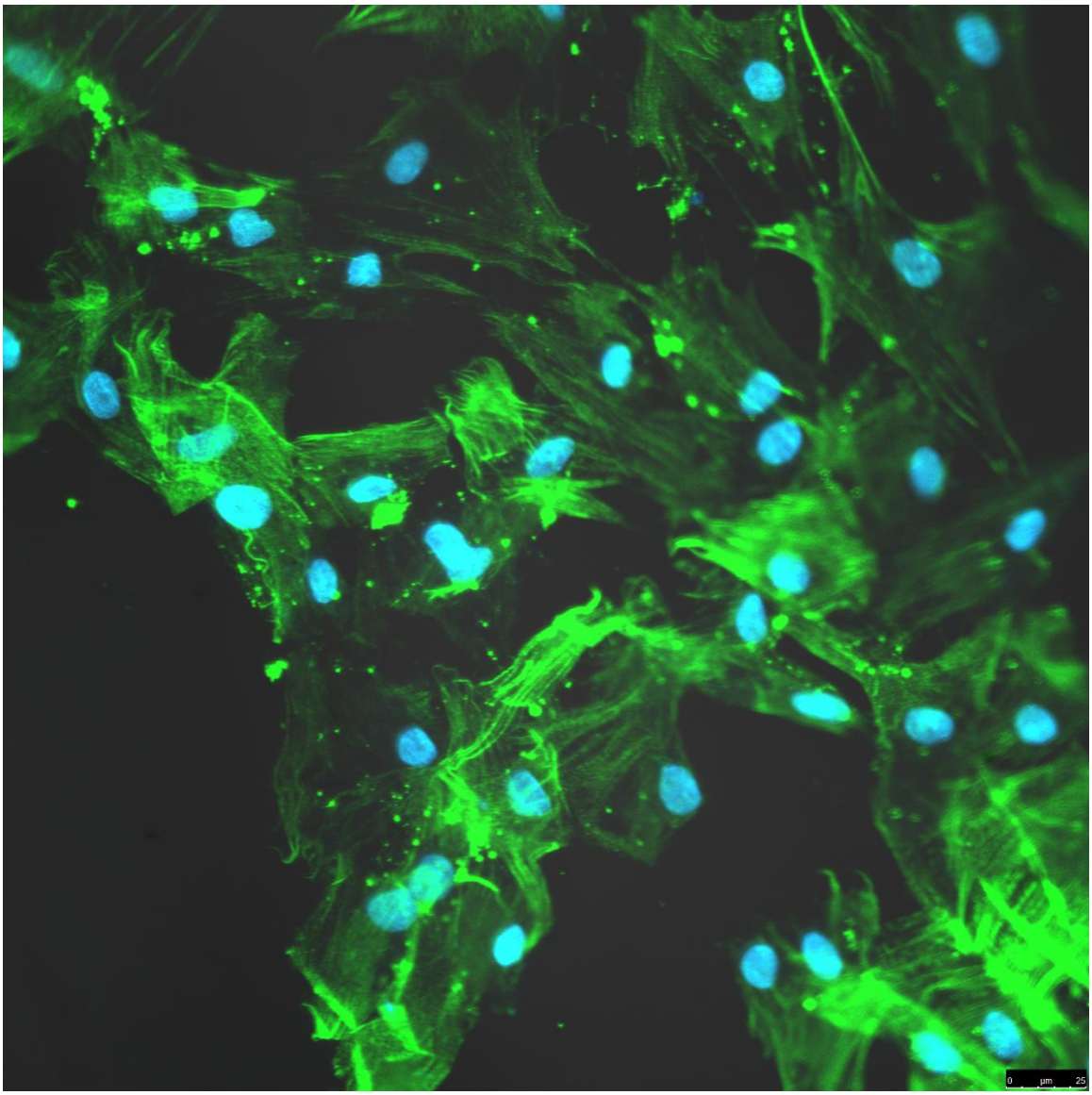

Figure 9-3: hMSCs cultured on polystyrene tissue culture dishes for 7 days. Green is actin staining and blue are nuclei. Note the random alignment of actin filaments.

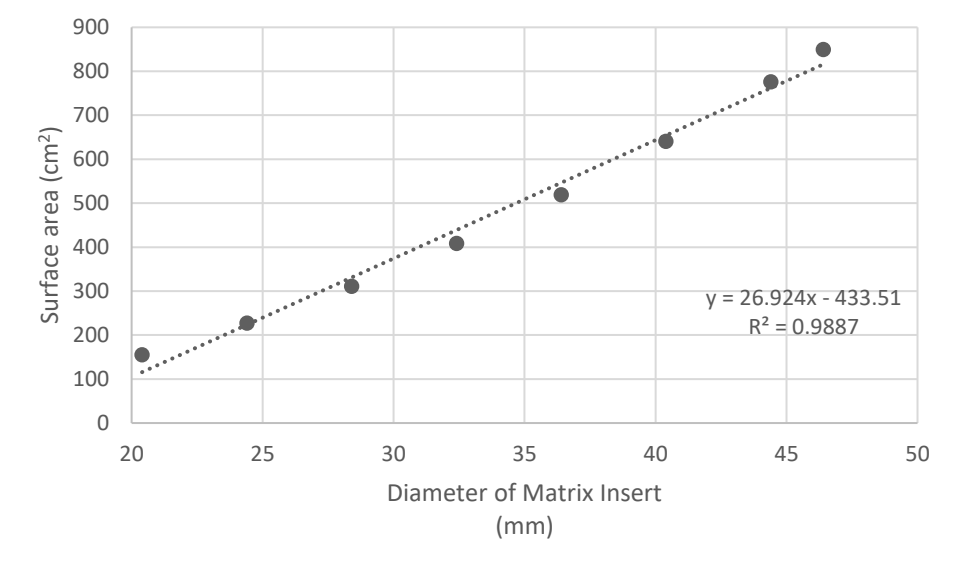

Figure 9-4: Total surface area vs diameter of 3D printed lattice insert. Calculated via Solidworks modeling.

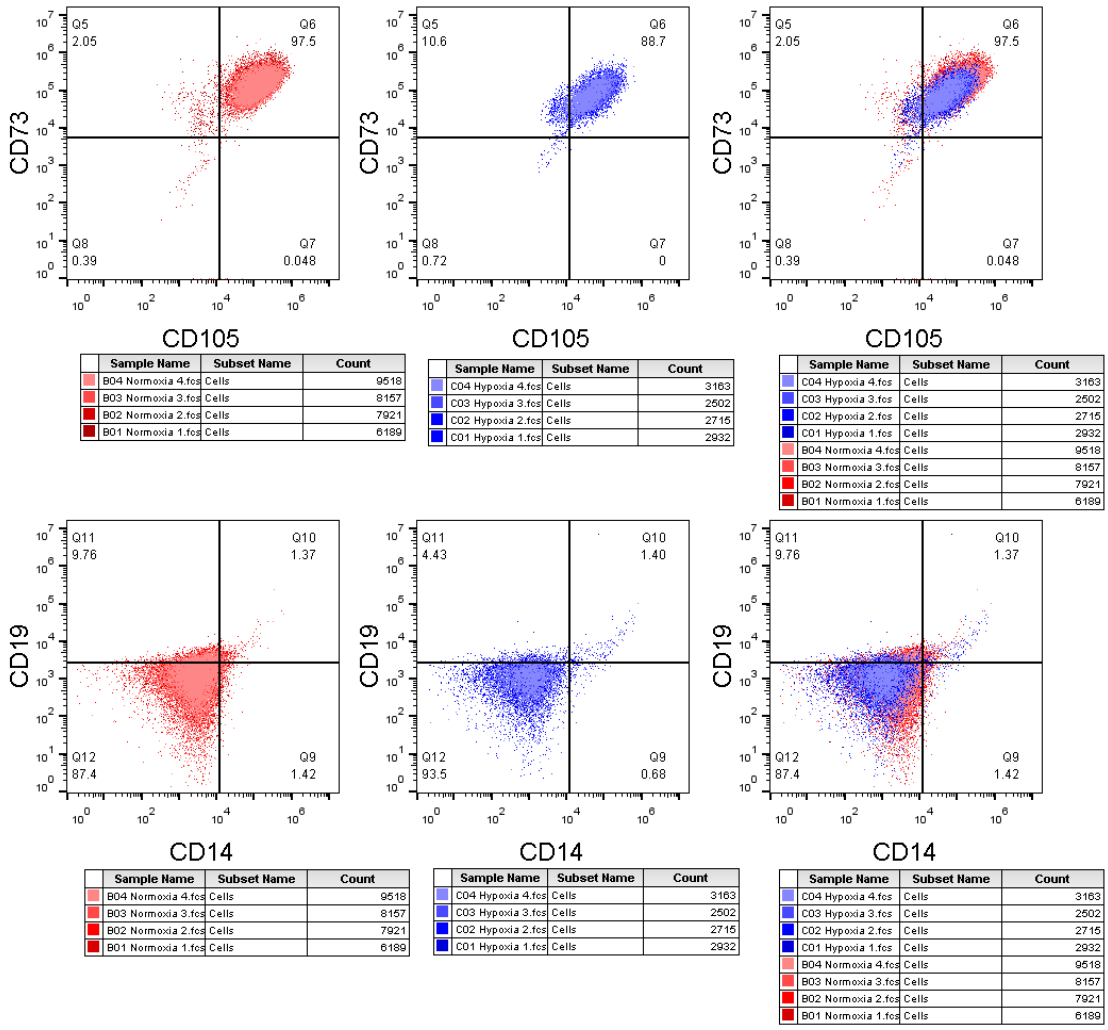

Figure 9-5: hMSC characterization of normoxic and hypoxic culture. Cells grown statically for 7 days on polystyrene tissue culture dishes and characterized via flow cytometry. Hypoxic treatment was for three days at 1.5% O_2. Red is normoxia and blue is hypoxia. The third column is the overlay of the first two columns for easier comparison.

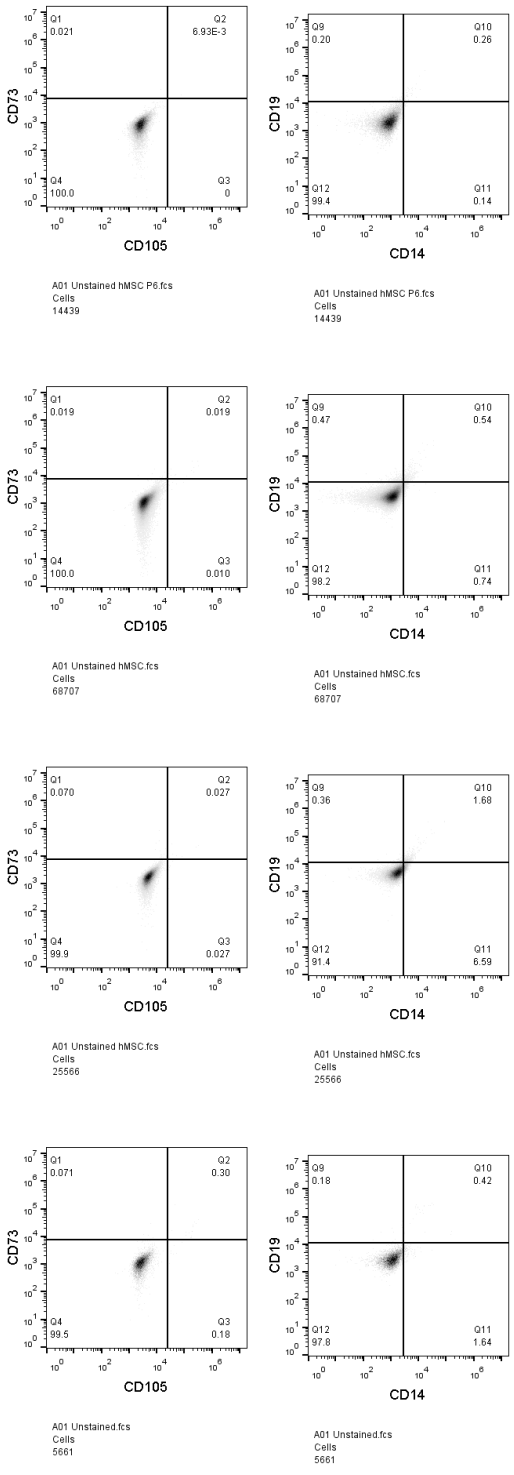

Figure 9-6: hMSC unstained Controls. Cultured for 7 days on polystyrene tissue culture dishes.

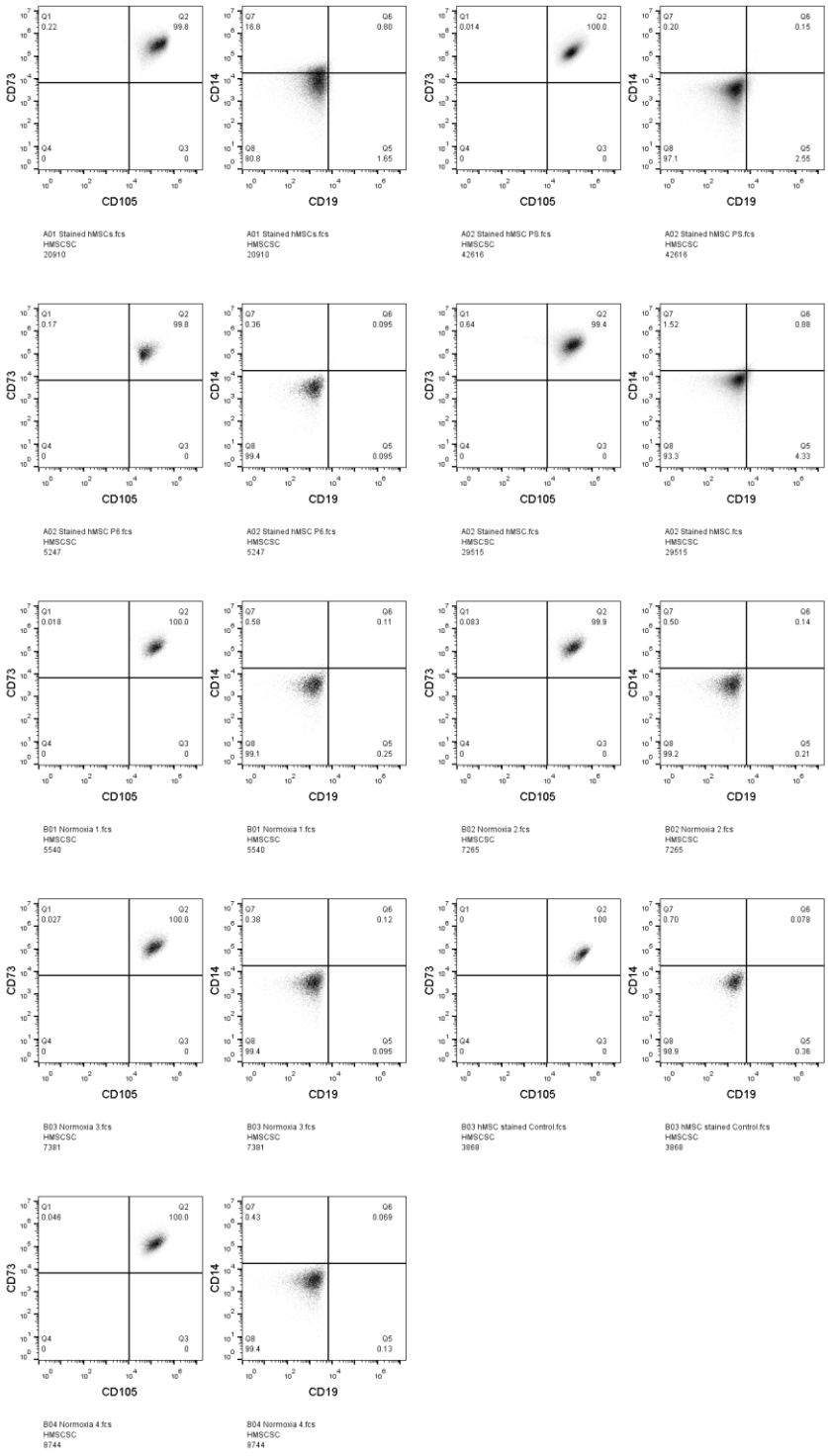

Figure 9-7:Stained control hMSCs. Cells cultured for 7 days on tissue culture polystyrene dishes and stained with hMSC markers according to protocol.

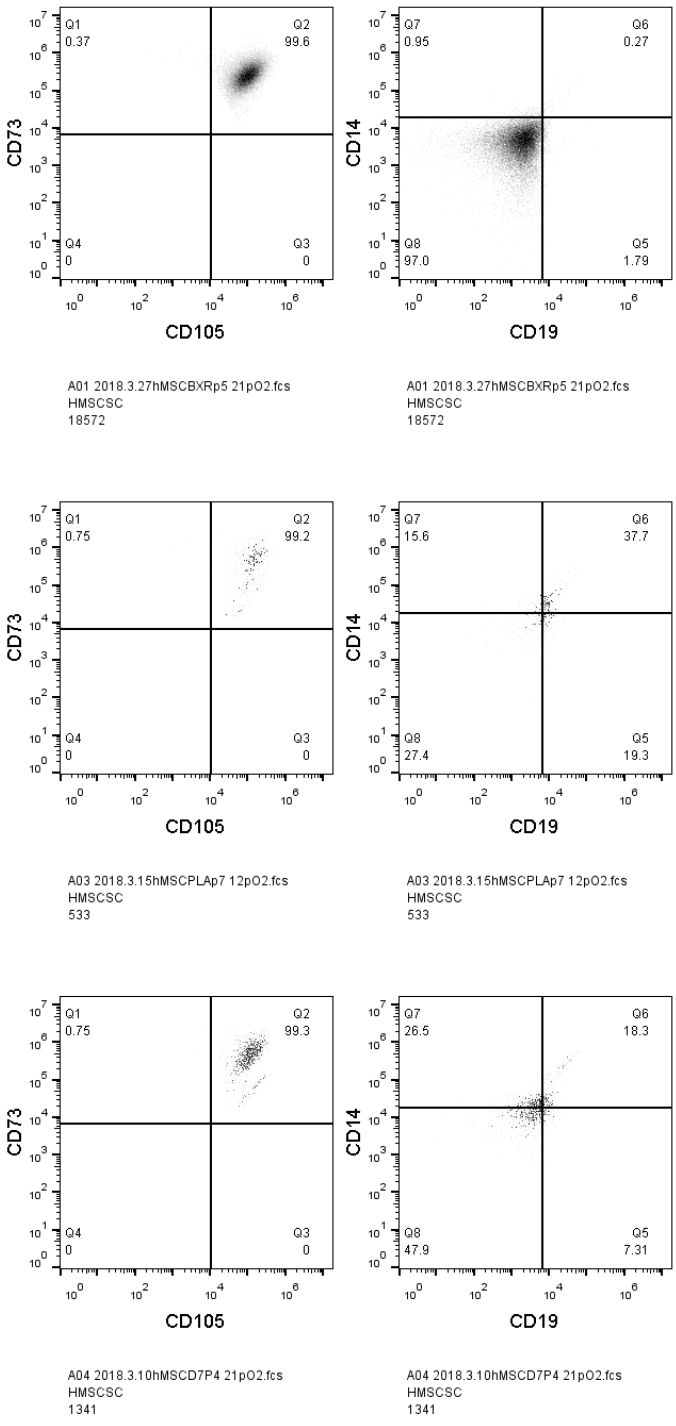

Figure 9-8: Flow Cytometer of 21% O_2 bioreactor cultured for 7 days at 0.25mL min^{-1}.

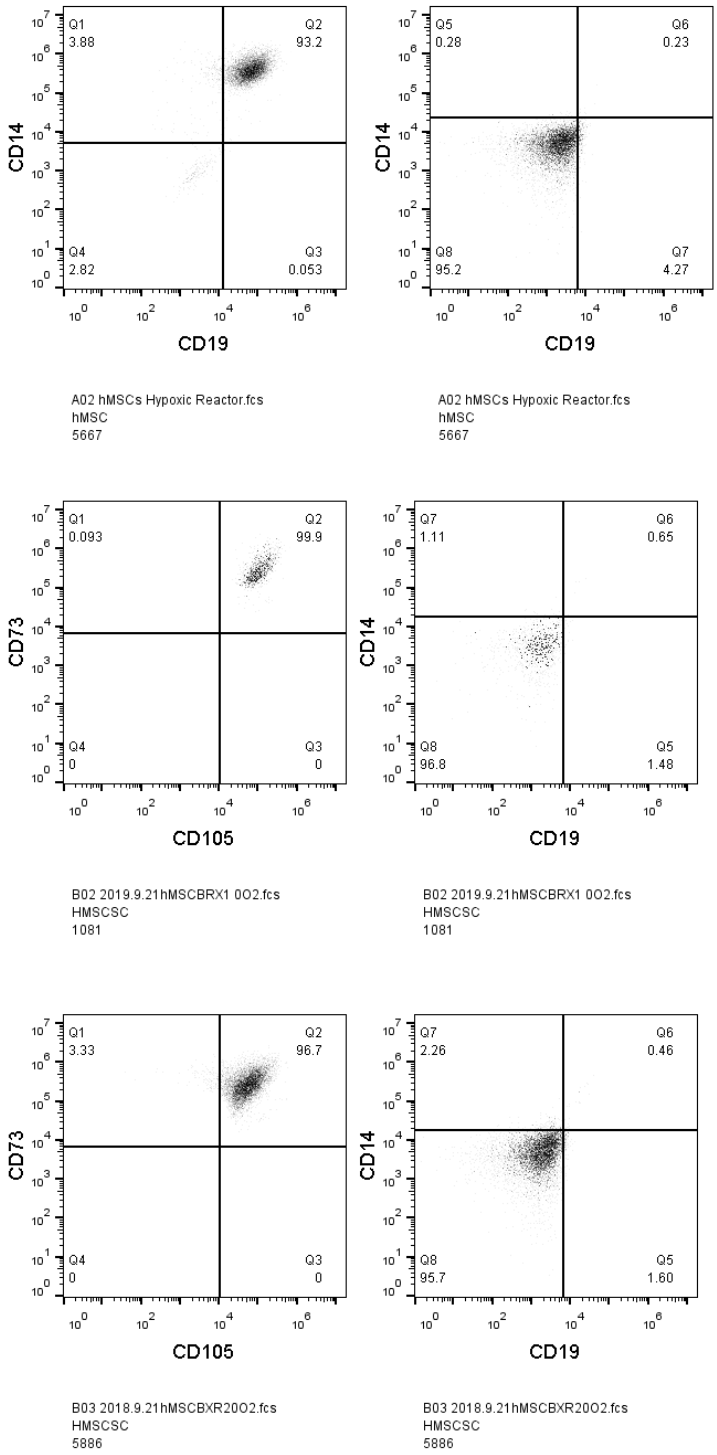

Figure 9-9: Flow Cytometry of hMSC primed at 0% O_2 for three days and cultured for a total of seven days in bioreactor at 0.25mL min^{-1}.

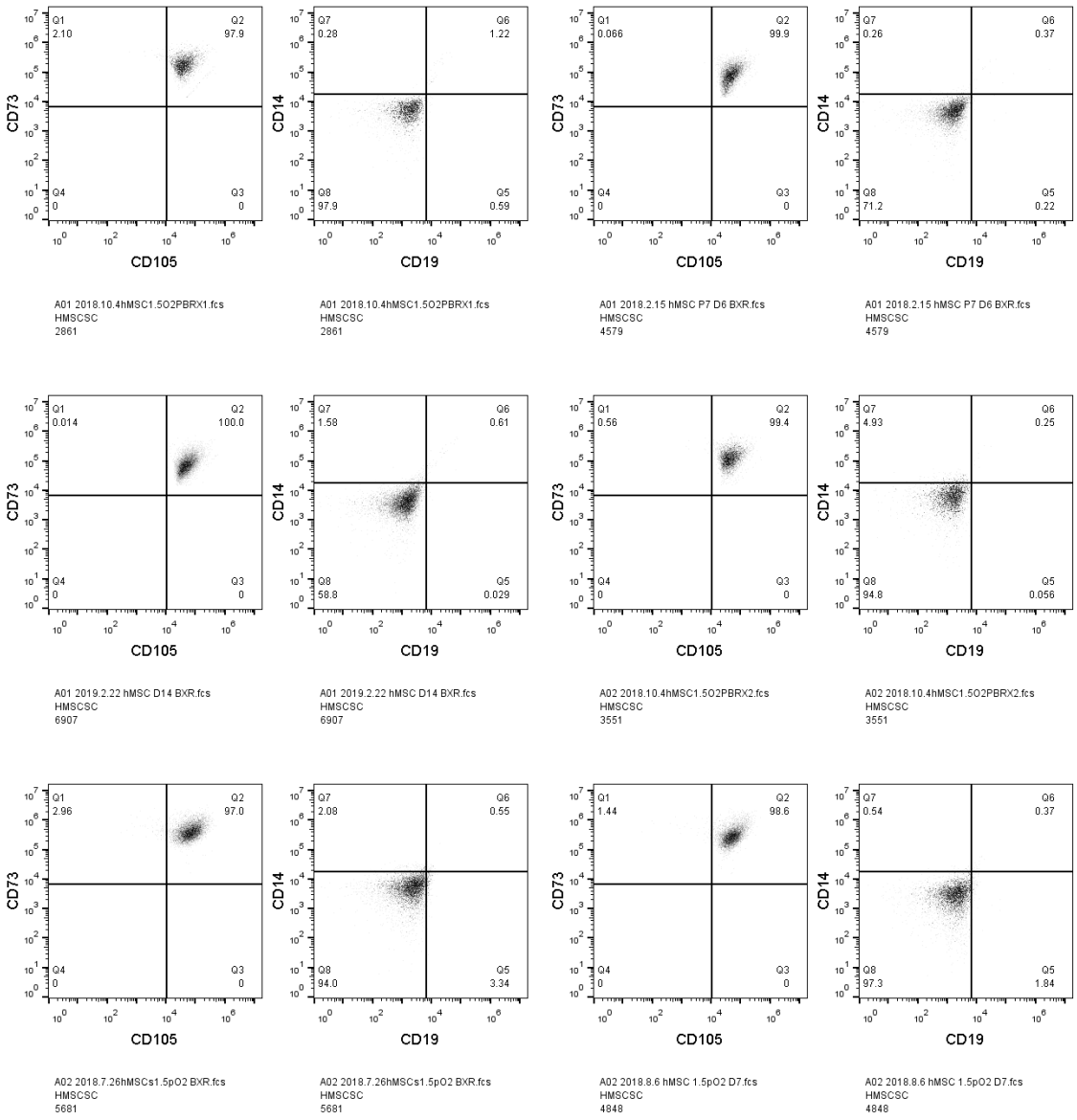

Figure 9-10: Flow Cytometry of hMSC primed at 1.5% O_2 for three days and cultured for a total of seven days in bioreactor at 0.25mL min^{-1}.

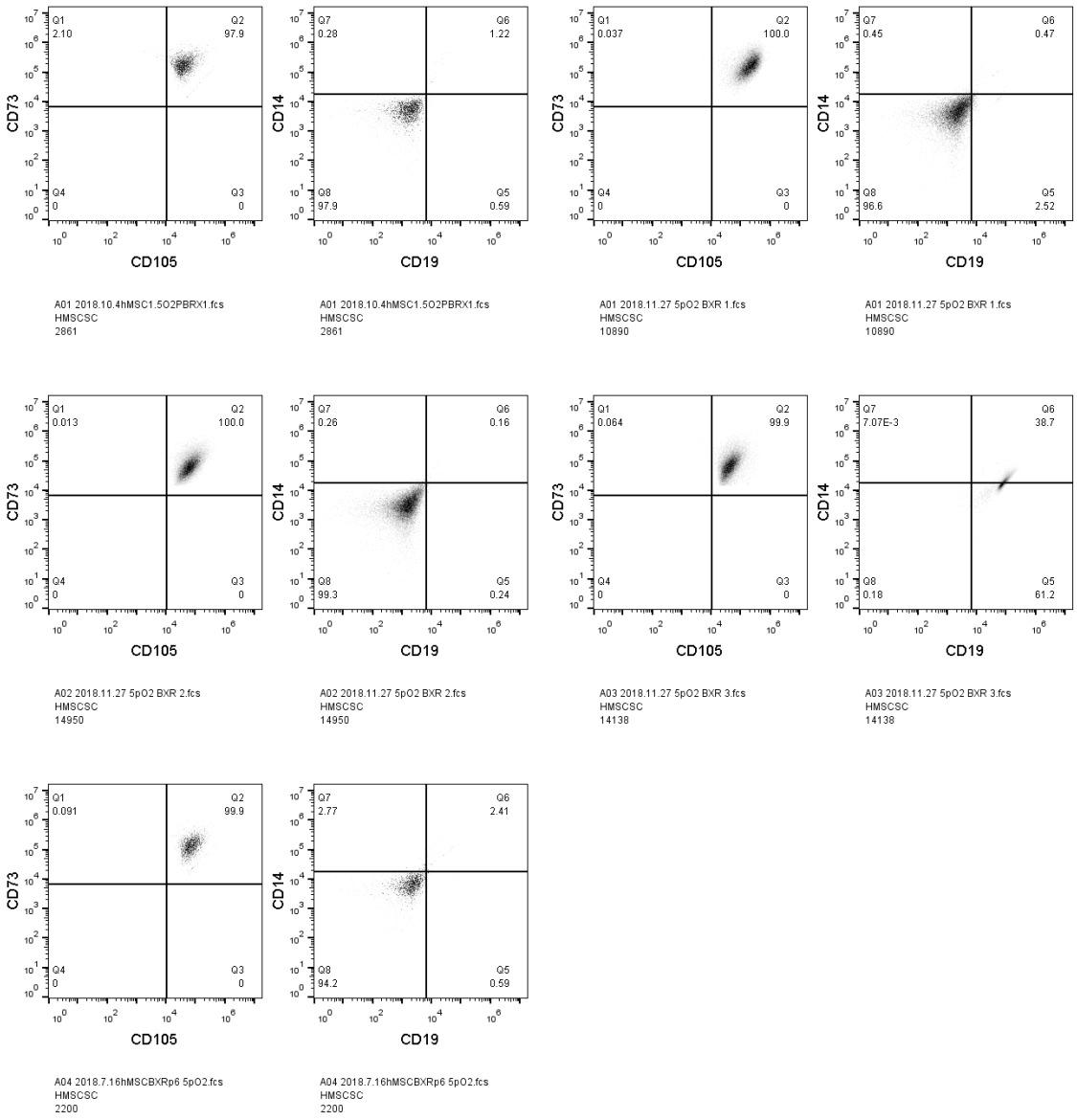

Figure 9-11: Flow Cytometry of hMSC primed at 5.0% O_2 for three days and cultured for a total of seven days in bioreactor at 0.25mL min^{-1}.